EFFECTS OF *DEEPWATER HORIZON* CRUDE OIL ON VISUAL FUNCTION IN TELEOST FISHES

Jason T. Magnuson

Dissertation Prepared for the Degree of

DOCTOR OF PHILOSOPHY

UNIVERSITY OF NORTH TEXAS

August 2018

APPROVED:

Aaron Roberts, Major Professor
Barney Venables, Committee Member
Ed Mager, Committee Member
Amie Lund, Committee Member
Jeff Morris, Committee Member
Art Goven, Chair of the Department of Biological Sciences
Su Gao, Dean of the College of Science
Victor Prybutok, Dean of the Toulouse Graduate School

Magnuson, Jason T. *Effects of* Deepwater Horizon *Crude Oil on Visual Function in Teleost Fishes*. Doctor of Philosophy (Biology), August 2018, 100 pp., 2 tables, 19 figures, chapter references.

The *Deepwater Horizon* oil spill released millions of barrels of oil into the Gulf of Mexico, impacting economically and ecologically important fishes. Polycyclic aromatic hydrocarbons (PAHs) present in the oil have been shown to cause developmental impairments in early life stage fishes, such as morphological and behavioral changes related to eye formation and visual processing following PAH exposure. Prior research reported reduced eye growth in open water, pelagic species, as well as reduced photoreceptor-specific transcription factors associated with eye development following exposure to crude oil. Though changes in transcriptomic-level pathways associated with vision and visual processing have been reported, it has yet to be determined how these changes relate to physiological or behavioral-level effects in fish. Therefore, the present studies evaluated the effect of weathered crude oil on eye development and visual function in mahi-mahi, red drum, sheepshead minnow, and zebrafish larvae. Fish were assessed through several visually-mediated behavioral assays, analyzed histologically and immunohistologically, along with subsequent transcriptomic analyses and associated gene expression changes. Larvae exposed to crude oil experienced significantly reduced abilities to exhibit optomotor or optokinetic responses relative to controls, with associated reductions in retinal development. Furthermore, genes associated with eye development and phototransduction were downregulated, with subsequent decreases in the immunofluorescence of neurological connections within the retina and a choroid-specific increase in apoptotic activity. We related oil-induced transcriptomic-level effects to morphological, physiological, and behavioral-level impairments in larval teleost fishes.

ACKNOWLEDGEMENTS

I thank my friends and family for their love and support through my graduate career. I thank my advisor, Dr. Aaron Roberts, for his help, guidance, and support, and my committee members, Drs. Barney Venables, Ed Mager, Amie Lund, and Jeff Morris for their help and assistance. I thank the RECOVER consortium and the Gulf of Mexico Research Initiative for their financial assistance the last three years. I thank my lab members for their help and support, and I especially thank Brittany for being understanding, supportive, and always willing to help, no matter the time of day. I finally thank Dr. Kerry Hansknecht and Dr. Mark Sandheinrich who have been mentors to me through the years and always willing to help in any way possible.

TABLE OF CONTENTS

Page

LIST OF TABLES AND FIGURES

Page

Tables

Figures

CHAPTER 1

INTRODUCTION

Crude oil is introduced to aquatic environments through natural seeps and anthropogenic actions such as oil extraction, transporting, refining, and spills. Though estimates of the contribution of oil deposited in the ocean from natural seeps have fluctuated in past studies, with estimates of a 10% input in 1975, 6% input in 1985, and 47% input in 2002, most recent estimates of contribution is around 180 million gallons added per year, worldwide [1]. Though not a main contributor of oil discharged into the ocean, oil spills have strong acute and long-lasting effects on marine ecosystems, such as seen with the *Exxon Valdez* and *Deepwater Horizon* oil spills [2,3]. With rising demand in the search for and transportation of crude oil internationally [1,4], the likelihood of oil spills is increasing.

The *Deepwater Horizon* oil spill persisted from April 20 to July 14, 2010, releasing 3.19 million barrels of oil into the Gulf of Mexico [2]. Developmental abnormalities have been shown as a result of polycyclic aromatic hydrocarbons (PAHs) present in the oil. Environmentally relevant concentrations of PAHs cause craniofacial and cardiotoxic defects, spinal curvature, pericardial edema, reduced growth, and visual impairment in several economically and ecologically important marine and estuarine fish species that had peak spawning periods at the time of the spill, such as the mahi-mahi (*Coryphaena hippurus*) and red drum (*Sciaenops ocellatus*) [5–15]. Despite the important role vision plays in fish growth, development, and reproduction, impacts of contaminants on visual function are not always assessed.

1.1 Approaches to Assess Visual Toxicity

The visual capability of fishes at different life-stages is an underlying factor for growth

and survival in teleosts [16]. Many marine pelagic embryos hatch in photopic environments where they rely on pure-cone retinas to aid in their ability to feed [17]. When added stressors occur in an environment, growth and survival can be impacted, especially in early life stages when fish are typically most sensitive [18–20]. In order to understand the impact of changing environmental factors on larval fishes it is important to first obtain baseline data to see how they respond without added stressors. However, baseline data for different species is not always available, rendering it difficult to make pre- and post-event comparisons. Understanding the sublethal effects of contaminants allows for insight on subtle ecological damage following chemical releases, spills, and exposure.

Various approaches have been used to assess visual function in fish exposed to toxicants. Developmental, histological, molecular, and behavioral assessments on eye development following toxicant exposure have been looked at, though not always concomitantly. Understanding the mechanism of toxicity of contaminants through morphometric, histological, and molecular-focused data is important to assess sublethal impacts on the visual system. However, few studies have focused on linking these physiological changes to behavioral effects in fish, as well as addressing subsequent ecological impacts these changes could possess. To measure visual function in the laboratory, optomotor response and optokinetic response assays have been used to assess visual function through both scotopic (light-limiting) and photopic (well-lit) light levels [21,22]. Optomotor responses focus on the ability of a fish to orient its body in the same direction as a designated stimulus, opposed to an optokinetic response, where a fish solely moves its eyes in the same direction as a stimulus [23,24]. A common approach in the laboratory is the use of a rotating drum apparatus, where a fish follows an alternating black or white stripe in a circle until unable to distinguish between individual stripes- referred to as a

flicker-fusion threshold. Use of behavioral endpoints, in conjunction with histological analysis of the retina, has been successful in determining the visual acuity of several fish species from freshwater and marine systems alike [21,22,25–27].

1.2 Eye Development Following Oil Exposure

Larval yellowfin tuna (*Thunnus albacares*), amberjack (*Seriola dumerili*), and bluefin tuna (*Thunnus thynnus*) exposed to *Deepwater Horizon* crude oil had a marked reduction in eye growth, with subsequent increases in edema and cardiac arrhythmia [5]. Ocular malformations, such as reduced eye diameter (microphthalmia) and pigment irregularities, were common craniofacial defects observed in embryonic and larval herring (*Clupea pallasi*) collected from previously oiled locations following the *Exxon Valdez* spill [28]. Similarly, herring exposed to oil contaminated sediment for 16 days had significant craniofacial and finfold defects, reduced brain size (microcephaly), and a significant reduction in retinal pigment [29]. Hose et al. (1996) didn't notice an increase in lens vacuolation between oiled an unoiled sites, though 29 percent of the Pacific herring larvae collected from oiled areas in Prince William Sound following the spill experienced lens vacuolation and increased retinal cell degeneration and necrosis [30]. Using mussel PAH concentrations as a reference for exposure to *Exxon Valdez* oil, Hose et al. (1996) found that microphthalmia in larvae was strongly correlated with measured *Exxon Valdez* PAH mussels' concentrations and suggested that histopathology be used to assess pathogenesis of ocular malformations in all future oil toxicity studies [28], as the composition of oil varies depending on location and weathering events.

Surf smelt (*Hypomesus pretiosus*) exposed to Cook Inlet crude oil had an increase in forebrain and retinal neuronal damage in 21 and 27 days post fertilization (dpf) embryos, though

all other tissues appeared normal in 21 dpf embryos [31]. Increased hypertrophy and vacuolation of retinal receptor cells was seen in 27 dpf embryos, with mitochondria in the damaged receptor cells beginning to lyse, yet no vacuolation or damage was seen 6 days prior in the retina [31]. Eye lens protrusion and reduced eye pigmentation in European flounder (*Pleuronectes flesus*) and cod (*Gadus* morhua) embryos exposed to Ekofisk oil and heavy fuel oil was seen by Lønning (1977). Newly hatched marine pejerrey (*Odontesthes argentinensis*) exposed to heavy petroleum, automotive diesel, and unleaded gasoline developed hyperplasia of psuedobranch epithelium [33], which is thought to play an important role in delivering oxygen to newly developing eyes. Cunners (*Tautogolabrus adspersus*) exposed to Venezuelan crude oil had a significant increase in eye lens diameter over a 6 month timespan [34], most likely contributed to increased edema.

1.3 Eye Development Following Oil Sand Exposure

Embryonic fathead minnows (*Pimephales promelas*) exposed to Athabasca River oil sands had increased eye alterations and reduced pigmentation, as well as signs of ocular hemorrhaging [35]. Similarly, newly hatched white sucker (*Catostomus commersoni*) larvae embryonically exposed to Athabasca River oil sands had noticeable ocular hemorrhaging [36]. Specifically looking at the toxicity and eye pathology of newly hatched fathead minnow and white sucker larvae exposed to collected oil sand sediment, Colavecchia et al. (2007) found that embryos exposed to oil sands with greater concentrations of PAHs had undifferentiated retinal layers with microphthalmia and optic fissures, though generally had a larger lens compared to control fish. The pigmented epithelium was detached in exposed larvae, which was also strongly correlated with the area where the greatest CYP1A expression in fathead minnows was seen [37].

Hargis et al. (1984) collected spot (*Leiostomus* xanthurus) from the Ware River, an unpolluted river in Virginia, and exposed them to collected sediment from the Elizabeth River, which has known PAH-contaminated sediment. The initial concentrations of PAHs in the sediment were 2,500 ppm, with phenanthrene and fluoranthene being the most prevalent PAHs, accounting for 5-12% TPAH. Additionally, effluent from sediment was used to expose spot to strictly waterborne fractions, with all spot developing cloudy or opaque eyes after 24 days of exposure [38]. Of the 56,505 sciaenids sampled by Hargis and Zwerner (1988) from the Elizabeth River, Atlantic croaker (*Micropogonias* undulates) had the highest incidence of cataracts (5%), followed by weakfish (*Cynoscion regalis*) (3.1%), and spot (2.9%). Several forms or features associated with cataracts such as simple hyperplastic growths, polymorphic cell growths, compacted fiber cells, fiber cell degeneration, and formation of vacuoles were seen in croaker, weakfish, and spot, with several mitotic anomalies and lesions seen in affected lens epithelial cells [40].

1.4 Eye Development Following Individual PAH and Dioxin Exposure

Rainbow trout (*Oncorhynchus mykiss*) alevins exposed to benzo(a)pyrene (BaP) predominately experienced cytological changes in the brain and neural retina [41]. Microphthalmia was the most prevalent ocular malformation seen, with 63% resulting from optic fissures, while retinal cell division was inhibited in 91% of exposed alevins with subsequent necrosis in these regions [41]. Significantly reduced ganglion cell densities were seen in BaP exposed zebrafish embryos, which could cause dysfunction in visual processing [42]. The outer nuclear layer, inner nuclear layer, inner plexiform layer, and retinal diameters did not differ compared to control retinas, though several genes associated with eye development and visual perception had

significant differential expression. They suggested that looking at changes in gene expression is an important sublethal endpoint as these changes could be occurring before subsequent protein translation and prior to notable histological damage. These larvae also had a significant reduction in phototactic response when exposed to higher concentrations of BaP, suggesting that BaP exposure may damage visual processing centers, specifically photoreceptors [42].

Williams et al. (1992) isolated spot lenses and cultured them in the presence of BaP medium with radiolabeled thymidine, uridine, and leucine present. The uptake of uridine and leucine, indicative of RNA and protein synthesis, respectively, was not influenced by BaP when compared to controls, though BaP had an inhibitory effect on RNA synthesis and protein reduction. Incorporation of thymidine, indicative of DNA synthesis, increased rapidly in BaP exposed lenses, though an inhibition of DNA synthesis was observed when compared to controls. Such reductions in macromolecule synthesis of lens cells indicates potential biochemical changes associated with PAH exposure that could lead to cataract formation [43].

Laycock et al. (2000) exposed dissected 6-18 month old rainbow trout lenses to increasing concentrations of BaP, fluoranthene, fluorene, or creosote, with or without the presence of UV radiation. Lenses co-exposed to fluoranthene or BaP with UV radiation weighed significantly more than controls and had a greater diameter due to lens edema, which is indicative of reduced activity in the lens epithelium. Lenses treated with fluoranthene, BaP, or creosote concomitantly with UV radiation became hazy. The haziness progressively worsened with time, becoming opaque by around 10 days post-exposure [44], however, no toxic effects of fluoranthene, BaP, or fluorene without the addition of UV radiation were noticed with concentrations used, nor was there a toxic effect when lenses were exposed to UV radiation

alone. Resulting creosote phototoxicity to the lens was thought to be due to the presence of anthracene, fluoranthene, and pyrene [44].

Rainbow trout exposed to creosote for 28 days had an increased focal length and reduced sharpness of focus, with a subsequent increase in mean diameter and weight of exposed fish lenses, which is possibly due to increased edema within the eye [45]. Huang et al. (2013) found that embryonic zebrafish (*Danio rerio*) exposed to phenanthrene had an undifferentiated retinal pigmented epithelium, outer nuclear layer, inner nuclear layer, inner plexiform layer, and ganglion cell layer, though retinal and lens diameters were significantly reduced with increasing phenanthrene concentrations, with subsequent reduction in phototactic response with increased exposure to phenanthrene. They also saw that exposed larvae had significantly increased apoptosis in retinas through the use of a TUNEL assay, increased caspase 3 activity, and reduced EdU positive cells [46].

Larval dourado (*Salminus brasiliensis*) exposed to phenanthrene had impaired visual acuity, with increases in acuity angles from 2.4° in controls to 3.3° in phenanthrene exposed [47]. Impaired prey capture ability was concomitantly seen with 2 to 5 days post hatch (dph) phenanthrene exposed larvae, reducing capture efficiency from 46% in controls to 13.4%. Capture ability significantly decreased with higher phenanthrene exposures, reducing prey capture to 2.3%. Six to 10 dph phenanthrene exposed larvae did not have any significantly reduced visual impairments, nor did any larvae exposed to any concentration of naphthalene used, regardless of age. Carvalho et al. (2008) indicated that swimming behavior was not impacted by phenanthrene exposure, and that visual impairment was the major ecological mechanism of effect. Carvalho and Tillitt (2004) looked at the biochemical, histological, and behavioral effects of TCDD exposure on 28 to 42 dph rainbow trout. Exposed larvae had a

significantly reduced visual acuity angle compared to controls, a decrease in photopic and scotopic flicker-fusion thresholds, and a reduced prey capture rate in those exposed to high concentrations of TCDD. Rod and cone densities did not significantly differ regardless of dose, though reductions in retinal ganglion cell densities and lens diameter decreases were seen.

1.5 Understanding the Mechanism of Oil-Induced Retinal Injury

It is currently not well understood the mechanism of oil-induced toxicity to retinal function in teleosts. Recent studies following the *Deepwater Horizon* oil spill have linked transcriptomic-level changes to morphological defects, specifically to eye development. Major biological processes impacted in mahi-mahi and red drum following oil exposure were associated with eye development and visual processing, with further dysregulations of genes important in proper visual function (Xu et al., 2016, 2017). These genes are regulated by microRNAs (miRNAs), which are dysregulated following oil exposure [49]. miRNAs impacted by oil exposure play important roles in visual function and processing, by regulating the activation and proliferation of proper capillary and choroidal vasculature, as well as mediating signals to the tectum [49]. Furthermore, processes important in the stability and function of Müller glial cells were impacted in mahi-mahi following oil exposure, such as CREB, Notch, Wnt, and Fgf [49]. *crx* plays in important role in the regulation of transcription of photoreceptors and is important in proper Müller cell function. It is primarily associated in the inner nuclear and photoreceptor area [50], and is inhibited following oil exposure, which has been linked to eye degradation [13].

1.6 References

(1) Kvenvolden, K. A.; Cooper, C. K. Natural Seepage of Crude Oil into the Marine Environment. *Geo-Marine Lett.* **2003**, *23* (3–4), 140–146.

(2) Beyer, J.; Trannum, H. C.; Bakke, T.; Hodson, P. V.; Collier, T. K. Environmental Effects of the Deepwater Horizon Oil Spill: A Review. *Mar. Pollut. Bull.* **2016**, *110* (1), 28–51.

(3) Peterson, C. H.; Rice, S. D.; Short, J. W.; Esler, D.; Bodkin, J. L.; Ballachey, B. E.; Irons, D. B. Long-Term Ecosystem Response to the Exxon Valdez Oil Spill. *Science (80-.).* **2003**, *302*, 2082–2086.

(4) NAS. *Oil in the Sea III: Inputs, Fates, and Effects*; National Academy of Sciences, National Academy Press: Washington, D.C., 2003.

(5) Incardona, J. P.; Gardner, L. D.; Linbo, T. L.; Brown, T. L.; Esbaugh, A. J.; Mager, E. M.; Stieglitz, J. D.; French, B. L.; Labenia, J. S.; Laetz, C. A.; et al. Deepwater Horizon Crude Oil Impacts the Developing Hearts of Large Predatory Pelagic Fish. *PNAS* **2014**, *111* (15), 1510–1518.

(6) Alloy, M.; Baxter, D.; Stieglitz, J.; Mager, E.; Hoenig, R.; Benetti, D.; Grosell, M.; Oris, J.; Roberts, A. Ultraviolet Radiation Enhances the Toxicity of Deepwater Horizon Oil to Mahi-Mahi (*Coryphaena Hippurus*) Embryos. *Environ. Sci. Technol.* **2016**, *50* (4), 2011–2017.

(7) Esbaugh, A. J.; Mager, E. M.; Stieglitz, J. D.; Hoenig, R.; Brown, T. L.; French, B. L.; Linbo, T. L.; Lay, C.; Forth, H.; Scholz, N. L.; et al. The Effects of Weathering and Chemical Dispersion on Deepwater Horizon Crude Oil Toxicity to Mahi-Mahi (*Coryphaena Hippurus*) Early Life Stages. *Sci. Total Environ.* **2016**, *543*, 644–651.

(8) Mager, E. M.; Esbaugh, A. J.; Stieglitz, J. D.; Hoenig, R.; Bodinier, C.; Incardona, J. P.; Scholz, N. L.; Benetti, D. D.; Grosell, M. Acute Embryonic or Juvenile Exposure to Deepwater Horizon Crude Oil Impairs the Swimming Performance of Mahi-Mahi (*Coryphaena Hippurus*). *Environ. Sci. Technol.* **2014**, *48* (12), 7053–7061.

(9) Pasparakis, C.; Mager, E. M.; Stieglitz, J. D.; Benetti, D.; Grosell, M. Effects of Deepwater Horizon Crude Oil Exposure, Temperature and Developmental Stage on Oxygen Consumption of Embryonic and Larval Mahi-Mahi (*Coryphaena Hippurus*). *Aquat. Toxicol.* **2016**, *181*, 113–123.

(10) Rooker, J. R.; Kitchens, L. L.; Dance, M. A.; Wells, R. J. D.; Falterman, B.; Cornic, M. Spatial, Temporal, and Habitat-Related Variation in Abundance of Pelagic Fishes in the Gulf of Mexico: Potential Implications of the Deepwater Horizon Oil Spill. *PLoS One* **2013**, *8* (10), 1–9.

(11) Stieglitz, J. D.; Mager, E. M.; Hoenig, R. H.; Benetti, D. D.; Grosell, M. Impacts of Deepwater Horizon Crude Oil Exposure on Adult Mahi-Mahi (*Coryphaena Hippurus*) Swim Performance. *Environ. Toxicol. Chem.* **2016**, *35* (10), 2613–2622.

(12) Sweet, L. E.; Magnuson, J.; Garner, T. R.; Alloy, M. M.; Stieglitz, J. D.; Benetti, D.; Grosell, M.; Roberts, A. P. Exposure to Ultraviolet Radiation Late in Development Increases the Toxicity of Oil to Mahi-Mahi (*Coryphaena Hippurus*) Embryos. *Environ.*

Toxicol. Chem. **2016**, 1–7.

(13) Xu, E. G.; Mager, E. M.; Grosell, M.; Pasparakis, C.; Schlenker, L. S.; Stieglitz, J. D.; Benetti, D.; Hazard, E. S.; Courtney, S. M.; Diamante, G.; et al. Time- and Oil-Dependent Transcriptomic and Physiological Responses to Deepwater Horizon Oil in Mahi-Mahi (*Coryphaena Hippurus*) Embryos and Larvae. *Environ. Sci. Technol.* **2016**, *50* (14), 7842–7851.

(14) Khursigara, A. J.; Perrichon, P.; Bautista, N. M.; Burggren, W. W.; Esbaugh, A. J. Cardiac Function and Survival Are Affected by Crude Oil in Larval Red Drum, *Sciaenops Ocellatus*. *Sci. Total Environ.* **2017**, *579*, 797–804.

(15) Xu, E. G.; Khursigara, A. J.; Magnuson, J.; Hazard, E. S.; Hardiman, G.; Esbaugh, A. J.; Roberts, A. P.; Schlenk, D. Larval Red Drum (*Sciaenops Ocellatus*) Sublethal Exposure to Weathered Deepwater Horizon Crude Oil: Developmental and Transcriptomic Consequences. *Environ. Sci. Technol.* **2017**, *51*, 10162–10172.

(16) Guthrie, D. M.; Muntz, W. R. A. Role of Vision in Fish Behaviour. In *The behaviour of teleost fishes*; Pitcher, T. J., Ed.; Springer: New York, 1986; pp 75–113.

(17) Blaxter, J. H. S. Development of Sense Organs and Behaviour of Teleost Larvae with Special Reference to Feeding and Predator Avoidance. *Trans. Am. Fish. Soc.* **1986**, *115*, 98–114.

(18) Incardona, J. P.; Collier, T. K.; Scholz, N. L. Defects in Cardiac Function Precede Morphological Abnormalities in Fish Embryos Exposed to Polycyclic Aromatic Hydrocarbons. *Toxicol. Appl. Pharmacol.* **2004**, *196* (2), 191–205.

(19) Jezierska, B.; Ługowska, K.; Witeska, M. The Effects of Heavy Metals on Embryonic Development of Fish (a Review). *Fish Physiol. Biochem.* **2009**, *35* (4), 625–640.

(20) Petersen, G. I.; Kristensen, P. Bioaccumulation of Lipophilic Substances in Fish Early Life Stages. *Environ. Toxicol. Chem.* **1998**, *17* (7), 1385–1395.

(21) Carvalho, P. S. M.; Noltie, D. B.; Tillitt, D. E. Ontogenetic Improvement of Visual Function in the Medaka *Oryzias Latipes* Based on an Optomotor Testing System for Larval and Adult Fish. *Anim. Behav.* **2002**, *64*, 1–10.

(22) Fuiman, L. A.; Delbos, B. C. Developmental Changes in Visual Sensitivity of Red Drum *Sciaenops Ocellatus*. *Copeia* **1998**, *1998* (4), 936–943.

(23) Muto, A.; Orger, M. B.; Wehman, A. M.; Smear, M. C.; Kay, J. N.; Page-McCaw, P. S.; Gahtan, E.; Xiao, T.; Nevin, L. M.; Gosse, N. J.; et al. Forward Genetic Analysis of Visual Behavior in Zebrafish. *PLoS Genet.* **2005**, *1* (5), 575–588.

(24) Orger, M. B.; Gahtan, E.; Muto, A.; Page-McCaw, P. S.; Smear, M. C.; Baier, H. Behavioral Screening Assays in Zebrafish. *Methods Cell Biol* **2004**, *77*, 53–68.

(25) Carton, A. G.; Vaughan, M. R. Behavioural and Anatomical Measures of Visual Acuity in First-Feeding Yellowtail Kingfish (*Seriola Lalandi*) Larvae. *Environ. Biol. Fishes* **2010**, *89* (1), 3–10.

(26) Job, S. D.; Bellwood, D. R. Visual Acuity and Feeding in Larval *Premnas Biaculeatus*. *J. Fish Biol.* **1996**, *48*, 952–963.

(27) Poling, K. R.; Fuiman, L. A. Sensory Development and Concurrent Behavioural Changes in Atlantic Croaker Larvae. *J. Fish Biol.* **1997**, *51*, 402–421.

(28) Hose, J. E.; McGurk, M. D.; Marty, G. D.; Hinton, D. E.; Brown, E. D.; Baker, T. T. Sublethal Effects of the Exxon Valdez Oil Spill on Herring Embyros and Larvae: Morphological, Cytogenetic, and Histopathological Assessments, 1989-1991. *Can. J. Fish. Aquat. Sci.* **1996**, *53* (10), 2355–2365.

(29) Carls, M. G.; Rice, S. D.; Hose, J. E. Sensitivity of Fish Embryos to Weathered Crude Oil: Part I. Low Level Exposure during Incubation Causes Malformations, Genetic Damage, and Mortality in Larval Pacific Herring (*Clupea Pallasi*). *Env. Toxicol Chem* **1999**, *18* (3), 481–493.

(30) Marty, G. D.; Hose, J. E.; McGurk, M. D.; Brown, E. D.; Hinton, D. E. Histopathology and Cytogenetic Evaluation of Pacific Herring Larvae Exposed to Petroleum Hydrocarbons in the Laboratory or in Prince William Sound, Alaska, after the Exxon Valdez Oil Spill. *Can. J. Fish. Aquat. Sci.* **1997**, *54* (8), 1846–1857.

(31) Hawkes, J. W.; Stehr, C. M. Cytopathology of the Brain and Retina of Embryonic Surf Smelt (*Hypomesus Pretiosus*) Exposed to Crude Oil. *Environ. Res.* **1982**, *27*, 164–178.

(32) Lønning, S. The Effects of Crude Ekofisk Oil and Oil Products on Marine Fish Larvae. *J. Arctiv Biol.* **1977**, *10* (1), 37–47.

(33) Rodrigues, R. V.; Miranda-Filho, K. C.; Gusmão, E. P.; Moreira, C. B.; Romano, L. A.; Sampaio, L. A. Deleterious Effects of Water-Soluble Fraction of Petroleum, Diesel and Gasoline on Marine Pejerrey *Odontesthes Argentinensis* Larvae. *Sci. Total Environ.* **2010**, *408* (9), 2054–2059.

(34) Payne, J. F.; Kiceniuk, J. W.; Squires, W. R. Pathological Changes in a Marine Fish after a 6-Month Exposure to Petroleum. *J. Fish. Res. Board Can.* **1978**, *35*, 665–667.

(35) Colavecchia, M. V.; Backus, S. M.; Hodson, P. V.; Parrott, J. L. Toxicity of Oil Sands to Early Life Stages of Fathead Minnows (*Pimephales Promelas*). *Environ. Toxicol.* **2004**, *23* (7), 1709–1718.

(36) Colavecchia, M. V.; Hodson, P. V.; Parrott, J. L. CYP1A Induction and Blue Sac Disease in Early Life Stages of White Suckers (*Catostomus Commersoni*) Exposed to Oil Sands. *J. Toxicol. Environ. Heal. Part A* **2006**, *69*, 967–994.

(37) Colavecchia, M. V.; Hodson, P. V.; Parrott, J. L. The Relationships among CYP1A

Induction, Toxicity, and Eye Pathology in Early Life Stages of Fish Exposed to Oil Sands. *J. Toxicol. Environ. Heal. Part A* **2007**, *70*, 1542–1555.

(38) Hargis, W. J. jr.; Roberts, M. H. jr.; Zwerner, D. E. Effects of Contaminanted Sediments and Sediment-Exposed Effluent Water on an Estuarine Fish: Acute Toxicity. *Mar. Environ. Res.* **1984**, *14*, 337–354.

(39) Hargis, W. J. jr.; Zwerner, D. E. Effects of Certain Contaminants on Eyes of Several Estuarine Fishes. *Mar. Environ. Res.* **1988**, *24*, 265–270.

(40) Hargis, W. J.; Zwerner, D. E. Some Effects of Sediment-Borne Contaminants on Development and Cytomorphology of Teleost Eye-Lens Epithelial Cells and Their Derivatives. *Mar. Environ. Res.* **1989**, *28*, 399–405.

(41) Hose, J. E.; Hannah, J. B.; Puffer, H. W.; Landolt, M. L. Histologic and Skeletal Abnormalities in Benzo(a)pyrene-Treated Rainbow Trout Alevins. *Arch. Environ. Contam. Toxicol.* **1984**, *13*, 675–684.

(42) Huang, L.; Zuo, Z.; Zhang, Y.; Wu, M.; Lin, J. J.; Wang, C. Use of Toxicogenomics to Predict the Potential Toxic Effect of Benzo(a)pyrene on Zebrafish Embryos: Ocular Developmental Toxicity. *Chemosphere* **2014**, *108*, 55–61.

(43) Williams, C. D.; Faisal, M.; Huggett, R. J. Polynuclear Aromatic Hydrocarbons and Fish Lens Cataract: Effects of Benzo[a]pyrene-7,8-Dihydordiol on the Macromolecular Synthesis of Cultured Eye Cells. *Mar. Environ. Res.* **1992**, *34*, 333–337.

(44) Laycock, N. L. C.; Schirmer, K.; Bols, N. C.; Sivak, J. G. Optical Properties of Rainbow Trout Lenses after in Vitro Exposure to Polycyclic Aromatic Hydrocarbons in the Presence or Absence of Ultraviolet Radiation. *Exp. Eye Res.* **2000**, *70*, 205–214.

(45) Whyte, J. J.; Herbert, K. L.; Karrow, N. A.; Dixon, D. G.; Sivak, J. G.; Bols, N. C. Effect of Maintaining Rainbow Trout in Creosote Microcosms on Lens Optical Properties and Liver 7-Ethoxyresorufin-O-Deethylase (EROD) Activity. *Arch. Environ. Contam. Toxicol.* **2000**, *38* (3), 350–356.

(46) Huang, L.; Wang, C.; Zhang, Y.; Wu, M.; Zuo, Z. Phenanthrene Causes Ocular Developmental Toxicity in Zebrafish Embryos and the Possible Mechanisms Involved. *J. Hazard. Mater.* **2013**, *261*, 172–180.

(47) Carvalho, P. S. M.; Kalil, D. da C. B.; Novelli, G. A. A.; Bainy, A. C. D.; Fraga, A. P. M. Effects of Naphthalene and Phenanthrene on Visual and Prey Capture Endpoints during Early Stages of the Dourado *Salminus Brasiliensis*. *Mar. Environ. Res.* **2008**, *66* (1), 205–207.

(48) Carvalho, P. S. M.; Tillitt, D. E. 2,3,7,8-TCDD Effects on Visual Structure and Function in Swim-up Rainbow Trout. *Environ. Sci. Technol.* **2004**, *38* (23), 6300–6306.

(49) Diamante, G.; Xu, E. G.; Chen, S.; Mager, E.; Grosell, M.; Schlenk, D. Differential

Expression of MicroRNAs in Embryos and Larvae of Mahi-Mahi (Coryphaena Hippurus) Exposed to Deepwater Horizon Oil. *Environ. Sci. Technol. Lett.* **2017**, *4*, 523–529.

(50) Shen, Y.; Raymond, P. A. Zebrafish Cone-Rod (Crx) Homeobox Gene Promotes Retinogenesis. *Dev. Biol.* **2004**, *269*, 237–251.

(51) Benetti, D. D.; Iversen, E. S.; Ostrowski, A. C. Growth Rates of Captive Dolphin, *Coryphaena Hippurus*, in Hawaii. *Fish. Bull.* **1995**, *93*, 152–157.

(52) Massutí, E.; Deudero, S.; Sánchez, P.; Morales-Nin, B. Diet and Feeding of Dolphin (*Coryphaena Hippurus*) in Western Mediterranean Waters. *Bull. Mar. Sci.* **1998**, *63* (2), 329–341.

(53) Rotschild, B. J. Observations on Dolphins (*Coryphaena* Spp.) in the Central Pacific Ocean. *Copeia* **1964**, *1964* (2), 445–447.

(54) Nelson, P. A.; Zamzow, J. P.; Losey, G. S. Ultraviolet Blocking in the Ocular Humors of the Teleost Fish *Acanthocybium Solandri* (Scombridae). *Can. J. Zool.* **2001**, *79* (9), 1714–1718.

(55) Palko, B. J.; Beardsley, G. L.; Richards, W. J. *Synopsis of the Biological Data on Dolphin-Fishes*, Coryphaena Hippurus *Linnaeus and* Coryphaena Equiselis *Linnaeus.*; 1982; Vol. 130.

(56) Munz, F. W.; McFarland, W. N. Part I: Presumptive Cone Pigments Extracted from Tropical Marine Fishes. *Vis. Res.* **1975**, *15*, 1045–1062.

(57) Kröger, R. H. H.; Fritsches, K. A.; Warrant, E. J. Lens Optical Properties in the Eyes of Large Marine Predatory Teleosts. *J. Comp. Physiol. A* **2009**, *195* (2), 175–182.

(58) Tamura, T.; Wisby, W. J. The Visual Sense of Pelagic Fishes Especially the Visual Axis and Accommodation. *Bull. Mar. Sci. Gulf Caribb.* **1963**, *13*, 433–448.

(59) McFarland, W. N.; Munz, F. W. Part III: The Evolution of Photopic Visual Pigments in Fishes. *Vis. Res.* **1975**, *15*, 1071–1080.

(60) Neave, D. A. The Development of Visual Acuity in Larval Plaice (*Pleuronectes Platessa* L.) and Turbot (*Scophthalmus Maximus* L.). *J. Exp. Mar. Biol. Ecol.* **1984**, *78*, 167–175.

(61) Kraul, S.; Brittain, K.; Cantrell, R.; Nagao, T. Nutritional Factors Affecting Stress Resistance in the Larval Mahimahi *Coryphaena Hippurus*. *J. World Aquac. Soc.* **1993**, *24* (2), 186–193.

(62) Benetti, D. D.; Orhun, M. R.; Sardenberg, B.; O'Hanlon, B.; Welch, A.; Hoenig, R.; Zink, I.; Rivera, J. A.; Denlinger, B.; Bacoat, D.; et al. Advances in Hatchery and Grow-out Technology of Cobia *Rachycentron Canadum* (Linnaeus). *Aquac. Res.* **2008**, *39* (7), 701–711.

(63) Kloeblen, S.; Stieglitz, J. D.; Suarez, J. A.; Grosell, M.; Benetti, D. D. Characterizing Egg Quality and Larval Performance from Captive Mahi-Mahi *Coryphaena Hippurus* (Linnaeus, 1758) Spawns over Time. *Aquac. Res.* **2018**, *49* (1), 282–293.

(64) Pankhurst, P. M. Age-Related Changes in the Visual Acuity of Larvae of New Zealand Snapper, *Pagrus Auratus*. *J. Mar. Biol. Ass. U.K.* **1994**, *74*, 337–349.

(65) Miller, T. J.; Crowder, L. B.; Rice, J. A. Ontogenetic Changes in Behavioural and Histological Measures of Visual Acuity in Three Species of Fish. *Environ. Biol. fishes* **1993**, *37*, 1–8.

(66) Blaxter, J. H. S.; Jones, M. P. The Development of the Retina and Retinomotor Responses in the Herring. *J. Mar. Biol.* **1967**, *47*, 677–697.

(67) Hilder, P. I. Development of Vision and Larval Feeding Responses in Southern Bluefin Tuna and Yellowtail Kingfish, University of Tasmania (Doctoral dissertation), 2013.

(68) Kotrschal, K.; Adam, H.; Brandstätter, R.; Junger, H.; Zaunreiter, M.; Goldschmid, A. Larval Size Constraints Determine Directional Ontogenetic Shifts in the Visual System of Teleosts. *Z. Zool. Syst. Evol.* **1990**, *28*, 166–182.

(69) Johns, P. R. Formation of Photoreceptors in Larval and Adult Goldfish. *J Neurosci* **1982**, *2* (2), 178–198.

(70) Flamarique, N. I.; Hawryshyn, C. W. Retinal Development and Visual Sensitivity of Young Pacific Sockeye Salmon (*Oncorhynchus Nerka*). *J. Exp. Biol.* **1996**, *199*, 869–882.

(71) Lyon, E. P. On Rheotropism. I.- Rheotropism in Fishes. *Am. J. Physiol.* **1904**, *12* (2), 149–161.

(72) Easter, S. S. Pursuit Eye Movements in Goldfish (*Carassius Auratus*). *Vision Res.* **1972**, *12* (1968), 673–688.

(73) Job, S. D.; Bellwood, D. R. Light Sensitivity in Larval Fishes: Implications for Vertical Zonation in the Pelagic Zone. *Limnol. Oceanogr.* **2000**, *45* (2), 362–371.

(74) Hylland, K. Polycyclic Aromatic Hydrocarbon (PAH) Ecotoxicology in Marine Ecosystems. *J. Toxicol. Environ. Health. A* **2006**, *69* (1–2), 109–123.

(75) Diamante, G.; Müller, S.; Menjivar-cervantes, N.; Genbo, E.; Volz, D. C.; Celso, A.; Bainy, D.; Schlenk, D. Developmental Toxicity of Hydroxylated Chrysene Metabolites in Zebrafish Embryos. *Aquat. Toxicol.* **2017**, *189* (June), 77–86.

(76) Liu, Z.; Liu, J.; Zhu, Q.; Wu, W. The Weathering of Oil after the Deepwater Horizon Oil Spill: Insights from the Chemical Composition of the Oil from the Sea Surface, Salt Marshes and Sediments. *Environ. Res. Lett.* **2012**, *7* (3), 35302.

(77) Pattillo, M. E.; Czapla, T. E.; Nelson, D. M.; Monaco, M. E. *Distribution and Abundance of Fishes and Invertebrates in Gulf of Mexico Estuaries, Volume II: Species Life History Summaries*; 1997; Vol. 11.

(78) Rooker, J. R.; Holt, S. A. Utilization of Subtropical Seagrass Meadows by Newly Settled Red Drum Sciaenops Ocellatus:patterns of Distribution and Growth. *Mar. Ecol. Prog. Ser.* **1997**, *158*, 139–149.

(79) Holt, S. A.; Kitting, C. L.; Arnold, C. R. Distribution of Young Red Drums among Different Sea-Grass Meadows. *Trans. Am. Fish. Soc.* **1983**, *112*, 267–271.

(80) Moreau, C. J.; Klerks, P. L.; Haas, C. N. Interaction between Phenanthrene and Zinc in Their Toxicity to the Sheepshead Minnow (*Cyprinodon Variegatus*). *Arch. Environ. Contam. Toxicol.* **1999**, *37* (2), 251–257.

(81) Jonsson, G.; Bechmann, R. K.; Bamber, S. D.; Baussant, T. Bioconcentration, Biotransformation, and Elimination of Polycyclic Aromatic Hydrocarbons in Sheepshead Minnows (*Cyprinodon Variegatus*) Exposed to Contaminated Seawater. *Environ. Toxicol. Chem.* **2004**, *23* (6), 1538–1548.

(82) Hawkins, W. E.; Walker, W. W.; Lytle, T. F.; Lytle, J. S.; Overstreet, R. M. Studies on the Carcinogenic Effects of Benzo(a)pyrene and 7,12-Dimethylbenz(a)anthracene on the Sheepshead Minnow (*Cyprinodon Variegatus*). *Aquat. Toxicol. Risk Assess.* **1991**, *14*, 97–104.

(83) Adams, G. G.; Klerks, P. L.; Belanger, S. E.; Dantin, D. The Effect of the Oil Dispersant Omni-Clean® on the Toxicity of Fuel Oil No. 2 in Two Bioassays with the Sheepshead Minnow *Cyprinodon Variegatus*. *Chemosphere* **1999**, *39* (12), 2141–2157.

(84) Finch, B. E.; Stubblefield, W. A. Photo-Enhanced Toxicity of Fluoranthene to Gulf of Mexico Marine Organisms at Different Larval Ages and Ultraviolet Light Intensities. *Environ. Toxicol. Chem.* **2016**, *35* (5), 1113–1122.

(85) Richards, F. M.; Alderton, W. K.; Kimber, G. M.; Liu, Z.; Strang, I.; Redfern, W. S.; Valentin, J.; Winter, M. J.; Hutchinson, T. H. Validation of the Use of Zebrafish Larvae in Visual Safety Assessment. *J. Pharmacol. Toxicol. Methods* **2008**, *58*, 50–58.

(86) Alloy, M. M.; Boube, I.; Griffitt, R. J.; Oris, J. T.; Roberts, A. P. Photo-Induced Toxicity of Deepwater Horizon Slick Oil to Blue Crab (*Callinectes Sapidus*) Larvae. *Environ. Toxicol. Chem.* **2015**, *34* (9), 2061–2066.

(87) Diercks, A. R.; Highsmith, R. C.; Asper, V. L.; Joung, D.; Zhou, Z.; Guo, L.; Shiller, A. M.; Joye, S. B.; Teske, A. P.; Guinasso, N.; et al. Characterization of Subsurface Polycyclic Aromatic Hydrocarbons at the Deepwater Horizon Site. *Geophys. Res. Lett.* **2010**, *37* (20), 1–6.

(88) Glover, C. N.; Bucking, C.; Wood, C. M. The Skin of Fish as a Transport Epithelium: A Review. *J. Comp. Physiol. B Biochem. Syst. Environ. Physiol.* **2013**, *183* (7), 877–891.

(89) Salem, M. A. Structure and Function of the Retinal Pigment Epithelium, Photoreceptors and Cornea in the Eye of *Sardinella Aurita* (Clupeidae, Teleostei). *J. Basic Appl. Zool.* **2016**, *75*, 1–12.

(90) Teo, S. L. H.; Block, B. A. Comparative Influence of Ocean Conditions on Yellowfin and Atlantic Bluefin Tuna Catch from Longlines in the Gulf of Mexico. *PLoS One* **2010**, *5* (5).

(91) Muhling, B. A.; Roffer, M. A.; Lamkin, J. T.; Ingram, G. W.; Upton, M. A.; Gawlikowski, G.; Muller-Karger, F.; Habtes, S.; Richards, W. J. Overlap between Atlantic Bluefin Tuna Spawning Grounds and Observed Deepwater Horizon Surface Oil in the Northern Gulf of Mexico. *Mar. Pollut. Bull.* **2012**, *64* (4), 679–687.

(92) *Deepwater Horizon Natural Resource Damage Assessment Trustees. (2016).* Deepwater Horizon Oil Spill: Final Programmatic Damage Assessment and Restoration Plan and Final Programmatic Environmental Impact Statement. *Retrieved from Http://www.gulfspill*.

(93) Mager, E. M.; Pasparakis, C.; Schlenker, L. S.; Yao, Z.; Bodinier, C.; Stieglitz, J. D.; Hoenig, R.; Morris, J. M.; Benetti, D. D.; Grosell, M. Assessment of Early Life Stage Mahi-Mahi Windows of Sensitivity during Acute Exposures to *Deepwater Horizon* Crude Oil. *Environ. Toxicol. Chem.* **2017**, *36* (7), 1887–1895.

(94) Edmunds, R. C.; Gill, J. A.; Baldwin, D. H.; Linbo, T. L.; French, B. L.; Brown, T. L.; Esbaugh, A. J.; Mager, E. M.; Stieglitz, J.; Hoenig, R.; et al. Corresponding Morphological and Molecular Indicators of Crude Oil Toxicity to the Developing Hearts of Mahi Mahi. *Sci. Rep.* **2015**, *5* (October), 1–18.

(95) Huang, L.; Xi, Z.; Wang, C.; Zhang, Y.; Yang, Z.; Zhang, S.; Chen, Y.; Zuo, Z. Phenanthrene Exposure Induces Cardiac Hypertrophy via Reducing miR-133a Expression by DNA Methylation. *Sci. Rep.* **2016**, *6*, 20105.

(96) Bianchi, M.; Renzini, A.; Adamo, S.; Moresi, V. Coordinated Actions of MicroRNAs with Other Epigenetic Factors Regulate Skeletal Muscle Development and Adaptation. *Int. J. Mol. Sci.* **2017**, *18* (4), 840.

(97) Goodson, J. M.; Weldy, C. S.; Macdonald, J. W.; Liu, Y.; Bammler, T. K.; Chien, W.; Chin, M. T. In Utero Exposure to Diesel Exhaust Particulates Is Associated with an Altered Cardiac Transcriptional Response to Transverse Aortic Constriction and Altered DNA Methylation. *FASEB J.* **2017**, *31*, 4935–4945.

(98) Xu, E. G.; Mager, E. M.; Grosell, M.; Hazard, E. S.; Hardiman, G.; Schlenk, D. Novel Transcriptome Assembly and Comparative Toxicity Pathway Analysis in Mahi-Mahi (*Coryphaena Hippurus*) Embryos and Larvae Exposed to Deepwater Horizon Oil. *Sci. Rep.* **2017**, *7*, 44546.

(99) Wu, J.; Bao, J.; Kim, M.; Yuan, S.; Tang, C.; Zheng, H.; Mastick, G. S. Two miRNA Clusters, *miR-34b/c* and *miR-499*, Are Essential for Normal Brain Development, Motile

Ciliogenesis, and Spermatogenesis. *PNAS* **2014**, *111* (28E2851-2857).

(100) Bhattacharya, M.; Sharma, A. R.; Sharma, G.; Patra, B. C.; Nam, J.; Chakraborty, C.; Lee, S.-S. The Crucial Role and Regulations of miRNAs in Zebrafish Development. *Protoplasma* **2017**, *254*, 17–31.

(101) Biyashev, D.; Veliceasa, D.; Topczewski, J.; Topczewska, J. M.; Mizgirev, I.; Vinokour, E.; Reddi, A. L.; Licht, J. D.; Revskoy, S. Y.; Volpert, O. V. miR-27b Controls Venous Specification and Tip Cell Fate. *Blood* **2012**, *119* (11), 2679–2688.

(102) Wilson, K. D.; Hu, S.; Venkatasubrahmanyam, S.; Fu, J.; Sun, N.; Abilez, O. J.; Baugh, J. J. A.; Jia, F.; Ghosh, Z.; Li, R. A.; et al. Dynamic microRNA Expression Programs during Cardiac Differentiation of Human Embryonic Stem Cells: Role for miR-499. *Circ. Cardiovasc. Genet.* **2010**, *3*, 426–435.

(103) Incardona, J. P.; Scholz, N. L. The Influence of Heart Developmental Anatomy on Cardiotoxicity-Based Adverse Outcome Pathways in Fish. *Aquat. Toxicol.* **2016**, *177*, 515–525.

(104) Sørhus, E.; Incardona, J. P.; Karlsen, Ø.; Linbo, T.; Sørensen, L.; Nordtug, T.; Meeren, T. Van Der; Thorsen, A.; Thorbjørnsen, M.; Jentoft, S.; et al. Crude Oil Exposures Reveal Roles for Intracellular Calcium Cycling in Haddock Craniofacial and Cardiac Development. *Sci. Rep.* **2016**, *6*.

(105) Wang, L.; Fu, C.; Fan, H.; Du, T.; Dong, M.; Chen, Y.; Jin, Y.; Zhou, Y.; Deng, M.; Gu, A.; et al. miR-34b Regulates Multiciliogenesis during Organ Formation in Zebrafish. *Development* **2013**, *140* (13), 2755–2764.

(106) Kapsimali, M.; Kloosterman, W. P.; de Bruijn, E.; Rosa, F.; Plasterk, R. H. A.; Wilson, S. W. MicroRNAs Show a Wide Diversity of Expression Profiles in the Developing and Mature Central Nervous System. *Genome Biol.* **2007**, *8* (8), R173.

(107) Bommer, G. T.; Gerin, I.; Feng, Y.; Kaczorowski, A. J.; Kuick, R.; Love, R. E.; Zhai, Y.; Giordano, T. J.; Qin, Z. S.; Moore, B. B.; et al. p53-Mediated Activation of miRNA34 Candidate Tumor-Suppressor Genes. *Curr. Biol.* **2007**, *17* (15), 1298–1307.

(108) Wienholds, E.; Kloosterman, W. P.; Miska, E.; Alvarez-Saavedra, E. MicroRNA Expression in Zebrafish Embryonic Development. *Science (80-.).* **2005**, *309*, 310–311.

(109) Carrella, S.; D'Agostino, Y.; Barbato, S.; Huber-Reggi, S. P.; Salierno, F. G.; Manfredi, A.; Neuhauss, S. C. F.; Banfi, S.; Conte, I. miR-181a/b Control the Assembly of Visual Circuitry by Regulating Retinal Axon Specification and Growth. *Dev. Neurobiol.* **2015**, *75* (11), 1252–1267.

(110) Zhou, Q.; Gallagher, R.; Ufret-vincenty, R.; Li, X.; Olson, E. N.; Wang, S. Regulation of Angiogenesis and Choroidal Neovascularization by Members of microRNA-23~27~24 Clusters. *PNAS* **2011**, *108* (20), 8287–8292.

(111) Agrawal, S.; Chaqour, B. MicroRNA Signature and Function in Retinal Neovascularization. *World J Biol Chem* **2014**, *5* (1), 1–11.

(112) Rajaram, K.; Harding, R. L.; Hyde, D. R.; Patton, J. G. miR-203 Regulates Progenitor Cell Proliferation during Adult Zebra Fish Retina Regeneration. *Dev. Biol.* **2014**, *392* (2), 393–403.

(113) Kohl, S.; Baumann, B.; Rosenberg, T.; Kellner, U.; Lorenz, B.; Jacobson, S. G.; Wissinger, B. Mutations in the Cone Photoreceptor G-Protein a -Subunit Gene GNAT2 in Patients with Achromatopsia. *Am. J. Hum. Genet.* **2002**, *71*, 422–425.

(114) Cai, K.; Itoh, Y.; Khorana, H. G. Mapping of Contact Sites in Complex Formation between Transducin and Light-Activated Rhodopsin by Covalent Crosslinking : Use of a Photoactivatable Reagent. *PNAS* **2001**, *98* (9), 4877–4882.

(115) Bringmann, A.; Pannicke, T.; Grosche, J.; Francke, M.; Wiedemann, P.; Skatchkov, S. N.; Osborne, N. N.; Reichenbach, A. Müller Cells in the Healthy and Diseased Retina. *Prog. Retin. Eye Res.* **2006**, *25*, 397–424.

(116) Westerfield, M. *The Zebrafish Book: A Guide for the Laboratory Use of Zebrafish (*Danio Rerio, 5th ed.; University of Oregon Press, 2007.

(117) Spence, R.; Gerlach, G.; Lawrence, C.; Smith, C. The Behaviour and Ecology of the Zebrafish, *Danio Rerio*. *Bio. Rev.* **2008**, *83*, 13–34.

(118) Pfaffl, M. W. *A New Mathematical Model for Relative Quantification in Real-Time RT–PCR*; 2001; Vol. 29.

(119) Blaxter, J. H. S. *The Eyes of Larval Fish. In: Vision in Fishes*, 1st ed.; Ali, M. A., Ed.; Plenum, New York, 1974.

(120) Schonthaler, H. B.; Lampert, J. M.; Isken, A.; Rinner, O.; Mader, A.; Gesemann, M.; Oberhauser, V.; Golczak, M.; Palczewski, K.; Neuhauss, S. C. F.; et al. Evidence for RPE65-Independent Vision in the Cone-Dominated Zebrafish Retina. *Eur. J. Neurosci.* **2007**, *26* (7), 1940–1949.

(121) Huang, L.; Zuo, Z.; Zhang, Y.; Wu, M.; Lin, J. J.; Wang, C. Use of Toxicogenomics to Predict the Potential Toxic Effect of Benzo(a)pyrene on Zebrafish Embryos: Ocular Developmental Toxicity. *Chemosphere* **2014**, *108*, 55–61.

(122) Billiard, S. M.; Hahn, M. E.; Franks, D. G.; Peterson, R. E.; Bols, N. C.; Hodson, P. V. Binding of Polycyclic Aromatic Hydrocarbons (PAHs) to Teleost Aryl Hydrocarbon Receptors (AHRs). *Comp. Biochem. Physiol. - B Biochem. Mol. Biol.* **2002**, *133* (1), 55–68.

(123) Aluru, N.; Jenny, M. J.; Hahn, M. E. Knockdown of a Zebrafish Aryl Hydrocarbon Receptor Repressor (AHRRa) Affects Expression of Genes Related to Photoreceptor Development and Hematopoiesis. *Toxicol. Sci.* **2014**, *139* (2), 381–395.

(124) Laranjeiro, R.; Whitmore, D. Transcription Factors Involved in Retinogenesis Are Co-Opted by the Circadian Clock Following Photoreceptor Differentiation. *Development* **2014**, *141*, 1–13.

(125) Peterson, R. E.; Fadool, J. M.; McClintock, J.; Linser, P. J. Müller Cell Differentiation in the Zebrafish Neural Retina: Evidence of Distinct Early and Late Stages in Cell Maturation. *J. Comp. Neurol.* **2001**, *429*, 530–540.

(126) Redmond, L.; Kashani, A. H.; Ghosh, A. Calcium Regulation of Dendritic Growth via CaM Kinase IV and CREB-Mediated Transcription. *Neuron* **2002**, *34*, 999–1010.

(127) Ramachandran, R.; Fausett, B. V; Goldman, D. Ascl1a Regulates Müller Glia Dedifferentiation and Retinal Regeneration through a Lin-28-Dependent, *Let-7* microRNA Signalling Pathway. *Nat. Cell Biol.* **2010**, *12* (11), 1101–1107.

(128) Easter, S. S.; Nicola, G. N. The Development of Vision in the Zebrafish (*Danio Rerio*). *Dev. Biol.* **1996**, *180* (2), 646–663.

(129) Brockerhoff, S. E.; Hurley, J. B.; Janssen-Bienhold, U.; Neuhauss, S. C.; Driever, W.; Dowling, J. E. A Behavioral Screen for Isolating Zebrafish Mutants with Visual System Defects. *Proc. Natl. Acad. Sci.* **1995**, *92* (23), 10545–10549.

(130) Makhankov, Y. V.; Rinner, O.; Neuhauss, S. C. F. An Inexpensive Device for Non-Invasive Electroretinography in Small Aquatic Vertebrates. *J. Neurosci. Methods* **2004**, *135* (1–2), 205–210.

(131) Freund, C. L.; Gregory-evans, C. Y.; Furukawa, T.; Papaioannou, M.; Looser, J.; Ploder, L.; Bellingham, J.; Ng, D.; Herbrick, J. S.; Duncan, A.; et al. Cone-Rod Dystrophy Due to Mutations in a Novel Photoreceptor-Specific Homeobox Gene (CRX) Essential for Maintenance of the Photoreceptor. *Cell* **1997**, *91*, 543–553.

CHAPTER 2

DEVELOPMENT OF THE OPTOMOTOR RESPONSE IN LARVAL MAHI-MAHI (*Coryphaena hippurus*)

2.1 Introduction

The visual capability of fishes at different life-stages is an underlying factor for growth and survival in teleosts [1]. Many marine pelagic embryos hatch in photopic (well-lit) conditions where they rely on pure cone retinas to aid in their ability to feed [2]. A majority of studies pertaining to the visual ability of fishes are focused on juveniles and adults with a limited number of studies that have looked at visual development in early life-stages. Improvements in aquaculture techniques allow for the study of larvae of appropriate age and health of what may otherwise be difficult to obtain. Visual development in early life-stage larvae happens rapidly, as retinal growth is related to overall size [3]. This is especially important in mahi-mahi, as their growth rate is one of the fastest among teleosts [4].

Mahi-mahi are opportunistic predators that utilize vision as an important component of their diel feeding behavior [5]. Though capable of feeding during moonlit nights [6], mahi-mahi predominately forage in epipelagic regions during the day [5,7], preying on fish and crustaceans associated with *Sargassum* mats [8]. This is reflected in the reduced ability to capture prey during scotopic (light-limiting) conditions [5], as mahi-mahi are associated with photopic feeding [9,10]. Prior work conducted on mahi-mahi vision has solely focused on juvenile and adult stages [9–12], with visual characterization lacking during early life-stage development.

Optomotor responses have been used as a common behavioral test to assess visual development in fishes [3,13–16]. Optomotor responses focus on the ability of a fish to orient its body in the same direction as a designated stimulus, opposed to an optokinetic response, where a fish

solely moves its eyes in the same direction as a stimulus. Use of this behavioral endpoint has been successful in determining visual function of several fish species from freshwater and marine systems alike [3,13,17–19], though current research on early life-stage marine pelagic larvae is lacking.

The objectives of this work were: 1) to measure the visual capabilities of larval mahi-mahi through optomotor behavioral assays, and 2) to see how these behavioral changes related to retinal morphological differences. Through combining both behavioral and morphometric results, we are better able to assess visual ability in early life-stage mahi-mahi.

2.2 Methods

2.2.1 Fish Larvae

Mahi-mahi embryos were obtained from spawning wild mahi-mahi broodstock maintained in captivity at the University of Miami Experimental Hatchery - Rosenstiel School of Marine and Atmospheric Science. Larvae were reared in 2.4 m^3 cylindrical fiberglass tanks equipped with aeration, supplemental oxygen, and flowing UV-sterilized seawater. Following hatching and yolk-sac absorption in the larvae, microalgae paste was added to the rearing water throughout the day to maintain low concentrations (~250,000 *Nannochloropsis* cells/mL) in the tank. Larval rearing protocols utilized in this study were similar to those reported by Kraul et al. (1993) and Benetti et al. (2008) for mahi-mahi and cobia (*Rachycentron canadum*), respectively. Mahi-mahi embryo quality remains consistently high for months of broodstock captivity [22]. In summary, the larvae were fed enriched rotifers (*Brachionus plicatilis*) 4-6 times daily using pulse feeding techniques. Beginning on 7 days post hatch (dph), larvae were co-fed rotifers and *Artemia nauplii* until 10 dph, after which the mahi-mahi larvae were pulse-fed enriched *Artemia*

nauplii. Water exchange rates ranged from 1000-1800% during the rearing period and tanks were routinely siphoned to remove negatively buoyant organic matter from the tank bottom.

2.2.2 Behavioral Assay

Larvae were placed in a closed bottom glass cylinder (inner diameter=20.82 mm) with an opaque bottom. A larger PVC cylinder (inner diameter=39.30 mm) was placed around the fixed glass cylinder where vertical, alternating black and white stripes (4 mm diameter) were adhered to the side. The glass cylinder sat on a clear Plexiglas disc to ensure the cylinder bottom was equidistant from the rotating stripes. The outer cylinder was driven by a 100 rpm motor with capabilities of being rotated both clock- and counter-clockwise. A potentiometer was used to control rotation speed, with speeds ranging from 6.6 rotations/min to 29.8 rotations/min. The only illumination provided to the system originated from the bottom of the chamber where light was emitted at 343lx (log I=2.54) through a clear Plexiglas disc onto the outer, rotating cylinder. Larvae were transferred to the chamber with a wide-mouth transfer pipette to help reduce stress. To view the larvae's behavior in the chamber, a GoPro Hero 4+ (San Mateo, California) was oriented above the rotating chamber where larval movement was recorded from first placement of the larvae into the chamber during acclimation until the behavioral assay was finished.

Fish larvae were acclimated in the chamber for one minute before assessing the optomotor response. One minute was chosen as an appropriate acclimation period based on preliminary data, as a greater period of time did not exhibit a change in normal swimming behavior (swimming around the chamber with short bursts opposed to irregular behavior, with sporadic swimming in fast circular motions). During the acclimation period the outer stripes were illuminated but not rotating. Once the larvae was acclimated, the outer cylinder was rotated

at an acuity visual angle of 11.4° from the center and at 22° from the outermost wall on the inner chamber to the plane of the rotating cylinder, and remained at a speed of 7.1 rotations/min until the larvae was able to follow in the same direction as the rotating stripes. The speed of the stripes was incrementally increased until the fish was no longer able to follow in the same direction as the stripes. At this point, the direction of the stripes was changed, and the same behavioral endpoints were recorded. In order for a larvae to be considered tracking, the larvae had to follow the stripes in both directions in an allotted three-minute time span. The starting direction of the stripes was alternated between larvae to avoid bias. The rotational speed of the stripes at which the larvae could no longer track was used as a threshold of developmental visual function.

Developmental periods used in this study were contingent upon certain limitations in working with early life-stage mahi-mahi. Larvae younger than 7 dph could not exhibit a consistent optomotor response, and therefore were not reflected in this study. Also, larvae older than 10 dph became too stressed while transferring into the behavioral assay, and would fail to acclimate to the chamber. No further ages were used due to sensitivity of larvae passed the developmental window where increased eye development is predominantly seen.

2.2.3 Histological Analysis

Larval mahi-mahi were fixed in Bouin's Solution for 24 hours, following completion of the behavioral assay, and stored in 70% ethanol. The larvae were subsequently dehydrated through a series of ethanol solutions and embedded in paraffin blocks with 5 µm sections made of the left eye. The sections were placed on poly-L-lysine coated slides and stained with hematoxylin and eosin. The whole retina (WR), lens (L), ganglion (G), inner plexiform (IP), inner nuclear (IN), outer plexiform (OP), outer nuclear (ON), photoreceptor layer (PL), and

pigmented epithelium (PE) (Figure 2.1) were imaged with an axio imager A1 Zeiss compound microscope (200x) and the diameter and area of each of these layers were measured using ImageJ (Version 1.47). The diameter of each layer was measured from the point where the lens diameter was largest across all layers examined. Further, the photoreceptor and ganglion cell densities were determined by counting photoreceptor and ganglion cells in a 100 µm transect along the central retina, as previously demonstrated [23] in larval fish with constraints imposed by small eye size and retinal curvature. A summation ratio (photoreceptor density/ganglion density) was used as a measure of assessing photoreceptor attachments to ganglion cells, with a value greater than 1.0 indicating multiple photoreceptors attaching to a single ganglion [3]. Anatomical determination of visual acuity was expressed as the minimum separable angle (α) [16], calculated as:

$$\alpha = \arcsin (1.11/ (10d \times F))$$

where d represents the number of cones per 100 µm of retina and F represents the focal length of the eye, which is estimated by multiplying the lens radius by 2.55 (Matthiessen's ratio).

2.2.4 Statistical Analysis

SPSS (version 20, Armonk, New York) was used to perform one-way ANOVA to assess differences in optomotor response between different age groups, as well as differences in morphological parameters (diameter and area of retinal layers, photoreceptor density, ganglion density, summation ratios, and anatomical visual acuity). Bonferroni post hoc multiple comparison tests were performed to determine if these parameters differed depending on age. Statistical significance was evaluated at alpha<0.05.

2.3 Results

2.3.1 Behavioral Analysis

A total of 90 larval mahi-mahi obtained from two sampling periods (October 2016) ranging from 7 to 10 dph were tested for an optomotor response. Of the 90 larvae tested, 79 acclimated to the chamber and were assessed in the behavioral assay. By the time larvae were 10 dph, only 10% of the larvae swam did not acclimate to the chamber, compared to 21% of the larvae at 7 dph. Mean tracking speeds ranged from 11, 15, 18, and 19 rotations/min in 7, 8, 9, and 10 dph larvae. There were significant increases in the ability of mahi-mahi to track at higher speeds at 9 ($p=0.047$) and 10 dph ($p=0.010$), relative to 7 dph, with an increase in average tracking speed by 42% between 7 and 10 dph (Figure 2.2).

2.3.2 Histological Analysis

A total of 41 larval mahi-mahi ranging from 7 to 10 dph were analyzed. Diameters of the whole retina ($p<0.001$), lens ($p=0.001$), outer nuclear layer ($p=0.029$), and photoreceptor layer ($p=0.042$) significantly increased with age, with the greatest increase from 7 to 10 dph larvae for each layer (20, 20, 31, and 22 %, respectively; Figure 2.3). There were no significant differences in the ganglion layer ($p=0.493$), inner plexiform layer ($p=0.068$), inner nuclear layer ($p=0.238$), outer plexiform layer ($p=0.260$), or pigmented epithelial layer ($p=0.789$) diameters (Figure 2.3).

The area of the whole retina ($p<0.001$), lens ($p<0.001$), ganglion layer ($p<0.001$), inner nuclear layer ($p<0.001$), outer plexiform layer ($p=0.003$), outer nuclear layer ($p<0.001$), and photoreceptor layer ($p<0.001$) significantly increased with age, with the greatest increase from 7 to 10 dph larvae for each layer (39, 37, 40, 35, 27, 38, and 37 %, respectively; Figure 2.4), with the inner plexiform area only significantly increasing in 7 to 10 dph ($p=0.048$) larvae. The

pigmented epithelial layer did not significantly differ in area from 7 to 10 dph (p=0.691; Figure 2.3).

There was a significantly lower visual acuity in larvae from 7 to 10 dph (p=0.005), from 0.99° to 0.77°, which is common among early life-stage larvae (Table 2.1). However, there were no significant differences in ganglion density (p=0.415), cone density (p=0.683), or photoreceptor density/ganglion density summation ratio (p=0.091) in larvae from 7 to 10 dph, though all mean summation ratios were >1 at all larval stages examined (Table 2.2).

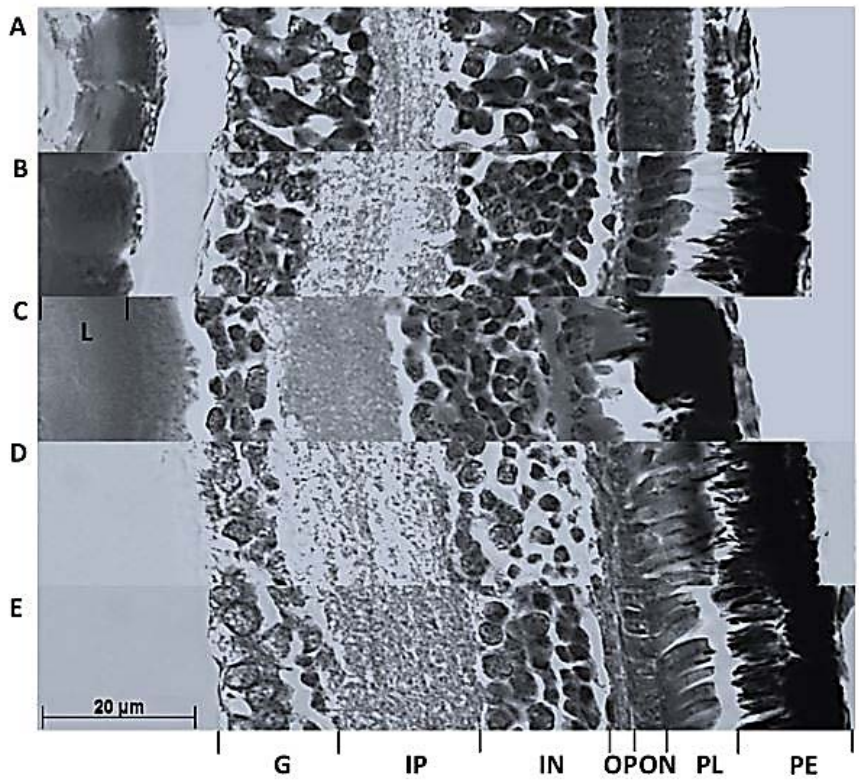

Figure 2.1: Transverse sections of larval mahi-mahi eyes at (A) 2 days post hatch (dph), (B) 4 dph, (C) 6 dph, (D) 8 dph, and (E) 10 dph. L-lens; G-ganglion; IP-inner plexiform; IN-inner nuclear; OP-outer plexiform; ON-outer nuclear; PL-photoreceptor layer; PE-pigmented epithelium.

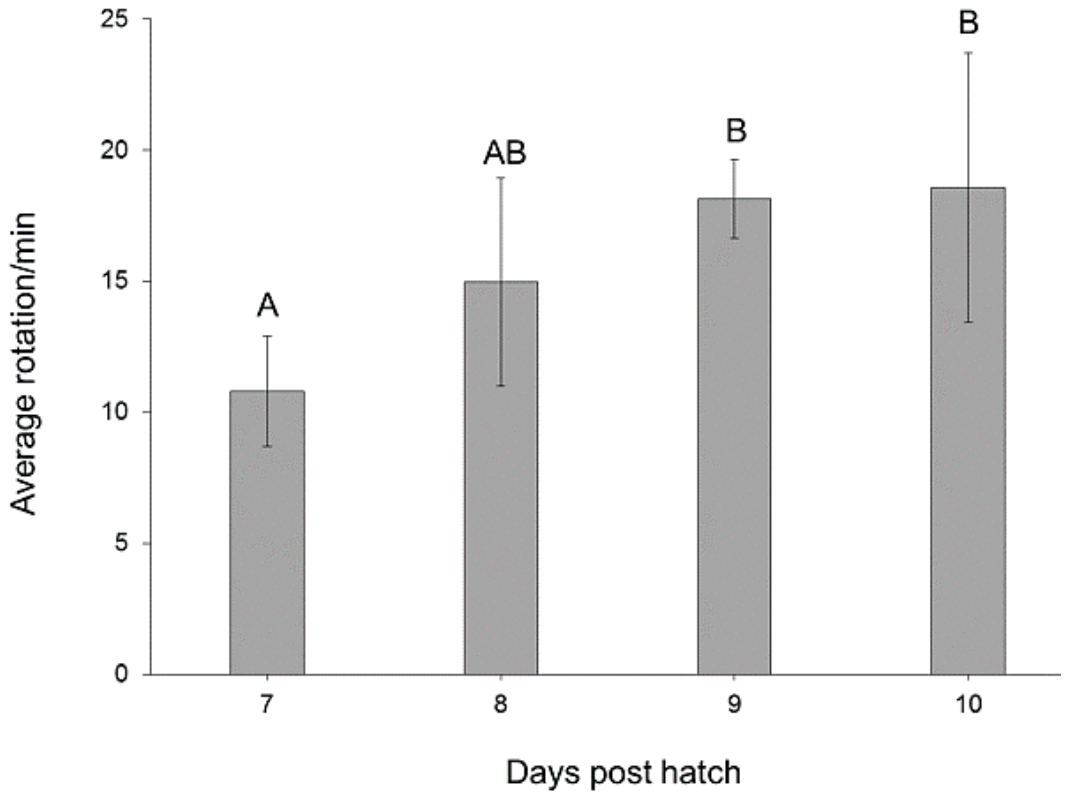

Figure 2.2: Maximum speed (average rpm (±SD)), attained for 7 to 10 day post hatch mahi-mahi. Uppercase letters denote statistical differences between development (p<0.05).

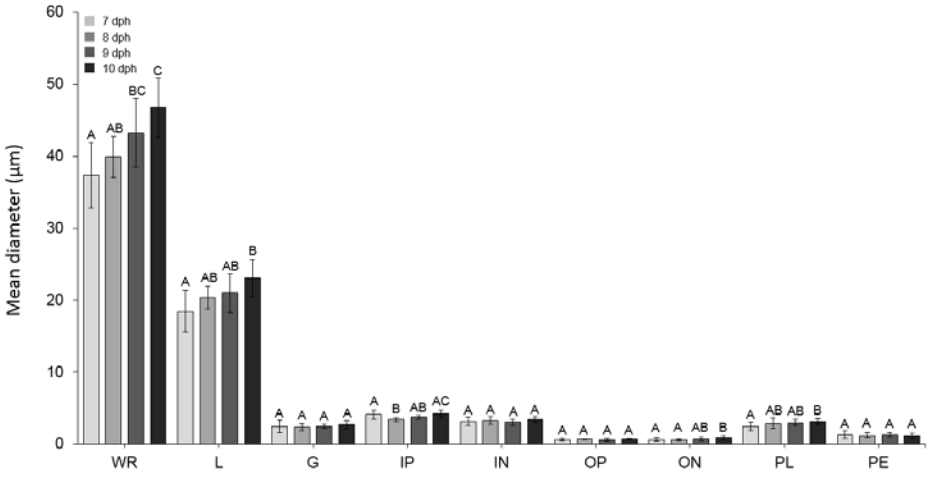

Figure 2.3: Mean diameter (µm) of retinal layers in 7 to 10 day post hatch (dph) mahi-mahi. WR-whole retina; L-lens; G-ganglion; IP-inner plexiform; IN-inner nuclear; OP-outer plexiform; ON-outer nuclear; PL-photoreceptor layer; PE-pigmented epithelium. Uppercase letters denote statistical differences between development (p<0.05).

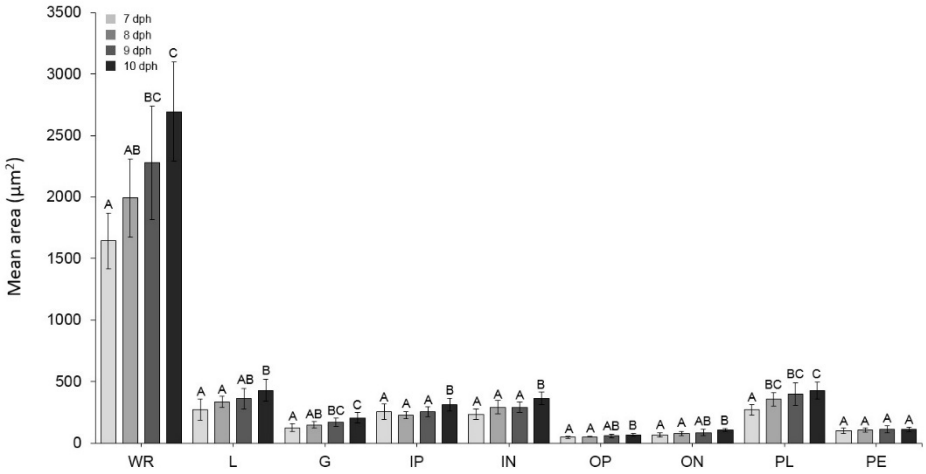

Figure 2.4: Mean area (µm^2) of retinal layers in 7 to 10 day post hatch (dph) mahi-mahi. WR-whole retina; L-lens; G-ganglion; IP-inner plexiform; IN-inner nuclear; OP-outer plexiform; ON-outer nuclear; PL-photoreceptor layer; PE-pigmented epithelium. Uppercase letters denote statistical differences between development (p<0.05).

2.4 Discussion

The results from the present study provide the first measure of optomotor response and visual acuity in larval mahi-mahi. Visual acuity, as determined by the minimum separable angle, in mahi-mahi is comparable to that of other early life-stage pelagic fish between 1-2° (Table 2.2). The minimum separable angles decreased rapidly between 7 and 10 dph mahi-mahi (by 22 %), which follows a similar pattern as other early life-stage fish [17,19,24]. While photoreceptor and ganglion densities did not differ with age, improvements in visual acuity are largely dependent on retinal and lens diameters [19,25,26], both of which increased with development. Increased visual acuity from 7 to 10 dph coincided with an increased optomotor response in larval mahi-mahi. Thus, this behavioral-level endpoint can be successfully used to determine development of visual function in a sensitive, early life-stage marine fish.

We did not observe a consistent optomotor response in larval mahi-mahi until 7 dph. Most teleost larvae have purely cone retinae with fully pigmented eyes by the time of first feed [2].

This was also true in mahi-mahi larvae where we observed increased pigmentation of the eye at 3 dph, the same point at which they start feeding exogenously. However, larval mahi-mahi hatch within 36-48 hours post fertilization, and like most pelagic marine larvae, are less developed at time of hatch than freshwater fishes [3]. Early life-stage fish primarily have myopic eyes and may rely on lateral line mechanoreceptors when feeding [23]. This helps explain the inconsistent response of larvae less than 7 dph to exhibit an optomotor response, though they are still able to feed at 3 dph.

Combining this behavioral assay with a histological approach further helped quantify the changes that were occurring within the eye during development. For example, the diameter of the photoreceptor layer in the mahi-mahi eye increased over time relative to the diameter of the whole retina, which has been shown to increase visual acuity in other teleosts [27]. However, the diameters of the inner nuclear and ganglion layers did not decrease between 7 and 10 dph mahi-mahi, as commonly seen during development [28,29]. While we did not observe a thinning of those layers, it is possible that by the time larval mahi-mahi were at an age that tolerated optomotor testing, these layers were already well-developed for processing and relaying information from photoreceptors to the brain. However, further study of the number of neural connections is needed. The outer nuclear layer, which contains nuclei of light detecting rods and cones, increased in size through development in larval mahi-mahi. This has also been previously reported in goldfish and is thought to contribute to a greater optomotor response [28].

Vision plays an important role in the phenomenon of rheotaxis in which fish orient their body against a water current by focusing on an external stimuli [30,31]. The ability to perceive light plays a key role in rheotactic-dependent activities such as vertical migration while feeding [32]. Increases in retinal diameter were seen with increased age, suggesting that vision also increased

as tracking ability increased, as well. Retinal diameter plays an important role in detecting different light intensities with the development of rods. Through development, larvae increase their ability to see in low light conditions, as seen during vertical migration events to deeper waters when following diurnal fluxes of plankton. The ability to migrate for food and avoid predation are important in larval fish, especially in species that are known to prey on its own species, such as the mahi-mahi [8].

The behavioral and visual capabilities of mahi-mahi have been well characterized in adults [5–10,12], though need to be better understood in early life-stages. There is limited data on visual function in early life-stage fish, especially in marine pelagic species, and this research helps contribute to the lack of data currently published, as well as provides a successful means of using both behavioral and histological assays to assess visual function in a sensitive, early life-stage fish.

Table 2.1: **Anatomical acuity in larval marine pelagic fish expressed as minimum separable angle (MSA) (degree).**

Species	MSA (°)	Developmental age: Days post hatch (dph)	Author
Anchoa mitchilli	4	At hatch	(Higgs and Fuiman, 1998)
Auxix spp.	1	First-feed	(Margulies, 1997)
Brevoortia tyrannus	2.1	At hatch	(Higgs and Fuiman, 1998)
Coryphaena hippurus	0.99	7 dph	Current work
Euthynnus lineatus	1	First-feed	(Margulies, 1997)
Harengula jaguana	1	At hatch	(Higgs and Fuiman, 1998)
Scomberomorus sierra	0.87	First-feed	(Margulies, 1997)
Seriola lalandi	1.39	4 dph	(Carton and Vaughan, 2010)
Seriola lalandi	0.97	7 dph	(Carton and Vaughan, 2010)
Seriola lalandi	1.1	First-feed (3 dph)	(Hilder, 2013)
Thunnus maccoyii	1.2	First-feed (3 dph)	(Hilder, 2013)

Table 2.2: **Morphological parameters used to assess visual acuity in 7 to 10 day post hatch (dph) larval mahi-mahi. Values are expressed as mean (±SD) per 100 µm retinal transect at 1000x magnification.**

	Larval age (days post hatch)			
Morphological parameters	7	8	9	10
Photoreceptor density (100 µm)	49.33 (4.37)	48.54 (2.67)	54.00 (6.71)	52.11 (4.37)
Ganglion density (100 µm)	44.83 (5.98)	44.00 (5.31)	40.91 (5.38)	44.89 (7.51)
Summation ratio	1.12 (0.23)	1.12 (0.17)	1.34 (0.20)	1.20 (0.27)
Visual acuity (degrees)	0.99 (0.08)	1.00 (0.15)	0.81 (0.10)	0.77 (0.08)

*Summation ratio= Photoreceptor density/ganglion density

2.5 References

(1) Guthrie, D. M.; Muntz, W. R. A. Role of Vision in Fish Behaviour. In *The behaviour of teleost fishes*; Pitcher, T. J., Ed.; Springer: New York, 1986; pp 75–113.

(2) Blaxter, J. H. S. Development of Sense Organs and Behaviour of Teleost Larvae with Special Reference to Feeding and Predator Avoidance. *Trans. Am. Fish. Soc.* **1986**, *115*, 98–114.

(3) Fuiman, L. A.; Delbos, B. C. Developmental Changes in Visual Sensitivity of Red Drum *Sciaenops Ocellatus*. *Copeia* **1998**, *1998* (4), 936–943.

(4) Benetti, D. D.; Iversen, E. S.; Ostrowski, A. C. Growth Rates of Captive Dolphin, *Coryphaena Hippurus*, in Hawaii. *Fish. Bull.* **1995**, *93*, 152–157.

(5) Massutí, E.; Deudero, S.; Sánchez, P.; Morales-Nin, B. Diet and Feeding of Dolphin (*Coryphaena Hippurus*) in Western Mediterranean Waters. *Bull. Mar. Sci.* **1998**, *63* (2), 329–341.

(6) Rotschild, B. J. Observations on Dolphins (*Coryphaena* Spp.) in the Central Pacific Ocean. *Copeia* **1964**, *1964* (2), 445–447.

(7) Nelson, P. A.; Zamzow, J. P.; Losey, G. S. Ultraviolet Blocking in the Ocular Humors of the Teleost Fish *Acanthocybium Solandri* (Scombridae). *Can. J. Zool.* **2001**, *79* (9), 1714–1718.

(8) Palko, B. J.; Beardsley, G. L.; Richards, W. J. *Synopsis of the Biological Data on Dolphin-Fishes,* Coryphaena Hippurus *Linnaeus and* Coryphaena Equiselis *Linnaeus.*; 1982; Vol. 130.

(9) Munz, F. W.; McFarland, W. N. Part I: Presumptive Cone Pigments Extracted from Tropical Marine Fishes. *Vis. Res.* **1975**, *15*, 1045–1062.

(10) Kröger, R. H. H.; Fritsches, K. A.; Warrant, E. J. Lens Optical Properties in the Eyes of Large Marine Predatory Teleosts. *J. Comp. Physiol. A* **2009**, *195* (2), 175–182.

(11) Tamura, T.; Wisby, W. J. The Visual Sense of Pelagic Fishes Especially the Visual Axis and Accommodation. *Bull. Mar. Sci. Gulf Caribb.* **1963**, *13*, 433–448.

(12) McFarland, W. N.; Munz, F. W. Part III: The Evolution of Photopic Visual Pigments in Fishes. *Vis. Res.* **1975**, *15*, 1071–1080.

(13) Carvalho, P. S. M.; Noltie, D. B.; Tillitt, D. E. Ontogenetic Improvement of Visual Function in the Medaka *Oryzias Latipes* Based on an Optomotor Testing System for Larval and Adult Fish. *Anim. Behav.* **2002**, *64*, 1–10.

(14) Carvalho, P. S. M.; Kalil, D. da C. B.; Novelli, G. A. A.; Bainy, A. C. D.; Fraga, A. P. M. Effects of Naphthalene and Phenanthrene on Visual and Prey Capture Endpoints during Early Stages of the Dourado *Salminus Brasiliensis*. *Mar. Environ. Res.* **2008**, *66* (1), 205–207.

(15) Carvalho, P. S. M.; Tillitt, D. E. 2,3,7,8-TCDD Effects on Visual Structure and Function in Swim-up Rainbow Trout. *Environ. Sci. Technol.* **2004**, *38* (23), 6300–6306.

(16) Neave, D. A. The Development of Visual Acuity in Larval Plaice (*Pleuronectes Platessa* L.) and Turbot (*Scophthalmus Maximus* L.). *J. Exp. Mar. Biol. Ecol.* **1984**, *78*, 167–175.

(17) Poling, K. R.; Fuiman, L. A. Sensory Development and Concurrent Behavioural Changes in Atlantic Croaker Larvae. *J. Fish Biol.* **1997**, *51*, 402–421.

(18) Job, S. D.; Bellwood, D. R. Visual Acuity and Feeding in Larval *Premnas Biaculeatus*. *J. Fish Biol.* **1996**, *48*, 952–963.

(19) Carton, A. G.; Vaughan, M. R. Behavioural and Anatomical Measures of Visual Acuity in First-Feeding Yellowtail Kingfish (*Seriola Lalandi*) Larvae. *Environ. Biol. Fishes* **2010**, *89* (1), 3–10.

(20) Kraul, S.; Brittain, K.; Cantrell, R.; Nagao, T. Nutritional Factors Affecting Stress Resistance in the Larval Mahimahi *Coryphaena Hippurus*. *J. World Aquac. Soc.* **1993**, *24* (2), 186–193.

(21) Benetti, D. D.; Orhun, M. R.; Sardenberg, B.; O'Hanlon, B.; Welch, A.; Hoenig, R.; Zink, I.; Rivera, J. A.; Denlinger, B.; Bacoat, D.; et al. Advances in Hatchery and Grow-

out Technology of Cobia *Rachycentron Canadum* (Linnaeus). *Aquac. Res.* **2008**, *39* (7), 701–711.

(22) Kloeblen, S.; Stieglitz, J. D.; Suarez, J. A.; Grosell, M.; Benetti, D. D. Characterizing Egg Quality and Larval Performance from Captive Mahi-Mahi *Coryphaena Hippurus* (Linnaeus, 1758) Spawns over Time. *Aquac. Res.* **2018**, *49* (1), 282–293.

(23) Pankhurst, P. M. Age-Related Changes in the Visual Acuity of Larvae of New Zealand Snapper, *Pagrus Auratus*. *J. Mar. Biol. Ass. U.K.* **1994**, *74*, 337–349.

(24) Miller, T. J.; Crowder, L. B.; Rice, J. A. Ontogenetic Changes in Behavioural and Histological Measures of Visual Acuity in Three Species of Fish. *Environ. Biol. fishes* **1993**, *37*, 1–8.

(25) Blaxter, J. H. S.; Jones, M. P. The Development of the Retina and Retinomotor Responses in the Herring. *J. Mar. Biol.* **1967**, *47*, 677–697.

(26) Hilder, P. I. Development of Vision and Larval Feeding Responses in Southern Bluefin Tuna and Yellowtail Kingfish, University of Tasmania (Doctoral dissertation), 2013.

(27) Kotrschal, K.; Adam, H.; Brandstätter, R.; Junger, H.; Zaunreiter, M.; Goldschmid, A. Larval Size Constraints Determine Directional Ontogenetic Shifts in the Visual System of Teleosts. *Z. Zool. Syst. Evol.* **1990**, *28*, 166–182.

(28) Johns, P. R. Formation of Photoreceptors in Larval and Adult Goldfish. *J Neurosci* **1982**, *2* (2), 178–198.

(29) Flamarique, N. I.; Hawryshyn, C. W. Retinal Development and Visual Sensitivity of Young Pacific Sockeye Salmon (*Oncorhynchus Nerka*). *J. Exp. Biol.* **1996**, *199*, 869–882.

(30) Lyon, E. P. On Rheotropism. I.- Rheotropism in Fishes. *Am. J. Physiol.* **1904**, *12* (2), 149–161.

(31) Easter, S. S. Pursuit Eye Movements in Goldfish (*Carassius Auratus*). *Vision Res.* **1972**, *12* (1968), 673–688.

(32) Job, S. D.; Bellwood, D. R. Light Sensitivity in Larval Fishes: Implications for Vertical Zonation in the Pelagic Zone. *Limnol. Oceanogr.* **2000**, *45* (2), 362–371.

CHAPTER 3

EFFECTS OF *DEEPWATER HORIZON* CRUDE OIL ON OCULAR DEVELOPMENT IN TWO ESTUARINE FISH SPECIES, RED DRUM (*Sciaenops ocellatus*) AND SHEEPSHEAD MINNOW (*Cyprinodon variegatus*)

3.1 Introduction

The *Deepwater Horizon* (DWH) oil spill occurred from April 20 to July 14, 2010, releasing 3.19 million barrels of oil into the Gulf of Mexico [1]. The spill coincided with peak spawning periods of economically and ecologically important marine and estuarine fish species[2]. The composition of crude oil varies widely, but predominantly consists of hydrocarbons (paraffins, naphthalene, aromatics, and asphaltics) and non-hydrocarbons (carbon, hydrogen, nitrogen, oxygen, sulfur, and trace metals) [3]. Polycyclic aromatic hydrocarbons (PAHs) present in oil have been known to cause morphological and behavioral changes related to eye formation and visual processing following PAH exposure [4–9].

Previous research has reported reduced eye growth in a variety of fish species exposed to PAHs found in DWH crude oil, such as larval bluefin tuna, yellowfin tuna, and amberjack [5]. Additionally, larval mahi-mahi and red drum exhibited reduced photoreceptor-specific transcription factors and reduced expression of genes associated with eye development following exposure to DWH oil [10,11]. Though changes in transcriptomic-level pathways associated with vision and visual processing have been reported, it has yet to be determined how these changes relate to physiological or behavioral-level effects in fish. Furthermore, PAHs present in sediments can be suspended during storm events or during dredging years following oil spills due to a reduced weathering in sediments compared to surface waters [12], enhancing toxicity in these environments.

Red drum and sheepshead minnow were selected as representative estuarine fish species. Red drum are a rapidly developing, economically important estuarine species, hatching within 20 to 30 hours post fertilization (hpf), and are widely distributed throughout the Gulf of Mexico [13]. Once hatched, larvae start exogenously feeding around 3 days post hatch (dph), when their eyes become pigmented. They remain suspended in the water column in estuaries until around 6 to 8 mm in size when they settle into seagrass and marsh-edge habitats [14,15].

Sheepshead minnows reside in estuarine waters ranging in distribution from the Atlantic coast of Cape Cod to Mexico. They have a longer embryonic developmental period than red drum, hatching around 6 days post fertilization (dpf) with fully pigmented eyes. Upon hatch, they are capable of actively swimming and foraging, and remain bottom-dwelling, diurnal feeders from larvae into adult-hood [13]. Sheepshead have been used as a model organism for a range of toxicological studies, including several with a focus on PAH and oil exposure [16–20]. Most of these studies have assessed mortality as an endpoint with none observing the effects of compounds on the visual system either behaviorally or morphometrically.

Based on previously reported changes in gene expression related to eye development in oil-exposed larvae [10,11], we hypothesized that oil-exposed red drum and sheepshead minnow larvae would have smaller, underdeveloped eyes and would exhibit reduced visual function compared to unexposed larvae. To determine visual function, an optomotor response (OMR) was assessed based on the concept of flicker-fusion. An OMR relies on the fish to orient its body in the same direction as a designated stimulus. This technique has previously been used in conjunction with histological analyses of the retina to assess visual function in marine pelagic and estuarine fishes [21,22], with relatively few studies using this assay to measure the influence of contaminants on fish vision [6,23,24].

Larvae were exposed to weathered crude oil and an OMR was assessed during early life-stages through use of a rotating drum apparatus. Additionally, histological analyses were conducted to assess eye development. We found that embryos of both species exposed to increasing concentrations of weathered oil had a reduced OMR, though this did not always correspond with the histological analysis of retinal layers examined.

3.2 Methods

3.2.1 Larval Rearing

Red drum embryos were collected from spawning broodstock tanks at the Texas Parks and Wildlife-CCA Marine Development Center in Corpus Christi, Texas, USA where they were aerated until arriving at the University of Texas Marine Science Institute. All procedures and animals used in this study were in accordance with the University of Texas Austin Institutional Animal Care and Use Committee (AUP-2014-00375). Embryos were formalin treated for 1 hour, rinsed with sterilized seawater, and assessed for buoyancy and viability using a stereoscope. Spawns with poor egg quality or low fertilization rates were not used.

Sheepshead minnow embryos were obtained from an existing culture at the University of North Texas. All procedures and animals used in the present study were conducted in accordance with the University of North Texas Institutional Animal Care and Use Committee (protocol number 17002). Adult sheepshead were fed *ad libitum* twice daily starting the week prior to spawning. Breeding baskets were placed at the bottom of rearing tanks the night prior to spawning and removed the following morning. Eggs were rinsed with fresh saltwater to remove any adhered food debris that may have resided on the chorion and were pooled together until exposed.

3.2.2 WAF Preparation

Embryos were exposed to high energy water accommodated fractions (HEWAFs) of weathered slick oil from the surface (OFS). This oil was obtained during the DWH spill by skimming oil from the ocean surface. HEWAFs were made using methods described previously [25,26]. Briefly, 1 g of oil was placed in 1 L of premade saltwater (35 ppt for red drum and 25 ppt for sheepshead) and blended on low for 30 sec. Following mixing, the WAF was poured into a 1 L separatory funnel, capped, and covered with aluminum foil. After settling for 1 h, 100 mL was drained from the bottom and discarded. Approximately 800 mL of the remaining WAF was drained and considered 100% HEWAF. This was subsequently diluted with seawater (35 ppt for red drum and 25ppt for sheepshead) and used to make exposure dilutions of 1 % HEWAF (2.72 ± 0.39 µg/L $tPAH_{50}$) for red drum and 25 and 50 % HEWAF (319 ± 30 and 159 ± 15 µg/L $tPAH_{50}$) for sheepshead. Water quality analysis was conducted daily with a 250 mL subset of the highest exposure dose taken and stored at 4°C until shipped to ALS Environmental (Kelso, WA, USA) for total PAH_{50} analysis (summation of 50 individual PAH concentrations).

3.2.3 Experimental Treatment

Embryonic red drum were collected the morning following spawning with approximately 2,500 embryos loaded into a 9 L pickle jar that contained either control seawater (35 ppt) or 2.72 µg/L $tPAH_{50}$ HEWAF until 24 hpf, with each treatment run in triplicate. Embryos were transferred to 164 L conical mesocosms containing clean saltwater, where they remained at 28°C with a 14 h:10 h light:dark photoperiod. Red drum were fed rotifers from 3 to 9 dpf, with supplemental *Artemia* added at 10 dpf.

Sheepshead embryos were exposed to control-saltwater, 159 µg/L, or 319 µg/L $tPAH_{50}$ of HEWAF. Each treatment was conducted in triplicate, with 30 embryos per 200 mL crystallizing dish. Embryos were exposed to newly mixed HEWAFs for six consecutive days, prior to hatching. Once hatched, larvae were transferred into, and remained in, fresh saltwater until behavioral analyses were conducted.

3.2.4 Behavioral and Histological Analysis

Visual function of individual larvae were measured in 10 to 14 dph red drum and in 4, 6, and 8 dph sheepshead to monitor an OMR using the same system described in Magnuson et al., (submitted). Briefly, an OMR was determined by a larval fish's ability to follow an individual black or white alternating vertical stripe in a circle. The rotational speed of the stripe was incrementally increased in either a clockwise or counterclockwise direction until the larvae was unable to following the rotating stripes. At this point, the stripes were rotated in the opposite direction, with the same behavioral endpoints recorded. Once tested behaviorally, larvae were fixed in Bouin's solution for 24 hours and then transferred to 70% ethanol. Larvae were subsequently dehydrated through a series of ethanol solutions and embedded in paraffin blocks. Sections of the left eye were made (5 µm), adhered to poly-L-lysine coated slides, and stained with hematoxylin and eosin. The whole retina, lens, ganglion, inner plexiform, inner nuclear, outer plexiform, outer nuclear, photoreceptor, and pigmented epithelial layers (Figure 3.1) were imaged on a compound scope (200x magnification) and the diameter of each retinal layer was measured using ImageJ (version 1.47). There were 3 red drum and sheepshead replicates of each exposure concentration, with 10 larvae taken from each replicate at 10 to 14 dph in red drum and 5 sheepshead larvae from each replicate at 4, 6, and 8 dph to assess histologically.

3.2.5 Statistical Analysis

Statistical analyses were performed using SPSS (version 20). Normal distribution was tested using Shapiro-Wilk test and homogeneity of variances was assessed using a Levene's test. Due to non-normality, a non-parametric Kruskal-Wallis test was used to test for differences in optomotor response between oil-exposed and control larvae. A Student's t-test was used to determine differences in the diameter of retinal layers between oil-exposed and control larvae. Alpha < 0.05 was used to determine statistical differences among treatments.

3.3 Results

3.3.1 HEWAF Chemistry

The prepared HEWAFs used for red drum exposures were comprised primarily of 3-ring PAHs (75%) followed by 4-ring PAHs (18%), with the majority represented as C1- and C2 phenanthrenes/anthracenes. The mean $tPAH_{50}$ concentration in the exposure WAF was 2.72 ± 0.39 µg/L. The prepared HEWAFs used for sheepshead exposures were comprised primarily of 3-ring PAHs (67%) followed by 4-ring PAHs (28%), with the majority represented as C1- and C2 phenanthrenes/anthracenes. The mean $tPAH_{50}$ concentrations in the exposure WAF were 319 ± 30 and 159 ± 15 µg/L $tPAH_{50}$.

3.3.2 Optomotor Response (OMR)

Control red drum larvae began to exhibit an OMR at 12 dph, however, OMR was not demonstrated in oil-exposed larvae until 13 dph. Further, at 13 dph, the OMR in oil-exposed larvae was 96 % slower than control larvae ($p = 0.026$). Similarly, oil-exposed 14 dph larvae were 32% slower than control individuals ($p < 0.001$; Figure 3.2).

In sheepshead larvae, controls and those exposed to 159 µg/L $tPAH_{50}$ were able to exhibit an OMR at 4 to 8 dph, while larvae exposed to 319 µg/L $tPAH_{50}$ were unable to exhibit an OMR until 8 dph. There was no significant difference in the ability of 4 dph ($p = 0.43$) or 8 dph ($p = 0.09$) larvae exposed to 159 µg/L $tPAH_{50}$ to track at speeds differing from control larvae, however, at 6 dph, oil-exposed larvae tracked at significantly reduced speeds compared to controls ($p = 0.04$). By 8 dph, larvae exposed to 319 µg/L $tPAH_{50}$ exhibited an OMR, though were 53% slower than control larvae ($p = 0.019$; Figure 3.3).

3.3.3 Histological Analysis

The retinas of 10 to 12 dph oil-exposed red drum larvae were 17 % smaller in diameter compared to control larvae ($p < 0.05$). The outer nuclear and pigmented epithelial layers were reduced in 10 to 11 dph oil-exposed larvae ($p < 0.05$), with 36 % and 21 % reduced diameters relative to controls, respectively. The ganglion layer ($p < 0.001$; 26 % reduced), inner plexiform layer ($p < 0.001$; 23 % reduced), inner nuclear layer ($p = 0.005$; 21 % reduced), and lens diameters ($p < 0.001$; 11 % reduced) in 11 dph oil-exposed larvae were reduced compared to controls, with 13 dph larvae only having a reduced photoreceptor layer ($p = 0.035$; 22 %). No other retinal layers significantly differed between exposed and control larvae (Figure 3.4).

There were no significant differences in the diameters of the retinas and lens nor in the diameter of the inner plexiform, inner nuclear, outer plexiform, and outer nuclear, and pigmented epithelial layers between 4 and 8 dph control sheepshead larvae and those exposed to 159 µg/L $tPAH_{50}$. However, there was a 17 % increase in the diameters of the ganglion layers ($p = 0.011$) and a 19 % decrease in the photoreceptor layers ($p = 0.004$) between 4 to 8 dph. Larvae exposed to 319 µg/L $tPAH_{50}$ had significantly reduced diameters of the whole retina ($p = 0.003$; 14 %),

lens (p = 0.014; 15 %), inner plexiform (p < 0.001; 19 %), inner nuclear (p < 0.001; 16 %), outer plexiform (p = 0.042; 4 %), and photoreceptor layers (p < 0.001; 34 %) compared to control larvae. However, there were no significant differences in the diameters of the ganglion, outer nuclear, or pigmented epithelial layers between control and exposed larvae (Figure 3.5).

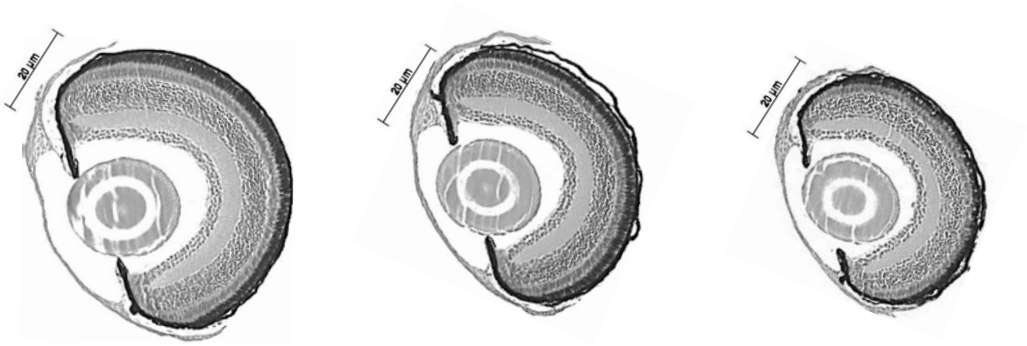

Figure 3.1: Hematoxylin and eosin stained retinal layers of 6 day post hatch control (A), 159 µg/L (B), and (C) 319 µg/L exposed sheepshead minnow.

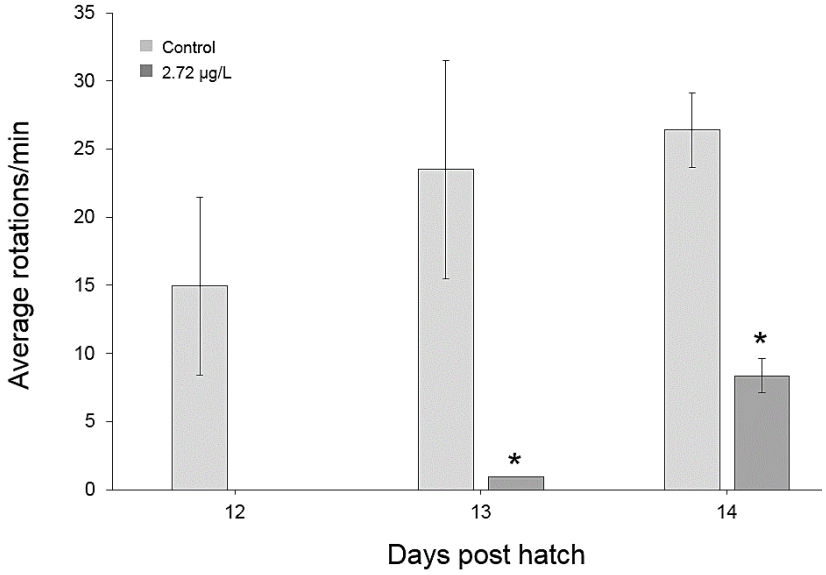

Figure 3.2: Maximum speed (average rotation/min ((±SD)), attained for 12, 13, and 14 day post hatch red drum. * Denotes significance at p < 0.05.

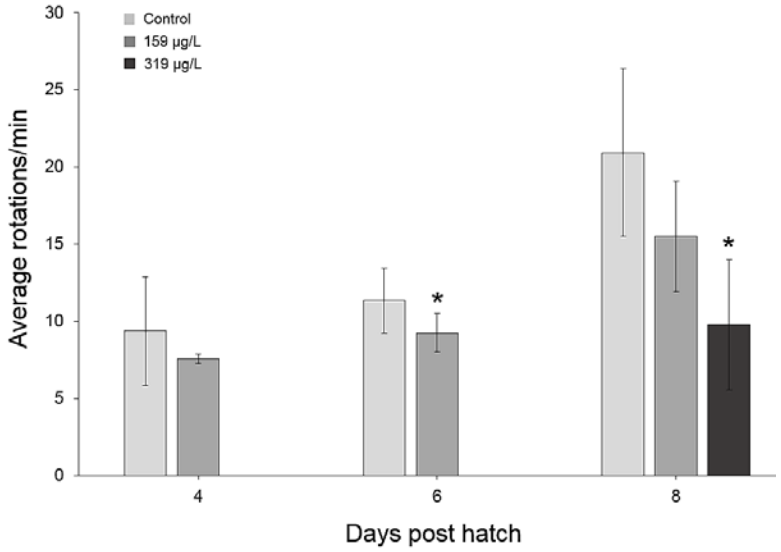

Figure 3.3: Maximum speed (average rotation/min (±SD)), attained for 4, 6, and 8 day post hatch sheepshead minnow. Asterisks (*) denote significance at p< 0.05.

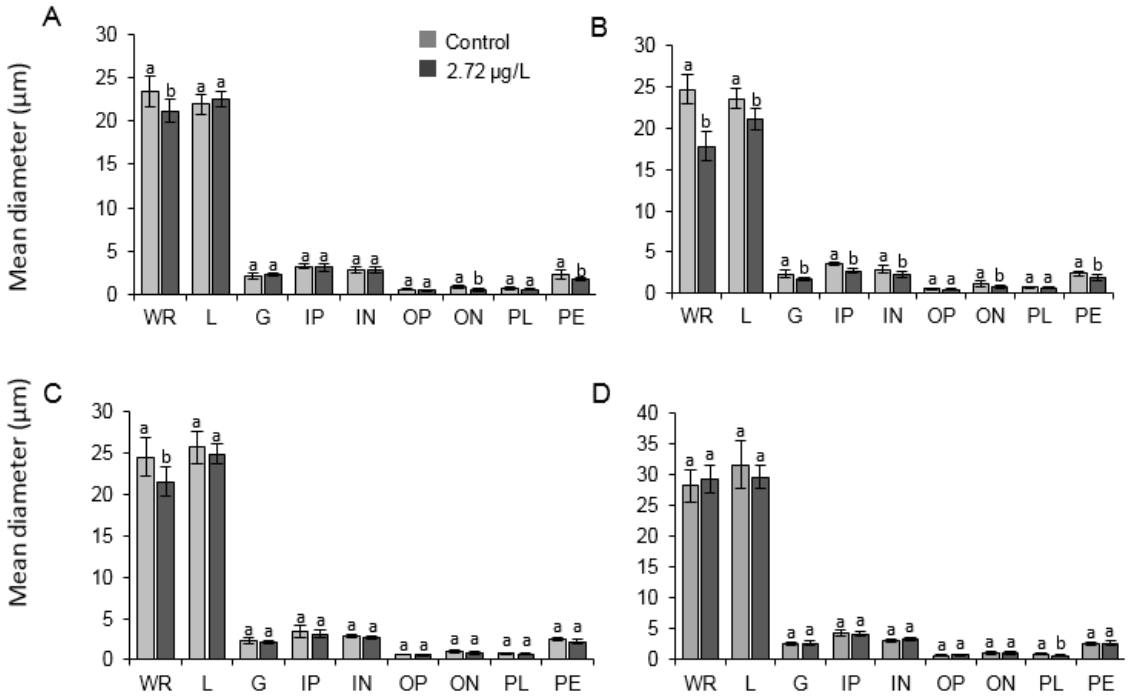

Figure 3.4: Mean diameter (µm) of retinal layers in 10 day post hatch (dph) (A), 11 dph (B), 12 dph (C), and 13 dph (D) red drum. WR-whole retina; L-lens; G-ganglion; IP-inner plexiform; IN-inner nuclear; OP-outer plexiform; ON-outer nuclear; PL-photoreceptor layer; PE-pigmented epithelium. Lowercase letters are used to denote significance between exposure treatments (p < 0.05).

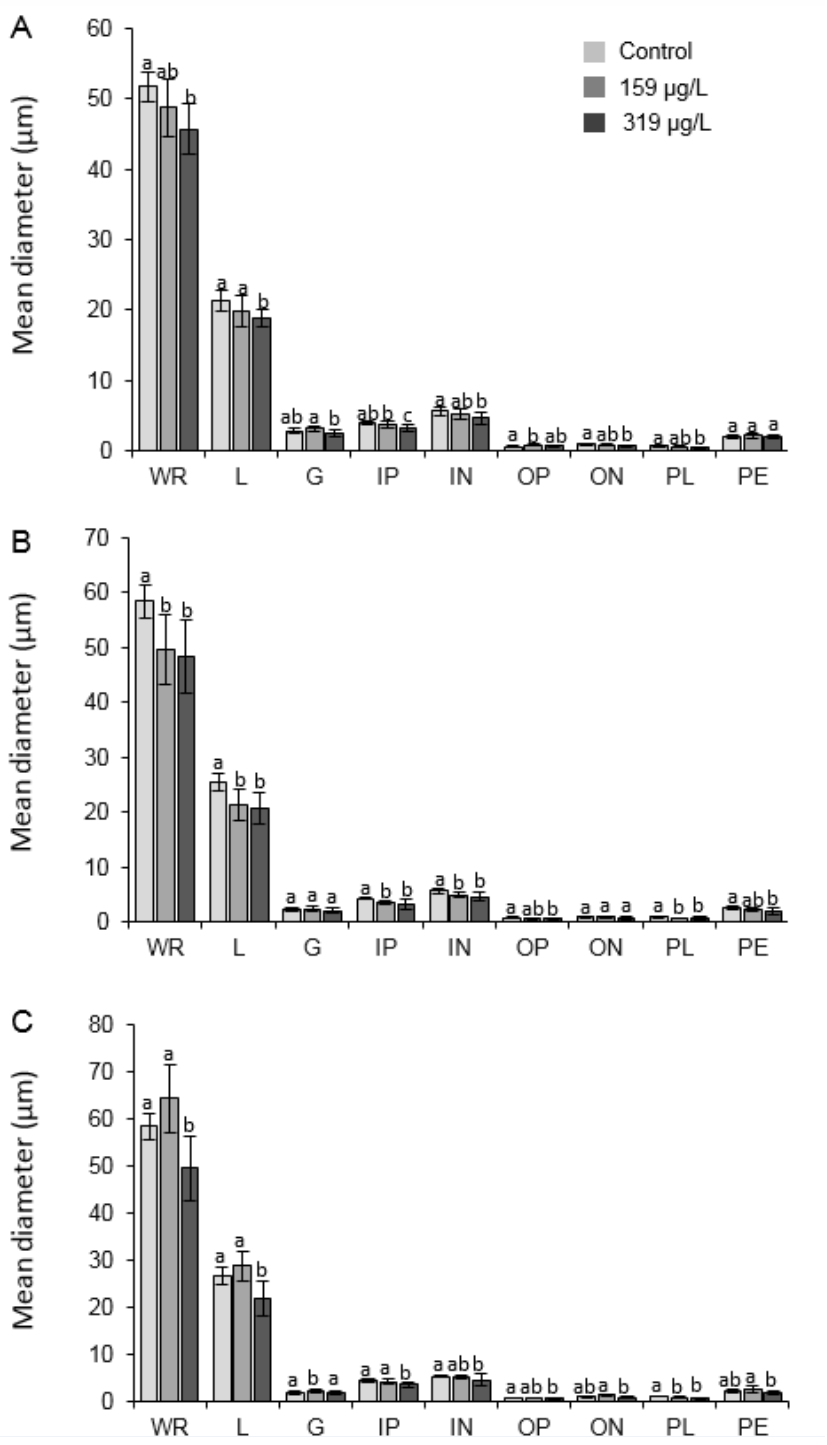

Figure 3.5: Mean diameter (µm) of retinal layers in 4 day post hatch (dph) (A), 6 dph (B), and 8 dph (C) sheepshead minnow. WR-whole retina; L-lens; G-ganglion; IP-inner plexiform; IN-inner nuclear; OP-outer plexiform; ON-outer nuclear; PL-photoreceptor layer; PE-pigmented epithelium. Lowercase letters are used to denote significance between exposure treatments ($p < 0.05$).

3.4 Discussion

The present study provides the first direct evidence that visual function and development are impaired in estuarine fish following exposure to PAHs in crude oil. Concentrations used in this study were within those reported during the DWH oil spill (0 - 84.8 µg/L; Diercks et al., 2010). Previous studies have shown molecular-level changes in genes associated with eye development and ocular diseases in larval mahi-mahi and red drum exposed to DWH oil [10,11]. Xu et al. (2017) reported the downregulation of genes related to eye diseases in red drum at 48 hpf when exposed to 4.74 µg/L slick oil, whereas we observed behavioral-level changes in 12 dph larvae exposed to lower concentrations of oil (2.72 µg/L). The present study demonstrates that the reported changes in gene expression likely manifest as behavioral-level changes in estuarine fish.

Oil-exposed red drum and sheepshead minnow had a reduced ability to exhibit an OMR when compared to controls. Similarly, Carvalho and Tillitt (2004) found that there was a concentration dependent decrease in OMR in trout exposed to TCDD, and in dourado exposed to individual PAHs [6]. The mechanism behind the reduced visual response seen in oiled animals has yet to be determined, with a possible mechanism involving reduced perfusion to the eye during development and another focusing more on a direct impact to the optic system itself. Microphthalmia (small eyes) and other craniofacial malformations have been considered a downstream developmental defect of cardiovascular dysfunction due to PAH exposure, predominantly associated with 3-ring PAHs [28]. However, embryonic and larval fish utilize cutaneous respiration for oxygen consumption [29], potentially reducing the reliance on the cardiovascular system during these early life stages for oxygen delivery.

When early life-stage mahi-mahi and red drum have been assessed for transcriptomic-level changes following oil exposure [10,11], subsequent downregulations of genes important in cardiac and visual abilities have been observed. Specifically, genes important to cardiac muscle contractions and cardiac hypertrophy, along with changes in pathways associated with visual function and development, have been seen concomitantly. Though craniofacial deformities were reported in 48 hpf red drum at 2.2 µg/L [30] and 4.74 µg/L [11], we found that when tested for OMR at 12 dph exposed red drum larvae did not experience any significant morphological or histological differences in eye/retinal size. However, a reduced OMR was exhibited when compared to controls. Oil-exposed sheepshead larvae had reduced development of the retinal layers, culminating in a reduced OMR.

To better assess impacts of oil exposure on eye development, histological assessments were used. The size of the pigmented epithelial layers in sheepshead larvae exposed to the highest PAH concentration were reduced. These layers play an important role in absorbing light, storing and modifying vitamin A precursors for photoreceptors, and delivering nutrients to photoreceptors [31]. The mean diameter of the photoreceptor layer, important for proper rod and cone function, was also reduced in oil-exposed sheepshead larvae. Similarly, Huang et al. (2013) found that embryonic zebrafish exposed to increasing concentrations of phenanthrene exhibited reduced retinal, pigmented epithelial, ganglion, and lens diameters. The authors additional suggest that phenanthrene could be damaging the photoreceptors themselves. It has further been shown that oil-exposed larvae have a downregulation in genes important in regulating photoreceptor function [10]. This further relates transcriptomic responses to physiological-level effects seen in layers important in visual function and phototransduction.

Furthermore, Huang et al. (2014) found that embryonic zebrafish exposed to benzo-a-pyrene had differential expression in 15 genes related to eye development and visual perception with a significantly decreased phototactic behavioral response. However, no significant differences were seen in the zebrafish retina, ganglion, outer nuclear, inner nuclear, inner plexiform, or pigmented epithelial diameters, when assessed histologically. The authors suggest that changes noticed during transcription could be occurring prior to protein translation and observable histological damage, while behavioral impacts were still seen. Similarly, the most prominent histological effect observed in red drum was a decrease in overall retina size, with slight reductions in the pigmented epithelial layer at 10 and 11 dph, and photoreceptor layer by 13 dph. Differences between sheepshead minnow and red drum responses following oil exposure could be due to overall sensitivity, exposure duration, differences in oil concentration, or developmental period in which larvae were taken and assessed for histological effects.

To our knowledge, this paper is the first report of behavioral or physiological-level visual impairment in fish exposed to DWH crude oil. Red drum and sheepshead minnow larvae exhibited reduced OMR following embryonic exposure which could lead to a reduced ability to capture prey and avoid predation in the wild. The underlying mechanisms by which changes in gene expression result in altered visual function or neural transmission are unknown. However, considering the importance of vision in growth and survival of fish, especially during sensitive life-stages, understanding these sublethal impacts of oil to embryonic and larval fish vision is important.

3.5 References

(1) Beyer, J.; Trannum, H. C.; Bakke, T.; Hodson, P. V.; Collier, T. K. Environmental Effects of the Deepwater Horizon Oil Spill: A Review. *Mar. Pollut. Bull.* **2016**, *110* (1),

28–51.

(2) Rooker, J. R.; Kitchens, L. L.; Dance, M. A.; Wells, R. J. D.; Falterman, B.; Cornic, M. Spatial, Temporal, and Habitat-Related Variation in Abundance of Pelagic Fishes in the Gulf of Mexico: Potential Implications of the Deepwater Horizon Oil Spill. *PLoS One* **2013**, *8* (10), 1–9.

(3) Hylland, K. Polycyclic Aromatic Hydrocarbon (PAH) Ecotoxicology in Marine Ecosystems. *J. Toxicol. Environ. Health. A* **2006**, *69* (1–2), 109–123.

(4) Hose, J. E.; McGurk, M. D.; Marty, G. D.; Hinton, D. E.; Brown, E. D.; Baker, T. T. Sublethal Effects of the Exxon Valdez Oil Spill on Herring Embyros and Larvae: Morphological, Cytogenetic, and Histopathological Assessments, 1989-1991. *Can. J. Fish. Aquat. Sci.* **1996**, *53* (10), 2355–2365.

(5) Incardona, J. P.; Gardner, L. D.; Linbo, T. L.; Brown, T. L.; Esbaugh, A. J.; Mager, E. M.; Stieglitz, J. D.; French, B. L.; Labenia, J. S.; Laetz, C. A.; et al. Deepwater Horizon Crude Oil Impacts the Developing Hearts of Large Predatory Pelagic Fish. *PNAS* **2014**, *111* (15), 1510–1518.

(6) Carvalho, P. S. M.; Kalil, D. da C. B.; Novelli, G. A. A.; Bainy, A. C. D.; Fraga, A. P. M. Effects of Naphthalene and Phenanthrene on Visual and Prey Capture Endpoints during Early Stages of the Dourado *Salminus Brasiliensis*. *Mar. Environ. Res.* **2008**, *66* (1), 205–207.

(7) Diamante, G.; Müller, S.; Menjivar-cervantes, N.; Genbo, E.; Volz, D. C.; Celso, A.; Bainy, D.; Schlenk, D. Developmental Toxicity of Hydroxylated Chrysene Metabolites in Zebrafish Embryos. *Aquat. Toxicol.* **2017**, *189* (June), 77–86.

(8) Huang, L.; Zuo, Z.; Zhang, Y.; Wu, M.; Lin, J. J.; Wang, C. Use of Toxicogenomics to Predict the Potential Toxic Effect of Benzo(a)pyrene on Zebrafish Embryos: Ocular Developmental Toxicity. *Chemosphere* **2014**, *108*, 55–61.

(9) Huang, L.; Wang, C.; Zhang, Y.; Wu, M.; Zuo, Z. Phenanthrene Causes Ocular Developmental Toxicity in Zebrafish Embryos and the Possible Mechanisms Involved. *J. Hazard. Mater.* **2013**, *261*, 172–180.

(10) Xu, E. G.; Mager, E. M.; Grosell, M.; Pasparakis, C.; Schlenker, L. S.; Stieglitz, J. D.; Benetti, D.; Hazard, E. S.; Courtney, S. M.; Diamante, G.; et al. Time- and Oil-Dependent Transcriptomic and Physiological Responses to Deepwater Horizon Oil in Mahi-Mahi (*Coryphaena Hippurus*) Embryos and Larvae. *Environ. Sci. Technol.* **2016**, *50* (14), 7842–7851.

(11) Xu, E. G.; Khursigara, A. J.; Magnuson, J.; Hazard, E. S.; Hardiman, G.; Esbaugh, A. J.; Roberts, A. P.; Schlenk, D. Larval Red Drum (*Sciaenops Ocellatus*) Sublethal Exposure to Weathered Deepwater Horizon Crude Oil: Developmental and Transcriptomic Consequences. *Environ. Sci. Technol.* **2017**, *51*, 10162–10172.

(12) Liu, Z.; Liu, J.; Zhu, Q.; Wu, W. The Weathering of Oil after the Deepwater Horizon Oil Spill: Insights from the Chemical Composition of the Oil from the Sea Surface, Salt Marshes and Sediments. *Environ. Res. Lett.* **2012**, *7* (3), 35302.

(13) Pattillo, M. E.; Czapla, T. E.; Nelson, D. M.; Monaco, M. E. *Distribution and Abundance of Fishes and Invertebrates in Gulf of Mexico Estuaries, Volume II: Species Life History Summaries*; 1997; Vol. 11.

(14) Rooker, J. R.; Holt, S. A. Utilization of Subtropical Seagrass Meadows by Newly Settled Red Drum *Sciaenops Ocellatus*:patterns of Distribution and Growth. *Mar. Ecol. Prog. Ser.* **1997**, *158*, 139–149.

(15) Holt, S. A.; Kitting, C. L.; Arnold, C. R. Distribution of Young Red Drums among Different Sea-Grass Meadows. *Trans. Am. Fish. Soc.* **1983**, *112*, 267–271.

(16) Moreau, C. J.; Klerks, P. L.; Haas, C. N. Interaction between Phenanthrene and Zinc in Their Toxicity to the Sheepshead Minnow (*Cyprinodon Variegatus*). *Arch. Environ. Contam. Toxicol.* **1999**, *37* (2), 251–257.

(17) Jonsson, G.; Bechmann, R. K.; Bamber, S. D.; Baussant, T. Bioconcentration, Biotransformation, and Elimination of Polycyclic Aromatic Hydrocarbons in Sheepshead Minnows (*Cyprinodon Variegatus*) Exposed to Contaminated Seawater. *Environ. Toxicol. Chem.* **2004**, *23* (6), 1538–1548.

(18) Hawkins, W. E.; Walker, W. W.; Lytle, T. F.; Lytle, J. S.; Overstreet, R. M. Studies on the Carcinogenic Effects of Benzo(a)pyrene and 7,12-Dimethylbenz(a)anthracene on the Sheepshead Minnow (*Cyprinodon Variegatus*). *Aquat. Toxicol. Risk Assess.* **1991**, *14*, 97–104.

(19) Adams, G. G.; Klerks, P. L.; Belanger, S. E.; Dantin, D. The Effect of the Oil Dispersant Omni-Clean® on the Toxicity of Fuel Oil No. 2 in Two Bioassays with the Sheepshead Minnow *Cyprinodon Variegatus*. *Chemosphere* **1999**, *39* (12), 2141–2157.

(20) Finch, B. E.; Stubblefield, W. A. Photo-Enhanced Toxicity of Fluoranthene to Gulf of Mexico Marine Organisms at Different Larval Ages and Ultraviolet Light Intensities. *Environ. Toxicol. Chem.* **2016**, *35* (5), 1113–1122.

(21) Fuiman, L. A.; Delbos, B. C. Developmental Changes in Visual Sensitivity of Red Drum *Sciaenops Ocellatus*. *Copeia* **1998**, *1998* (4), 936–943.

(22) Poling, K. R.; Fuiman, L. A. Sensory Development and Concurrent Behavioural Changes in Atlantic Croaker Larvae. *J. Fish Biol.* **1997**, *51*, 402–421.

(23) Carvalho, P. S. M.; Tillitt, D. E. 2,3,7,8-TCDD Effects on Visual Structure and Function in Swim-up Rainbow Trout. *Environ. Sci. Technol.* **2004**, *38* (23), 6300–6306.

(24) Richards, F. M.; Alderton, W. K.; Kimber, G. M.; Liu, Z.; Strang, I.; Redfern, W. S.; Valentin, J.; Winter, M. J.; Hutchinson, T. H. Validation of the Use of Zebrafish Larvae

in Visual Safety Assessment. *J. Pharmacol. Toxicol. Methods* **2008**, *58*, 50–58.

(25) Alloy, M. M.; Boube, I.; Griffitt, R. J.; Oris, J. T.; Roberts, A. P. Photo-Induced Toxicity of Deepwater Horizon Slick Oil to Blue Crab (*Callinectes Sapidus*) Larvae. *Environ. Toxicol. Chem.* **2015**, *34* (9), 2061–2066.

(26) Alloy, M.; Baxter, D.; Stieglitz, J.; Mager, E.; Hoenig, R.; Benetti, D.; Grosell, M.; Oris, J.; Roberts, A. Ultraviolet Radiation Enhances the Toxicity of Deepwater Horizon Oil to Mahi-Mahi (*Coryphaena Hippurus*) Embryos. *Environ. Sci. Technol.* **2016**, *50* (4), 2011–2017.

(27) Diercks, A. R.; Highsmith, R. C.; Asper, V. L.; Joung, D.; Zhou, Z.; Guo, L.; Shiller, A. M.; Joye, S. B.; Teske, A. P.; Guinasso, N.; et al. Characterization of Subsurface Polycyclic Aromatic Hydrocarbons at the Deepwater Horizon Site. *Geophys. Res. Lett.* **2010**, *37* (20), 1–6.

(28) Incardona, J. P.; Collier, T. K.; Scholz, N. L. Defects in Cardiac Function Precede Morphological Abnormalities in Fish Embryos Exposed to Polycyclic Aromatic Hydrocarbons. *Toxicol. Appl. Pharmacol.* **2004**, *196* (2), 191–205.

(29) Glover, C. N.; Bucking, C.; Wood, C. M. The Skin of Fish as a Transport Epithelium: A Review. *J. Comp. Physiol. B Biochem. Syst. Environ. Physiol.* **2013**, *183* (7), 877–891.

(30) Khursigara, A. J.; Perrichon, P.; Bautista, N. M.; Burggren, W. W.; Esbaugh, A. J. Cardiac Function and Survival Are Affected by Crude Oil in Larval Red Drum, *Sciaenops Ocellatus*. *Sci. Total Environ.* **2017**, *579*, 797–804.

(31) Salem, M. A. Structure and Function of the Retinal Pigment Epithelium, Photoreceptors and Cornea in the Eye of *Sardinella Aurita* (Clupeidae, Teleostei). *J. Basic Appl. Zool.* **2016**, *75*, 1–12.

CHAPTER 4

DEEPWATER HORIZON OIL CHANGES GLOBAL MICRO-RNA-mRNA SIGNATURE IN LARVAL FISH: TOXICITY PATHWAY AND FUNCTIONAL NETWORK ANALYSIS

4.1 Introduction

In 2010, the *Deepwater Horizon* (DWH) blowout released millions of barrels of oil into the Gulf of Mexico [1], coinciding with peak spawning periods of economically and ecologically important pelagic fishes [2–4]. Measured concentrations of polycyclic aromatic hydrocarbons (PAHs) in the Gulf of Mexico surrounding the spill ranged from 0 - 84.8 µg/L tPAH [5]. Some samples were as high as 240 µg/L (Deepwater Horizon Natural Resource Damage Assessment Trustees, 2016) in the upper subsurface. The composition of PAHs in crude oil can be altered by natural weathering, which can increase the amount of high molecular weight PAHs and increase toxicity to larval fish [7]. Furthermore, PAHs present in DWH crude oil have been related to a high incidence of developmental impairments and mortality in pelagic fishes, such as yellowfin tuna, bluefin tuna, amberjack, and mahi-mahi [7,8].

Marine pelagic fish develop rapidly, with mahi-mahi hatching within 36 hours post fertilization (hpf). Due to their fast development, these early stages are particularly vulnerable to PAH toxicity, with LC_{50} concentrations ranging from 19 µg/L to 146 µg/L $tPAH_{50}$ during the first 48 hours of mahi-mahi development [9]. Furthermore, pericardial edema, abnormal looping, and reduced contractility were seen in larval mahi-mahi following exposures to < 10 µg/L tPAH [10], with swimming performance also impaired in larval mahi-mahi exposed to 1.2 µg/L tPAH [11]. In a transcriptomic-based approach to determine effects of DHW crude oil on larval mahi-mahi development, Xu et al. (2016) found that cardiac impairment was among the highest impacted biological pathway following exposure, along with reduced photoreceptor-specific transcription

factors, with a subsequent downregulation of genes important in cardiovascular system development and function and eye development.

Recent studies found that PAH exposure can regulate the expression of microRNAs (miRNAs) [13–15], which can further influence mRNA expression. As previous research has shown alterations in gene expression in mahi-mahi exposed to crude oil [12], we evaluated miRNA-mRNA interactions associated with DWH oil exposure and their influence on subsequent morphological, physiological, and visual-mediated behavioral impairments in larval fish.

4.2 Methods

4.2.1 Animals and DHW Oil Exposure

Mahi-mahi broodstock were caught off the coast of South Florida using hook and line angling techniques and then directly transferred to the University of Miami Experimental Hatchery (UMEH). Broodstock were acclimated in 80 m^3 fiberglass maturation tanks equipped with recirculating and temperature-controlled water. All embryos used in the experiments described here were collected within 2-10 h following a volitional (non-induced) spawn using standard UMEH methods. Two sources of crude oil from the DWH spill that varied with respect to weathering state were obtained from British Petroleum under chain of custody for testing purposes: (1) slick oil collected from surface skimming operations (sample ID: OFS-20100719-Juniper-001 A0091G) and (2) oil from the Massachusetts barge (sample ID: SO-20100815-Mass-001 A0075K) which received oil collected from the subsea containment system positioned directly over the well (referred to herein as slick and source oil, respectively). Preparation of high energy water accommodated fractions (HEWAFs) of two oil types and oil exposures were performed at the University of Miami as outlined previously. For miRNA-mRNA and 48-hour morphometric

analyses, exposures were started at 6 hpf until 48 hpf at three nominal concentrations based on LC_{25} in previous study: 0.5%, 1%, and 2% HEWAF of slick oil (3.11, 6.22, 12.45 µg/L) or 0.125%, 0.25% and 0.5% HEWAF of source oil (4.54, 9.08, 13.62 µg/L). Three replicates were used per time point with 25 embryos per replicate. Slick and source oil HEWAF exposures were run concurrently using the same batch of embryos and a shared set of controls for both sets of experiments. Subsequently, 7 to 10 day post hatch (dph) mahi-mahi were assessed for morphological, histological, and behavioral effects following exposure to 0.08% (0.67 µg/L) and 0.2% (1.14 µg/L) slick oil HEWAFs from 6 hpf until 36 hours. All animal experiments were performed ethically and in accordance with Institutional Animal Care and Use Committee (IACUC protocol number 15-019) approved by the University of Miami IACUC committee, and the institutional assurance number is A-3224-01.

4.2.2 Water Chemistry Analysis

Water quality was monitored throughout the experiment and PAH concentrations were measured by gas chromatography/mass spectrometry – selective ion monitoring (GC/MS-SIM; based on EPA method 8270D) according to Xu et al. (2016). Briefly, 250 mL subsamples of diluted HEWAF were collected in an amber bottle for each exposure dilution and stored at 4°C until shipped to ALS Environmental (Kelso, WA, USA) for total PAH_{50} analysis (summation of 50 individual PAH concentrations).

4.2.3 Physiological, Morphological, and Histological Measurements

Larvae were mounted on a Nikon SMZ800 stereomicroscope with images collected at 48 hours for pericardial area, eye area, and heart rate using iMovie software on a MacBook laptop.

Seven to 10 dph larvae were imaged prior to fixation in Bouin's solution, and later assessed for total length and eye measurements. Larvae were subsequently dehydrated in ethanol solutions and embedded in paraffin. A microtome was used to make 5 µm sections of the left eye, with sections adhered to poly-L-lysine- coated slides and stained with hematoxylin and eosin. The retina, lens, ganglion, inner plexiform layer, inner nuclear layer, outer plexiform layer, outer nuclear layer, photoreceptor layer, and the pigmented epithelial layer diameters were imaged on a Axio imager A1 Zeiss compound microscope (200x magnification), with images analyzed using ImageJ (version 1.47).

4.2.4 Behavioral Assessment- Optomotor Response (OMR)

An OMR was assessed in 7 to 10 dph larvae as previously described. Briefly, an OMR was determined by the ability of a larvae to following a rotating black or white vertical stripe in both clockwise and counterclockwise directions. The rotation of the stripes were increased incrementally until the larvae was unable to follow the rotating stipes, at which point the maximum rotational speed was recorded.

4.2.5 Statistical Analysis

One-way analysis of variances (ANOVAs) were used to determine differences in optomotor response in exposed versus control 7 to 10 dph, as well as differences in morphology and histology of the eye. A Bonferroni post hoc was run to determine if these parameters differed depending on age and oil concentration. Linear regression was used to evaluate the relationship between total standard length and eye diameters in relation to larval age and oil exposure. An alpha < 0.05 was used to determine statistical significance among treatments.

4.2.6 mRNA Sequencing, Assembly, and Annotation

A detailed method of mRNA sequencing is presented in [16]. The surviving larvae from each replicate were pooled and RNA was isolated and purified with RNeasy Mini Kit (Qiagen, Valencia, California). The total RNA sample was quantified by NanoDrop ND-1000 Spectrophotometer (Nanodrop Technologies, Wilmington, DE, USA). 200 ng of total RNA was used to prepare RNA-Seq libraries using the NEBNext® Ultra™ II Directional RNA Library Prep Kit for Illumina following the protocol described by the manufacturer (Ipswich, MA). The size distribution and concentration of the libraries were determined using the Agilent High Sensitivity DNA Assay Chip (Santa Clara, CA). Single Read 1 x 75 sequencing was performed on an Illumina NextSEQ v2 at the Institute of Integrative Genome Biology, University of California, Riverside with each individual sample sequenced to a minimum depth of ~50 million reads. Data were subjected to Illumina quality control (QC) procedures (>85% of the data yielded a Phred score of 30).

Raw sequences were trimmed off Illumina adapter sequences and filtered out sequences that did not meet the quality thresholds using Trimmomatic (version 0.33). All reads were pooled and assembled *de novo* using Trinity (version 2.2.0) with k-mer length set at 25. Subsequently, the high-quality reads were mapped to the Trinity assembled *de novo* mahi-mahi transcriptome to estimate the transcript/Unigene abundance using RSEM (RNA-Seq by Expectation-Maximization) (version 1.2.21) with the default aligner Bowtie (version 1.1.1). The expression level of each transcript/Unigene was measured with FPKM (fragments per kilobase per million reads). A script 'PtR' in Trinity was used to compare the biological replicates for each of the samples and generate a correlation matrix and Principal Component Analysis (PCA) plot. Statistical differences in gene expression levels between mahi larvae exposed to slick oil and

controls were calculated using DEseq2. Genes were considered differentially expressed when false discovery rate (FDR) < 0.01 (Benjamini−Hochberg correction). Trinotate (2.0.2) was used for functional annotation, including homology search to known sequence data (BLAST+/SwissProt), protein domain identification (HMMER/PFAM), protein signal peptide and transmembrane domain prediction (signalP/tmHMM), and leveraging various annotation databases (eggNOG/GO/Kegg databases), reporting the best hits in the databases (http://trinotate.github.io/).

4.2.7 Gene Ontology and Ingenuity Pathway Analyses

The sorted transcript lists were mapped to human orthologs to generate HGNC (HUGO Gene Nomenclature Committee) gene symbols for downstream gene ontology (GO) term analysis, using DAVID Bioinformatics Resources 6.8 (Danio rerio as reference) and ToppGene Suite. GO terms for molecular function, molecular component, biological process, pathway and phenotype were considered significantly enriched when $p < 0.05$. The analysis was performed on categories for biological process (GOTERM_BP_FAT), cellular component (GOTERM_CC_FAT) and molecular function (GOTERM_MF_FAT) using the functional annotation tool with a modified Fisher exact p-value (EASE score) < 0.01.

Comparative toxicity pathway (tox-pathway) analysis was further conducted. If individual genes are not commonly regulated between methods/conditions, commonality may still exist on the level of pathway regulation. Comparative pathway analysis could also provide additional information on modes of action of toxicants. This comparative toxicity pathway analysis closely relates to the concept of adverse outcome pathways determining toxicity. Ingenuity Pathway Analyses (IPA) (Ingenuity Systems Inc., Redwood City, CA, USA) was used

to compare at different oil types and concentration conditions to identify similarities and differences in canonical pathways and toxicity functions (IPA-Comparison analysis). Fisher's exact test was used to calculate a p-value determining the probability that the association between the genes in the dataset and the IPA-Tox pathways as opposed to this occurring by chance alone.

4.2.8 miRNA Isolation, Sequencing, and Annotation

The miRNA sequencing and annotation followed Diamante et al. (2017) with minor modifications. miRNAs of pooled samples were isolated using the miRNeasy mini kit from Qiagen (Valenica, CA). The quality and concentration of miRNA were determined using the Agilent 2100 small RNA chip (Santa Clara, CA). miRNA libraries were made using the New England Biolabs NEBNext Multiplex Small RNA Sample Prep kit (Ipswich, MA) following the manufacturer's protocol. The size distribution and concentration of the libraries were determined using the Agilent High Sensitivity DNA Assay Chip (Santa Clara, CA). Single Read 1 x 75 sequencing was performed on an Illumina NextSEQ v2 at the Institute of Integrative Genome Biology, University of California, Riverside.

The quality of the raw miRNA sequences was evaluated by FastQC toolkit (Cambridge, UK). Adaptor sequences were trimmed off using the FASTX toolkit (Cambridge, UK), to obtain a mean Phred score ≥30. Only reads that are longer than 18 bp and shorter than 30 bp were kept for downstream alignment. The processed reads were mapped to the *Fugu rubripes* genome, and both known and novel miRNAs were identified using miRDeep2, a probabilistic algorithm based on the miRNA biogenesis model and designed to detect miRNAs from deep sequencing reads. Read counts generated from miRDeep2 were used for differential expression analysis using

DESeq2. Differential expression analysis was conducted using DESeq2 with default independent filtering. miRNAs were considered differentially expressed when false discovery rate (FDR) < 0.01 (Benjamini−Hochberg correction). Identified differentially expressed miRNAs and mRNA-seq data from the sample samples were analyzed using the microRNA Target Filter in IPA to identify experimentally demonstrated miRNA-mRNA relationships and predict the impact of expression changes of miRNA and its target mRNA on biological processes and pathways. A miRNA was considered to be regulatory only if the expression levels of miRNA and its mRNA targets are reversely correlated.

4.3 Results

4.3.1 Chemical Composition of Weathered Slick Oil and Source Oil

The concentrations of PAHs in weathered slick oil and source oil were measured before and after exposures. A loss of 2-ring PAHs, as well as enrichment of 3-ring and larger PAHs, was observed during weathering process. The weathered slick oil predominantly consisted of 3-ring (initial, 72%; after, 79%) (Figure 4.1a), while the source oil was comprised predominantly of 2-ring PAHs (initial, 59%; after, 45%) followed by 3-ring PAHs (initial, 39%; after, 52%) (Figure 4.1b), represented largely by the naphthalenes and phenanthrenes/anthracenes, respectively.

4.3.2 Morphological and Physiological Measurements

Both slick and source oil increased the mean pericardial area in mahi-mahi larvae at 48 h. The slick oil treatment significantly increased pericardial area at 3.11, 6.22, and 12.45 µg/L concentrations compared to controls, and this was also significant under 9.08 µg/L source oil

treatment (Figure 4.1c). In addition, the 3.11, 6.22, and 12.45 µg/L slick oil and 3.62 µg/L source oil treatments significantly decreased heart rate at 48 h compared to controls (Figure 4.1d). The size of eyes of larvae was not significantly affected by slick or source oil treatment at 48 h (Figure 4.1e). Furthermore, the eye diameters and total standard length (TSL) of 7 to 10 dph oil-exposed larvae did not significantly differ from controls ($p > 0.05$). There was, however, a strong relationship between eye diameter and TSL in control ($F_{1,78} = 362.193$, $R^2 = 0.823$, $p < 0.0001$), 0.67 µg/L exposed ($F_{1,78} = 522.810$, $R^2 = 0.870$, $p < 0.0001$), and 1.14 µg/L exposed ($F_{1,78} = 335.648$, $R^2 = 0.811$, $p < 0.0001$) larvae. Larvae exposed to oil had 7 to 8% larger retinas than controls (0.67 and 1.14 µg/L exposed, respectively), with a 7 and 11% larger inner nuclear and ganglion layer diameter in 0.67 µg/L exposed larvae. No other retinal diameters in exposed larvae (lens, inner plexiform, outer plexiform, outer nuclear, photoreceptor layer, pigmented epithelium) were significantly different than control larvae ($p > 0.05$; Figure 4.5).

4.3.3 Behavioral Response

Oil-exposed larvae exhibited a significantly reduced OMR compared to controls (52.5 ± 12.7% slower; $p < 0.0001$; Figure 4.6). At 7 dph, larvae exposed to 0.67 and 1.14 µg/L $tPAH_{50}$ exhibited an OMR at 1.1 and 1.5 rpm (revolutions per minute), respectively, which was significantly slower than control larvae (3.8 rpm; $p < 0.0001$; Figure 4.6). By 10 dph, oil-exposed larvae increased their OMR by 7-fold from 7 dph, though still exhibited a significantly reduced speed compared to control larvae ($p < 0.0001$; Figure 4.6).

4.3.4 Transcriptome of Larval Mahi-Mahi Assembled by Trinity

Due to the lack of reference genome for mahi-mahi, the transcriptome was *de novo* assembled with Trinity. Over 50 million Illumina HiSeq reads were generated from each pooled larval sample. After trimming the adapters, 170,183,689 bases were assembled, resulting in 258,722 transcript contigs with an average length of 658 bp and an N50 of 967 bases. 17,370 HMMER/PFAM protein domains (Pfam), 31,432 non-supervised orthologous groups of genes (eggNOG), 34,847 GO_blast, and 18,375 GO_pfam were determined using Trinotate pipeline. The final transcriptome assembly provided a high-quality template for further global gene differential expression analysis in this study.

4.3.5 Global Profiles of Differentially Expressed Genes (DEGs) and microRNAs (DE miRNAs)

Overall, the unexposed control samples clustered separately from the slick or source oil treated sample, indicating global transcriptomic differences between the treatments. The numbers of DEGs were 540, 419, and 1304 after 3.11, 6.22, 12.45 µg/L slick oil exposure, respectively (Figure 4.3). After 5.54, 9.08, 13.62 µg/L source oil exposure, 1106, 1392, and 320 genes were significantly differentially expressed at FDR < 0.01, respectively. As for DE miRNAs, the numbers were 74, 50 and 60 after 3.11, 6.22, 12.45 µg/L slick oil exposure, respectively (Figure 4.2a). Exposure to 5.54, 9.08, 13.62 µg/L source oil resulted in 62, 98 and 84 altered miRNAs, respectively. 29 and 30 common DE miRNAs were identified among different concentrations of slick and source oil exposure, respectively (Figure 4.2a). Nine miRNAs were consistently up- (e.g. miR-23b, miR-181b, mi-34b-5p) or down-regulated (e.g. miR-203a-3p) at all exposure conditions, with dose-dependent fold change (Figure 4.2b).

4.3.6 Biological Processes Affected by Slick and Source Oil Exposure

To determine the potential biological impact of oil exposure at system level, a gene ontology (GO) term analysis on biological processes (BPs) was conducted by analyzing the DEGs using ToppGene and DAVID. The profile of BPs was dose- and oil type- dependent (Figure 4.3**)**. After exposure to 3.11 µg/L slick oil, the top enriched biological processes were RNA processing and RNA metabolism terms (blue in Figure 4.3a) by ToppGene. Metabolic and catabolic process (e.g. carboxylic acid, organonitrogen compounds) and terms associated with embryo development (e.g. anatomical structure in morphogenesis, muscle cell differentiation, and neurogenesis) were some of the most enriched BPs at 6.22 µg/L slick oil (Figure 4.3b). The top enriched BPs at 12.45 µg/L slick oil were organic acid metabolic process and cardiovascular system development (green in Figure 4.3c). For source oil, cell cycle process, metabolic process, and RNA processing were the most enriched by 4.54 µg/L source oil exposure (Figure 4.3d), which were also highly enriched by 9.08 µg/L source oil exposure, while more 'response' BPs were enriched by 9.08 µg/L source oil exposure, such as regulation of response to stress, response to endogenous stimulus, response to hormone, cellular response to light stimulus, etc. (Figure 4.3e). The most significantly enrich BP by 13.62 µg/L source oil was cardiovascular system development followed by organic acid metabolic process and cell junction assembly (Figure 4.3f). Similar BP profile to the ToppGene results, DAVID also predicted regulation of transcription, heart development, and cell proliferation as the top enriched terms for both slick and source oil, with more embryonic and system development BPs at higher concentrations.

4.3.7 Toxicity Pathways Identified Using IPA

Canonical pathways and toxicity lists in mahi larvae after slick and source oil exposure were analyzed by IPA. The representative activated canonical pathways included EIF2 signaling, intrinsic prothrombin activation pathway, integrin signaling, signaling by RhoA family GTPases, cardiac β-adrenergic signaling, NRF2-mediated oxidative stress responses, apoptosis pathway etc., and the representative inhibited canonical pathways included Huntington's disease signaling, Gαq signaling, eNOS signaling, CREB signaling in neurons, synaptic long term potentiation pathway, etc. Notably, a number of significantly enriched canonical pathways such as aryl hydrocarbon receptor pathway, calcium signaling, and nNOS signaling in neurons interacted with other canonical pathways, and the complexity of the pathway networks depend on the concentrations of oil. Ingenuity Toxicity Pathways focusing on the assessment of toxicity were further enriched using IPA. AhR signaling, Fatty Acid Metabolism, Cell cycle, Liver necrosis/cell death, Positive Acute Phase Responses Proteins, Cardiac Necrosis/Cell death, Long-term Renal Injury, Increases Heart Failure, and Oxidative Stress were the 10 most significantly predicted toxicity pathways (Figure 4.4).

4.3.8 Meta-Analysis on miRNA-mRNA Functional Networks

Based on the differentially expressed (DE) miRNAs and mRNAs (DEGs) identified from deep sequencing, the interaction of miRNA-mRNA and their downstream functional consequences were predicted by using MicroRNA Target Filter in IPA database. Among 101 and 126 significant DE miRNAs, we obtained 31 and 51 DE miRNAs and inversely correlated target DEGs after slick and source oil exposure, respectively. Four dose-dependent DE miRNAs (miR-34b, miR-181b, miR-23b, and miR-203a) responsive to both slick and source oil exposure were

further filtered to predict downstream biological functions. Consistent with biological process analysis by ToppGene/DAVID and toxicity pathway analysis by IPA, the target genes of these four miRNAs were involved AhR signaling, Cardiac β-adrenergic signaling, nNOS signaling in neurons, xenobiotic metabolism signaling, p53 signaling, cell cycle regulation, etc., as well as potential diseases including cardiovascular disease, neurological disease, developmental disorder, ophthalmic disease, metabolism disease, etc. (Figure 4.2c).

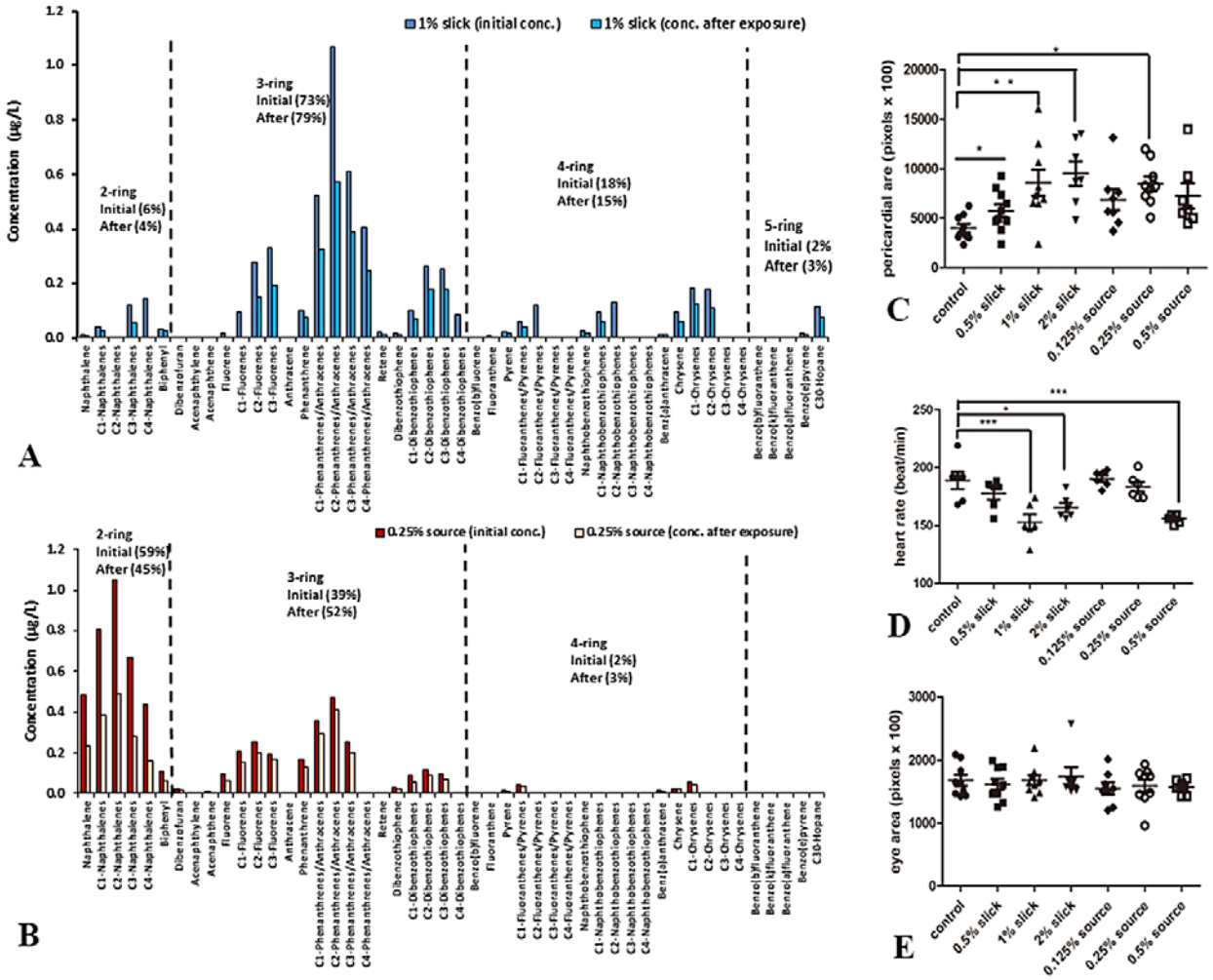

Figure 4.1: **Percent composition for 50 PAH analytes as determined by GC-MS for HEWAF of 1% slick (3.22 µg/L) (A) and 0.25% source (9.08 µg/L) DHW oil (B). Assessment of pericardial area (C), heart rate (D), and eye area (E) in mahi-mahi exposed to slick or source oil HEWAF. Data are presented as mean ± SEM. * indicate significant differences between control and oil exposed larvae.**

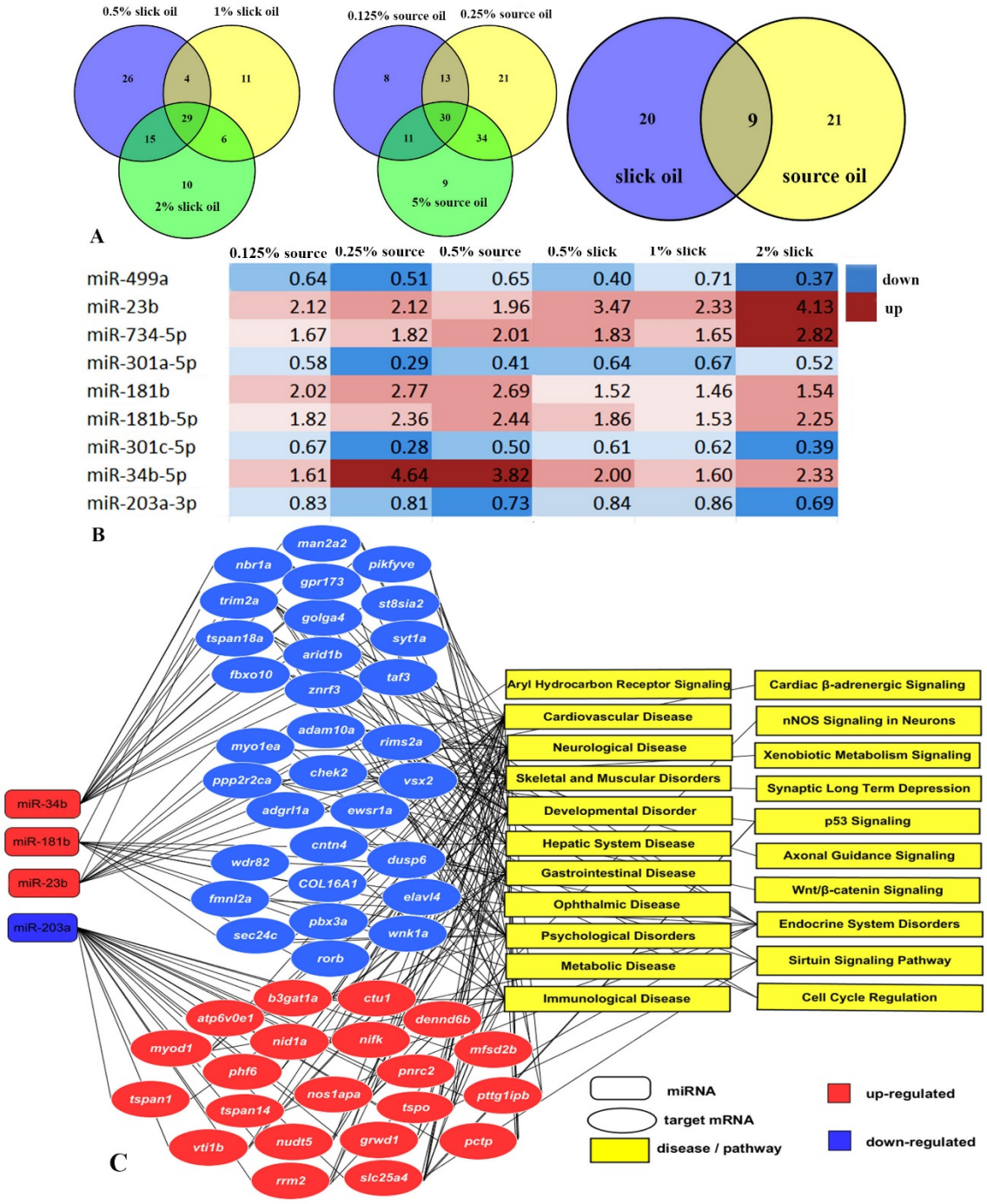

Figure 4.2: Venn diagrams of shared differentially expressed miRNA at the 3 different concentrations of slick and source oil exposure (A). Nine shared differentially expressed miRNA between slick and source oil exposure (B). Interaction network of DE miRNAs identified potential DEGs involved in important signaling pathways and diseases by using the tool microRNA Target Filter of IPA (C).

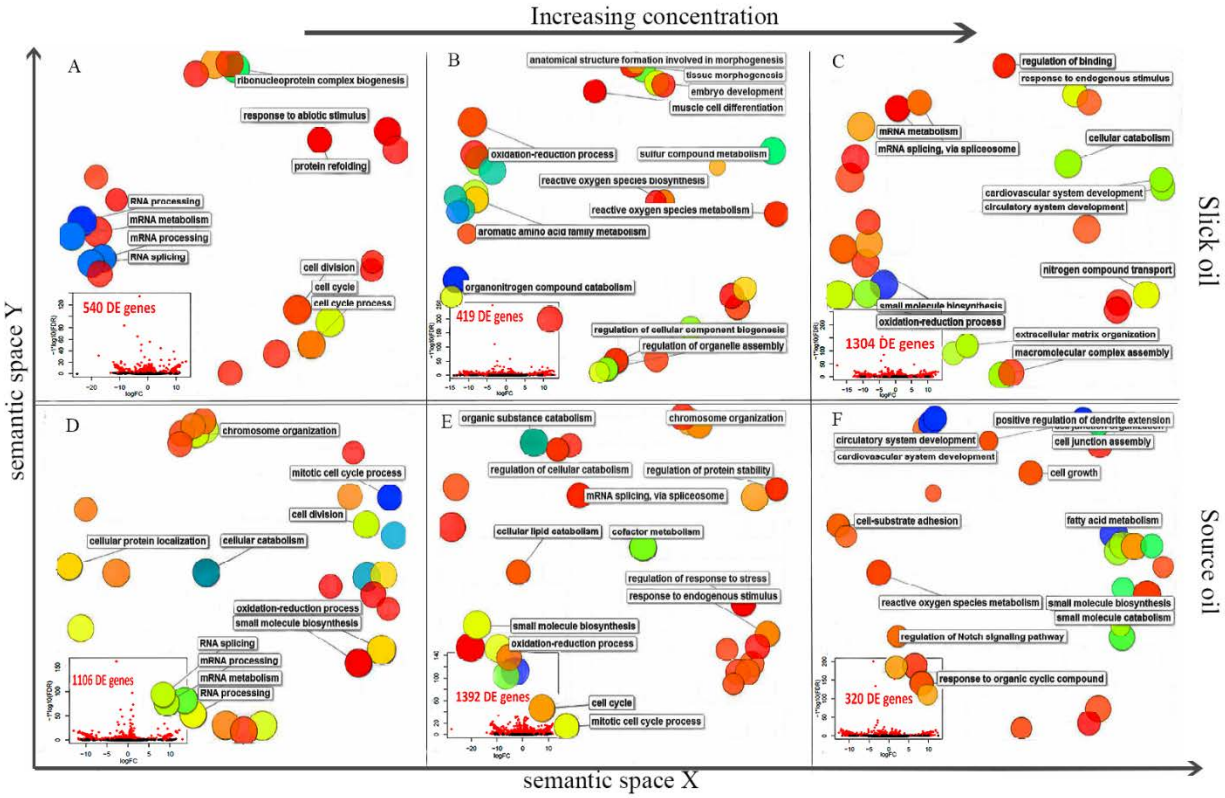

Figure 4.3: Enriched biological process in mahi-mahi exposed to different concentrations of slick or source oil HEWAF by ToppGene. The scatterplots show cluster members in a two-dimensional space obtained by applying multi-dimensional scaling of a matrix of the gene ontology (GO) terms' semantic similarities. The proximity on the plot reflects the semantic similarity. Blue and green circles indicate greater significant p-values than the orange and red circles. The size of the circle indicates the GO term frequency in the GO database.

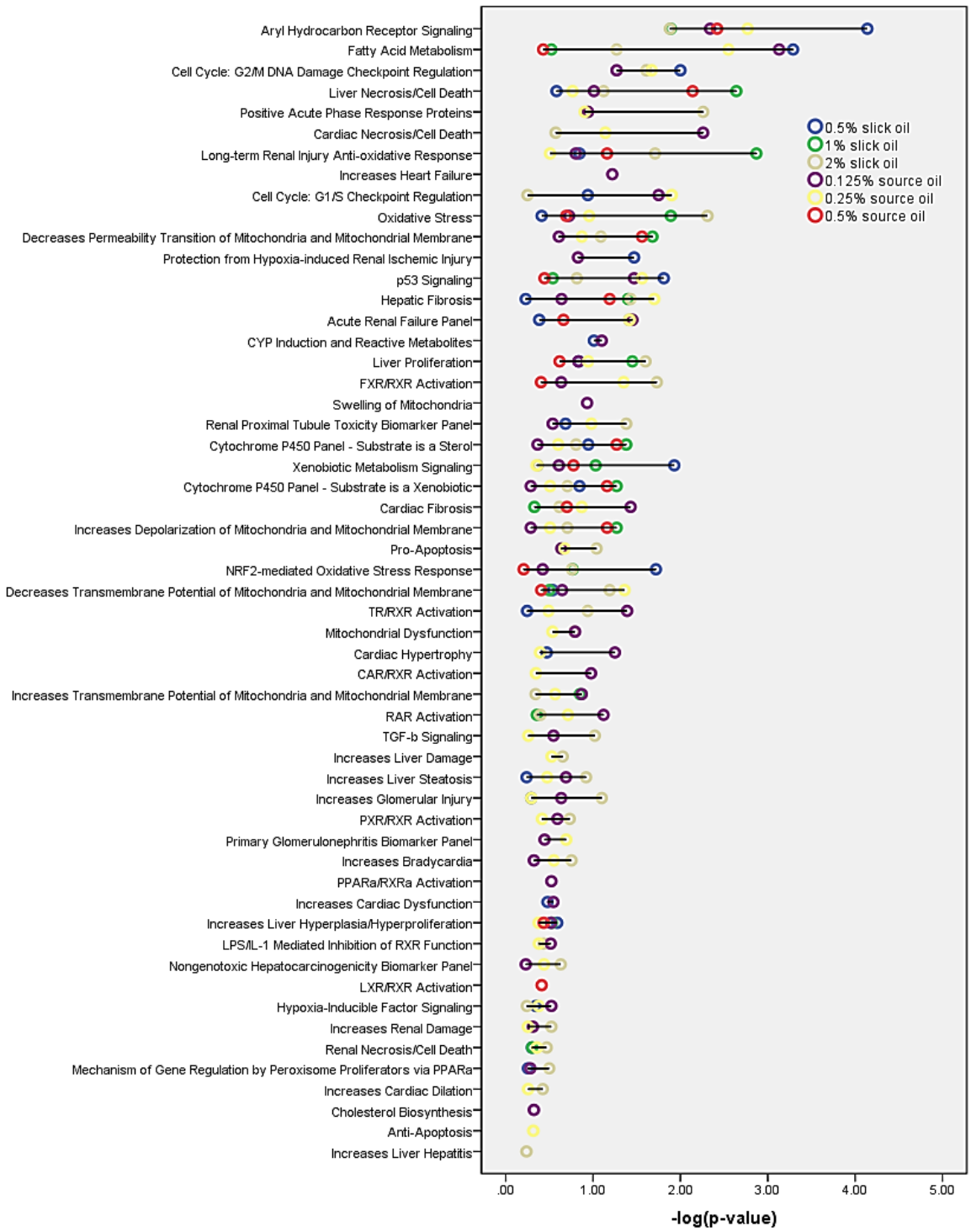

Figure 4.4: **Common Ingenuity Toxicity Lists for slick and source oil. The x-axis displays the -log of p-value which is calculated by Fisher's exact test right-tailed.**

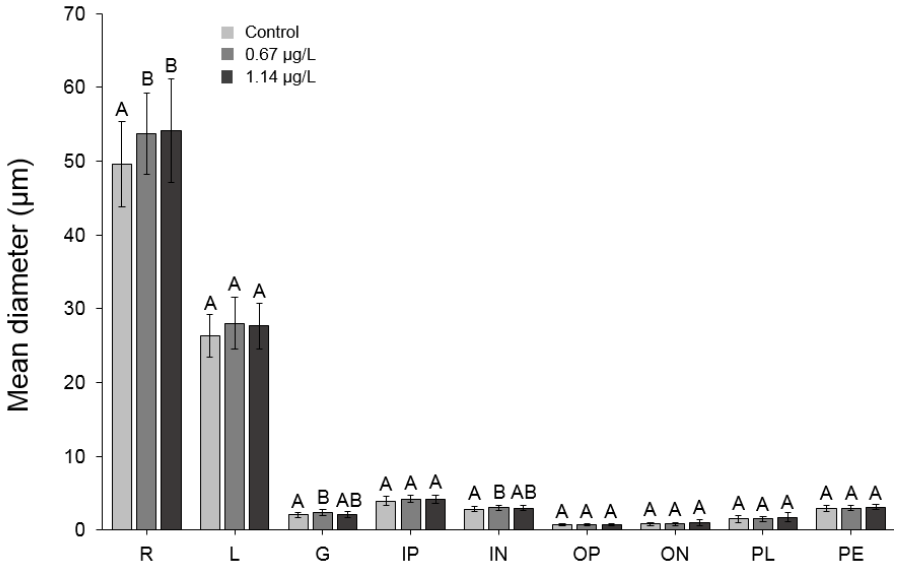

Figure 4.5: Effects of 0.67 µg/L and 1.14 µg/L $tPAH_{50}$ exposure on the mean diameters (µm) of 7 to 10 day post hatch larval mahi-mahi. One-way ANOVA, Bonferroni post hoc. Data presented as mean ± standard deviation (SD). Uppercase letters are used to denote significance between exposure treatments ($p < 0.05$). (R- retina; L-lens; G-ganglion; IP-inner plexiform; IN-inner nuclear; OP-outer plexiform; ON-outer nuclear; PL-photoreceptor layer; PE-pigmented epithelium).

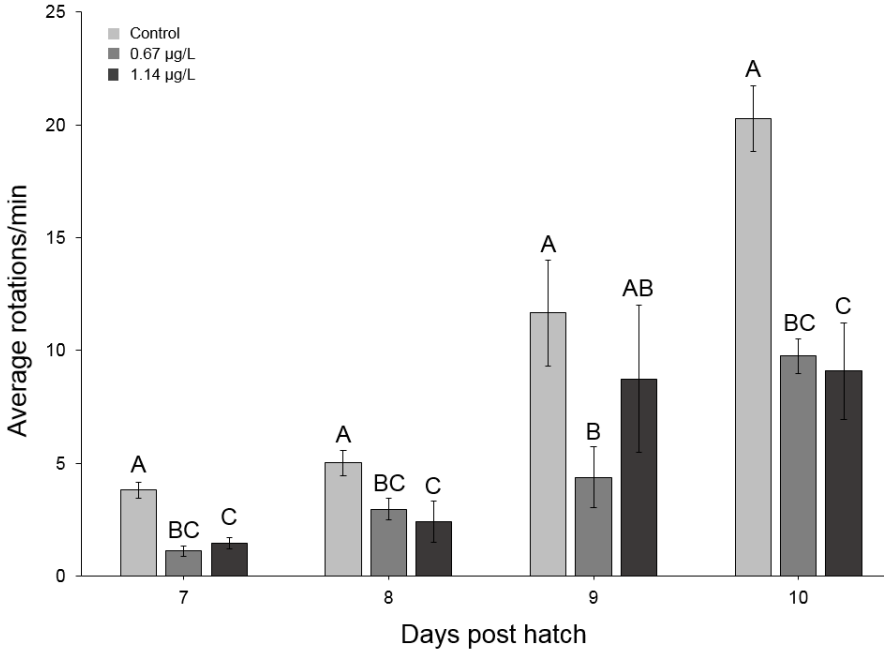

Figure 4.6: Effects of 0.67 µg/L and 1.14 µg/L $tPAH_{50}$ exposure on the average rotations/min of 7 to 10 day post hatch larval mahi-mahi. One-way ANOVA, Bonferroni post hoc. Data presented as mean ± standard deviation (SD). Uppercase letters are used to denote significance between exposure treatments ($p < 0.05$).

4.4 Discussion

To our knowledge, this is the first study to determine miRNA-mRNA interactions and their target genes in relation to a highly weathered and non-weathered oil, while providing several novel miRNA biomarkers that can be used in subsequent oil studies. miRNAs have an important role in regulating mRNA stability and translation, with potential influences in PAH-associated toxicity. We were able to relate the expression of these miRNAs to morphological, physiological, and behavioral-level responses associated with cardiac and visually mediated effects following oil exposure. Of the 29 common slick and 30 source oil DE miRNAs, 9 were consistently up- (miR-23b; miR-734-5p; mir-181b; miR-181b-5p; miR-34b-5p) or down-regulated (miR-499a; miR-301a-5p; miR-301c-5p; miR-203a-3p). These miRNAs are predominantly associated with proper vascular, heart, eye, and brain development [18–21].

Through the use of ToppGene the major biological processes following exposure to weathered slick oil were involved with RNA processing and metabolism, catabolic processes, embryo development, organic acid metabolism, and cardiovascular system development. Though, following non-weathered source oil exposure, one of the major processes was involved in responses such as stress and hormone responses and cellular response to light stimuli. However, similarities were seen between oil types with regard to RNA processing, metabolism, and cardiovascular system development. DAVID predicted similar processes, with major processes involved in the regulation of transcription, heart development, and cell proliferation.

These commonly affected pathways [12,17,22] following oil exposure have been shown to have subsequent morphological and behavioral effects in larval fish. The weathering state of oil further influences toxicity, with weathered oils containing more 3-ring PAHs than non-weathered oils, which can increase cardiotoxicity and visual effects following exposure [7,8,11,13,23,24]. To

further relate these transcriptomic level effects to a higher level or organization, larvae were assessed morphologically for incidence of pericardial area, heart rate, and eye size, with additional histological and behavioral assessments conducted to assess visual function.

There was a significantly increased pericardial area and bradycardia in larvae exposed to slick oil relative to control, with larvae exposed to 9.08 µg/L source oil having a significantly increased pericardial area and bradycardia when exposed to 13.62 µg/L source oil. This response is consistent to what was observed previously in larval mahi-mahi, as weathered slick oil tends to induce a greater cardiotoxic effect than non-weathered source oil [12]. A similar finding was seen in 48 to 72 hpf larval red drum exposed to slick oil, with a significantly increased pericardial area following exposure [22,25], as others noticed a similar response in larval, pelagic fishes [7,10].

Though various craniofacial deformities are commonly observed following oil exposure in larval fish (Hose et al., 1996; Incardona et al., 2014; Sørhus et al., 2016), there were no difference in eye size between exposed and control larvae at 48 hpf, regardless of concentration or oil type, as previously seen by others in larval mahi-mahi [10]. As larvae develop, their eyes grow proportional to their length [28], with subsequent increases in visual acuity observed. We found a similar response, regardless of oil-exposure, with a strong relationship between eye size and total body length in larvae from 7 to 10 dph. Morphometric and histological assessment may not fully assess the effect of oil-exposure on eye development, as processes involved in visual signaling pathways are among the most impacted following oil exposure. When larval zebrafish were observed for visually-induced effects following benzo-a-pyrene (BaP) exposure, Huang et al. (2014) found that, regardless of exposure concentration, histological differences in retinal layers did not significantly differ from controls. However, transcriptomic-level dysregulation of

eye-associated genes was reported following BaP exposure. Similarly, no reductions in morphometric nor histological measures of retinal size were observed in oil-exposed larval mahi-mahi, though transcriptomic-level effects related to vision and visual function were impacted. A subsequent explanation could be due to densities of mahi-mahi following oil exposure. Larvae exposed to oil had an overall reduced survivability compared to controls, as mahi-mahi are also known to prey among themselves, with larger larvae remaining by the time an optomotor response was exhibited. This is the same time as which morphometric measurements were conducted and larvae preserved for histological assessment.

However, when a visually-mediated behavioral assay was used to determine visual function in 7 to 10 dph larvae, oil-exposed larvae exhibited a significantly reduced optomotor response compared to control. The maximum velocity of the rotating drum (122 mm/min) would subtend a speed at which the average body length per second of a 7 to 10 dph mahi-mahi would be ~0.21 mm/sec at maximum speed (unpublished). Due to such a short duration at this speed- less than 10 seconds- it can further be determined that visual function is directly impacted, as prior studies have demonstrated that larval mahi-mahi are capable of swimming long durations at greater speeds than through the use of an optomotor response [11]. This behavioral assay has been used in several fishes to assesses visual function following exposure to contaminants [30], including 2- and 3- ring PAHs [31].

To further assess the interaction among miRNA-mRNA and their associated function, four DE miRNAs were filtered to predict downstream biological functions. The four miRNAs (miR-34b, miR-181b, miR-23b, and miR-203a) have consistent toxicity pathways as demonstrated with ToppGene and DAVID. miR-34b functions in kidney morphogenesis and olfactory organ development as seen in zebrafish [32], where it also plays a role in neuronal brain

cells [33]. miR-34b is further induced by p53, as is serves as a direct transcriptional target of p53 [34]. p53 signaling was a major downstream biological pathway among the miRNAs consistently dysregulated following oil-exposure, and could play a part in the upregulation of the upstream miRNA-34b.

miR-181b is predominately found associated with visual function in the tectum and telencephalon in the brain and within the eyes [35], particularly retinal ganglion cells and inner nuclear layers [36]. The pretectal and tectal areas play an important role in visual function and processing as correct neuronal circuitry is dependent upon the upstream expression of miR-181a,b [36]. Furthermore, the expression of miR-23b is involved in the activation, proliferation, and migration of endothelial cells in the eyes and heart [37], where it plays an important role in the vascular branching[20], mediating proper capillary formation and choroidal neovascularization[38]. Whereas, a downregulation of miR-203a has been shown to increase proliferation of progenitor cells associated with retinal regeneration [39].

In conclusion, this study related several miRNA-mRNA interactions associated with developmental impairments following the DWH spill. We related transcriptomic-level effects to morphological, physiological, and behavioral-level impairments in larval fish exposed to several doses of oil both source and slick oil, suggesting that miRNAs play an important role in regulating impairments following oil exposure. The results of this study further provide the potential of using these DE miRNAs as novel biomarkers in oil studies.

4.5 References

(1) Beyer, J.; Trannum, H. C.; Bakke, T.; Hodson, P. V.; Collier, T. K. Environmental Effects of the Deepwater Horizon Oil Spill: A Review. *Mar. Pollut. Bull.* **2016**, *110* (1), 28–51.

(2) Rooker, J. R.; Kitchens, L. L.; Dance, M. A.; Wells, R. J. D.; Falterman, B.; Cornic, M.

Spatial, Temporal, and Habitat-Related Variation in Abundance of Pelagic Fishes in the Gulf of Mexico: Potential Implications of the Deepwater Horizon Oil Spill. *PLoS One* **2013**, *8* (10), 1–9.

(3) Teo, S. L. H.; Block, B. A. Comparative Influence of Ocean Conditions on Yellowfin and Atlantic Bluefin Tuna Catch from Longlines in the Gulf of Mexico. *PLoS One* **2010**, *5* (5).

(4) Muhling, B. A.; Roffer, M. A.; Lamkin, J. T.; Ingram, G. W.; Upton, M. A.; Gawlikowski, G.; Muller-Karger, F.; Habtes, S.; Richards, W. J. Overlap between Atlantic Bluefin Tuna Spawning Grounds and Observed Deepwater Horizon Surface Oil in the Northern Gulf of Mexico. *Mar. Pollut. Bull.* **2012**, *64* (4), 679–687.

(5) Diercks, A. R.; Highsmith, R. C.; Asper, V. L.; Joung, D.; Zhou, Z.; Guo, L.; Shiller, A. M.; Joye, S. B.; Teske, A. P.; Guinasso, N.; et al. Characterization of Subsurface Polycyclic Aromatic Hydrocarbons at the Deepwater Horizon Site. *Geophys. Res. Lett.* **2010**, *37* (20), 1–6.

(6) *Deepwater Horizon Natural Resource Damage Assessment Trustees. (2016).* Deepwater Horizon Oil Spill: Final Programmatic Damage Assessment and Restoration Plan and Final Programmatic Environmental Impact Statement. *Retrieved from Http://www.gulfspill*.

(7) Esbaugh, A. J.; Mager, E. M.; Stieglitz, J. D.; Hoenig, R.; Brown, T. L.; French, B. L.; Linbo, T. L.; Lay, C.; Forth, H.; Scholz, N. L.; et al. The Effects of Weathering and Chemical Dispersion on Deepwater Horizon Crude Oil Toxicity to Mahi-Mahi (*Coryphaena Hippurus*) Early Life Stages. *Sci. Total Environ.* **2016**, *543*, 644–651.

(8) Incardona, J. P.; Gardner, L. D.; Linbo, T. L.; Brown, T. L.; Esbaugh, A. J.; Mager, E. M.; Stieglitz, J. D.; French, B. L.; Labenia, J. S.; Laetz, C. A.; et al. Deepwater Horizon Crude Oil Impacts the Developing Hearts of Large Predatory Pelagic Fish. *PNAS* **2014**, *111* (15), 1510–1518.

(9) Mager, E. M.; Pasparakis, C.; Schlenker, L. S.; Yao, Z.; Bodinier, C.; Stieglitz, J. D.; Hoenig, R.; Morris, J. M.; Benetti, D. D.; Grosell, M. Assessment of Early Life Stage Mahi-Mahi Windows of Sensitivity during Acute Exposures to *Deepwater Horizon* Crude Oil. *Environ. Toxicol. Chem.* **2017**, *36* (7), 1887–1895.

(10) Edmunds, R. C.; Gill, J. A.; Baldwin, D. H.; Linbo, T. L.; French, B. L.; Brown, T. L.; Esbaugh, A. J.; Mager, E. M.; Stieglitz, J.; Hoenig, R.; et al. Corresponding Morphological and Molecular Indicators of Crude Oil Toxicity to the Developing Hearts of Mahi Mahi. *Sci. Rep.* **2015**, *5* (October), 1–18.

(11) Mager, E. M.; Esbaugh, A. J.; Stieglitz, J. D.; Hoenig, R.; Bodinier, C.; Incardona, J. P.; Scholz, N. L.; Benetti, D. D.; Grosell, M. Acute Embryonic or Juvenile Exposure to Deepwater Horizon Crude Oil Impairs the Swimming Performance of Mahi-Mahi (*Coryphaena Hippurus*). *Environ. Sci. Technol.* **2014**, *48* (12), 7053–7061.

(12) Xu, E. G.; Mager, E. M.; Grosell, M.; Pasparakis, C.; Schlenker, L. S.; Stieglitz, J. D.; Benetti, D.; Hazard, E. S.; Courtney, S. M.; Diamante, G.; et al. Time- and Oil-Dependent Transcriptomic and Physiological Responses to Deepwater Horizon Oil in Mahi-Mahi (*Coryphaena Hippurus*) Embryos and Larvae. *Environ. Sci. Technol.* **2016**, *50* (14), 7842–7851.

(13) Huang, L.; Xi, Z.; Wang, C.; Zhang, Y.; Yang, Z.; Zhang, S.; Chen, Y.; Zuo, Z. Phenanthrene Exposure Induces Cardiac Hypertrophy via Reducing miR-133a Expression by DNA Methylation. *Sci. Rep.* **2016**, *6*, 20105.

(14) Bianchi, M.; Renzini, A.; Adamo, S.; Moresi, V. Coordinated Actions of MicroRNAs with Other Epigenetic Factors Regulate Skeletal Muscle Development and Adaptation. *Int. J. Mol. Sci.* **2017**, *18* (4), 840.

(15) Goodson, J. M.; Weldy, C. S.; Macdonald, J. W.; Liu, Y.; Bammler, T. K.; Chien, W.; Chin, M. T. In Utero Exposure to Diesel Exhaust Particulates Is Associated with an Altered Cardiac Transcriptional Response to Transverse Aortic Constriction and Altered DNA Methylation. *FASEB J.* **2017**, *31*, 4935–4945.

(16) Xu, E. G.; Mager, E. M.; Grosell, M.; Hazard, E. S.; Hardiman, G.; Schlenk, D. Novel Transcriptome Assembly and Comparative Toxicity Pathway Analysis in Mahi-Mahi (<i>Coryphaena Hippurus<i/>) Embryos and Larvae Exposed to Deepwater Horizon Oil. *Sci. Rep.* **2017**, *7*, 44546.

(17) Diamante, G.; Xu, E. G.; Chen, S.; Mager, E.; Grosell, M.; Schlenk, D. Differential Expression of MicroRNAs in Embryos and Larvae of Mahi-Mahi (*Coryphaena Hippurus*) Exposed to Deepwater Horizon Oil. *Environ. Sci. Technol. Lett.* **2017**, *4*, 523–529.

(18) Wu, J.; Bao, J.; Kim, M.; Yuan, S.; Tang, C.; Zheng, H.; Mastick, G. S. Two miRNA Clusters, *miR-34b/c* and *miR-499*, Are Essential for Normal Brain Development, Motile Ciliogenesis, and Spermatogenesis. *PNAS* **2014**, *111* (28E2851-2857).

(19) Bhattacharya, M.; Sharma, A. R.; Sharma, G.; Patra, B. C.; Nam, J.; Chakraborty, C.; Lee, S.-S. The Crucial Role and Regulations of miRNAs in Zebrafish Development. *Protoplasma* **2017**, *254*, 17–31.

(20) Biyashev, D.; Veliceasa, D.; Topczewski, J.; Topczewska, J. M.; Mizgirev, I.; Vinokour, E.; Reddi, A. L.; Licht, J. D.; Revskoy, S. Y.; Volpert, O. V. miR-27b Controls Venous Specification and Tip Cell Fate. *Blood* **2012**, *119* (11), 2679–2688.

(21) Wilson, K. D.; Hu, S.; Venkatasubrahmanyam, S.; Fu, J.; Sun, N.; Abilez, O. J.; Baugh, J. J. A.; Jia, F.; Ghosh, Z.; Li, R. A.; et al. Dynamic microRNA Expression Programs during Cardiac Differentiation of Human Embryonic Stem Cells: Role for miR-499. *Circ. Cardiovasc. Genet.* **2010**, *3*, 426–435.

(22) Xu, E. G.; Khursigara, A. J.; Magnuson, J.; Hazard, E. S.; Hardiman, G.; Esbaugh, A. J.; Roberts, A. P.; Schlenk, D. Larval Red Drum (*Sciaenops Ocellatus*) Sublethal Exposure

to Weathered Deepwater Horizon Crude Oil: Developmental and Transcriptomic Consequences. *Environ. Sci. Technol.* **2017**, *51*, 10162–10172.

(23) Incardona, J. P.; Scholz, N. L. The Influence of Heart Developmental Anatomy on Cardiotoxicity-Based Adverse Outcome Pathways in Fish. *Aquat. Toxicol.* **2016**, *177*, 515–525.

(24) Huang, L.; Wang, C.; Zhang, Y.; Wu, M.; Zuo, Z. Phenanthrene Causes Ocular Developmental Toxicity in Zebrafish Embryos and the Possible Mechanisms Involved. *J. Hazard. Mater.* **2013**, *261*, 172–180.

(25) Khursigara, A. J.; Perrichon, P.; Bautista, N. M.; Burggren, W. W.; Esbaugh, A. J. Cardiac Function and Survival Are Affected by Crude Oil in Larval Red Drum, *Sciaenops Ocellatus*. *Sci. Total Environ.* **2017**, *579*, 797–804.

(26) Sørhus, E.; Incardona, J. P.; Karlsen, Ø.; Linbo, T.; Sørensen, L.; Nordtug, T.; Meeren, T. Van Der; Thorsen, A.; Thorbjørnsen, M.; Jentoft, S.; et al. Crude Oil Exposures Reveal Roles for Intracellular Calcium Cycling in Haddock Craniofacial and Cardiac Development. *Sci. Rep.* **2016**, *6*.

(27) Hose, J. E.; McGurk, M. D.; Marty, G. D.; Hinton, D. E.; Brown, E. D.; Baker, T. T. Sublethal Effects of the Exxon Valdez Oil Spill on Herring Embyros and Larvae: Morphological, Cytogenetic, and Histopathological Assessments, 1989-1991. *Can. J. Fish. Aquat. Sci.* **1996**, *53* (10), 2355–2365.

(28) Blaxter, J. H. S.; Jones, M. P. The Development of the Retina and Retinomotor Responses in the Herring. *J. Mar. Biol.* **1967**, *47*, 677–697.

(29) Huang, L.; Zuo, Z.; Zhang, Y.; Wu, M.; Lin, J. J.; Wang, C. Use of Toxicogenomics to Predict the Potential Toxic Effect of Benzo(a)pyrene on Zebrafish Embryos: Ocular Developmental Toxicity. *Chemosphere* **2014**, *108*, 55–61.

(30) Carvalho, P. S. M.; Tillitt, D. E. 2,3,7,8-TCDD Effects on Visual Structure and Function in Swim-up Rainbow Trout. *Environ. Sci. Technol.* **2004**, *38* (23), 6300–6306.

(31) Carvalho, P. S. M.; Kalil, D. da C. B.; Novelli, G. A. A.; Bainy, A. C. D.; Fraga, A. P. M. Effects of Naphthalene and Phenanthrene on Visual and Prey Capture Endpoints during Early Stages of the Dourado *Salminus Brasiliensis*. *Mar. Environ. Res.* **2008**, *66* (1), 205–207.

(32) Wang, L.; Fu, C.; Fan, H.; Du, T.; Dong, M.; Chen, Y.; Jin, Y.; Zhou, Y.; Deng, M.; Gu, A.; et al. miR-34b Regulates Multiciliogenesis during Organ Formation in Zebrafish. *Development* **2013**, *140* (13), 2755–2764.

(33) Kapsimali, M.; Kloosterman, W. P.; de Bruijn, E.; Rosa, F.; Plasterk, R. H. A.; Wilson, S. W. MicroRNAs Show a Wide Diversity of Expression Profiles in the Developing and Mature Central Nervous System. *Genome Biol.* **2007**, *8* (8), R173.

(34) Bommer, G. T.; Gerin, I.; Feng, Y.; Kaczorowski, A. J.; Kuick, R.; Love, R. E.; Zhai, Y.; Giordano, T. J.; Qin, Z. S.; Moore, B. B.; et al. p53-Mediated Activation of miRNA34 Candidate Tumor-Suppressor Genes. *Curr. Biol.* **2007**, *17* (15), 1298–1307.

(35) Wienholds, E.; Kloosterman, W. P.; Miska, E.; Alvarez-Saavedra, E. MicroRNA Expression in Zebrafish Embryonic Development. *Science (80-.).* **2005**, *309*, 310–311.

(36) Carrella, S.; D'Agostino, Y.; Barbato, S.; Huber-Reggi, S. P.; Salierno, F. G.; Manfredi, A.; Neuhauss, S. C. F.; Banfi, S.; Conte, I. miR-181a/b Control the Assembly of Visual Circuitry by Regulating Retinal Axon Specification and Growth. *Dev. Neurobiol.* **2015**, *75* (11), 1252–1267.

(37) Zhou, Q.; Gallagher, R.; Ufret-vincenty, R.; Li, X.; Olson, E. N.; Wang, S. Regulation of Angiogenesis and Choroidal Neovascularization by Members of microRNA-23~27~24 Clusters. *PNAS* **2011**, *108* (20), 8287–8292.

(38) Agrawal, S.; Chaqour, B. MicroRNA Signature and Function in Retinal Neovascularization. *World J Biol Chem* **2014**, *5* (1), 1–11.

(39) Rajaram, K.; Harding, R. L.; Hyde, D. R.; Patton, J. G. miR-203 Regulates Progenitor Cell Proliferation during Adult Zebra Fi Sh Retina Regeneration. *Dev. Biol.* **2014**, *392* (2), 393–403.

CHAPTER 5

OIL-INDUCED NEURONAL DEATH IN THE EYE OF TELEOST FISH

5.1 Introduction

In 2010, the *Deepwater Horizon* (DWH) oil spill released millions of barrels of oil into the Gulf of Mexico [1]. Polycyclic aromatic hydrocarbons (PAHs) present in the oil have been shown to cause developmental malformations, such as cardiac defects, craniofacial abnormalities, dysregulation of genes important in development, and behavioral-level effects [2–8]. These effects are both dose and oil dependent, as highly weathered oil contains higher molecular weight PAHs than non-weathered oil resulting in greater toxicity in larval fish [6]. Recent studies have found reduced eye development and dysregulation of miRNAs and associated mRNAs following exposure to DWH oil [2–4].

To further understand the mechanism of oil-induced toxicity to visual function in fish, gene expression, immunohistochemistry, and behavior were assessed in oil-exposed larval zebrafish. Several genes involved in phototransduction and eye development were assessed. *opn1mw*, *arr3b*, and *sws1* are expressed in green-, blue-, and UV-sensitive cones, respectively. *pde6c* and *pde6h* make up the alpha and gamma subunits of cGMP, cone-specific phosphodiesterase, respectively. *gnat2* is responsible for encoding a cone photoreceptor-specific transducin, which further couples to visual pigments in the photoreceptor cell layer [9]. The associated transducin is a G-protein of the phototransduction cascade, which is initiated by *rho*, an essential G-protein receptor. This interaction between *rho* and transducing further generates a visual signal transduction [10], whereas *rpe65a* plays an important role in visual pigment regeneration and *rgr* catalyzes the conversion of all-trans-retinal to 11-cis-retinal, which is expressed exclusively in the retinal pigment epithelium and Müller glial cells. *crx* plays an

important role in the regulation of transcription for several genes including as *gnat2*, *pde6c*, *pde6h*, and *arr3* [11].

Müller glial cells were examined through immunofluorescence, as they play an important role in forming a neuronal network in the retina, while providing cellular structure and integrity. They are further involved in the regulation of ion and gas exchange in the retina [12]. miRNAs specific to Müller glial cell function have been shown to be dysregulated in mahi-mahi following oil exposure [3], with further process involved in ion exchange and gene regulation also impaired [2,4]- directly impacting Müller glia. Furthermore, as phenanthrene exposure can have a photoreceptor-specific toxicity in zebrafish [13], a TUNEL assay was used to assess apoptosis in the eye following oil exposure. We hypothesized that there would be an increased level of apoptotic cells associated with Müller glial processes in the photoreceptor layer of the cell. Furthermore, to determine what impact cell apoptosis would have on visual function, we used an optokinetic response (OKR) assay to record eye saccades in oil exposed larvae. The objectives of this study were to determine the impact of oil exposure on visual function by examining: 1) alterations in gene expression important in eye development and visual processing, 2) neuronal connections in the brain and associated apoptosis, and 3) visually-mediated behavioral function in larval zebrafish.

We found that oil-exposed larvae had a significant downregulation of vision-related genes, an increased level of apoptosis in the retina, and decreased Müller glial cell activity. Subsequent reductions in visually-mediated behavioral assays were observed in oil-exposed larvae. These findings help further our knowledge of oil-induced toxicity to vision in fish following exposure.

5.2 Methods

5.2.1 Fish Rearing

Adult AB strain zebrafish were obtained from a local supplier and maintained in 600 L, recirculating systems at the University of North Texas. The fish were kept in a 14:10 h light:dark cycle under standard conditions as recommended by Westerfield (2007) and Spence et al. (2008). Fish were fed commercial flake food twice per day for a total of ~3% of body weight per day, with supplemental brine shrimp twice per week.

5.2.2 Oil Exposure

Embryonic zebrafish were exposed less than 4 hours post fertilization (hpf) to a diluted, weathered high energy water accommodated fraction (HEWAF) of DWH crude oil. HEWAFs were made as previously reported (Sweet et al. 2016; Alloy et al. 2015). A 100 % HEWAF (1 g oil/ 1000 mL E3 water) was diluted in E3 water (5mM NaCl, 0.17 mM KCl, 0.33 mM $CaCl_2$, 0.33 mM $MgSO_4$, 0.1% methylene blue) into concentrations of 0, 1, 3, 5, and 7% HEWAF. A total of 5 concentrations, with 5 replicates per concentration, containing 30 embryos per replicate was prepared. Embryos remained at 28 ± 1˚C throughout development. HEWAFs were renewed daily until hatch (~48 hours post fertilization), and then transferred into clean, 200 mL crystallizing dishes containing E3 water for the duration of the experiment.

5.2.3 Morphological Assessment

Larvae were anesthetized with buffered MS-222 and mounted on a Nikon SMZ800 stereoscope at 96 hpf, where images were collected to assess total standard length and eye measurements (n=20 per treatment). All images were analyzed using ImageJ (version 1.47).

5.2.4 Optokinetic Response (OKR)

An OKR was used to assess visual function in 96 hpf larvae (n = 20 per treatment). Larvae were positioned in a 35 mm Petri dish containing 3% methylcellulose to immobilize the larvae from moving side to side. Larvae were oriented so that they remained equidistant to each side of a circular drum containing alternating black and white vertical stripes. The stipes subtended an angle of 9° to the larvae, and were rotated by an attached motor at 6 rotations per minute. The stripes were rotated in both clockwise and counterclockwise directions. The larvae were viewed from a stereoscope, with videos recording eye saccades at 30 frames/sec.

5.2.5 Tissue Preparation

Larvae were fixed in 4% paraformaldehyde (1x PBS; pH 7.4) at 4˚C overnight, followed by 3 washes in 1X PBS for 5 minutes, each. Larvae were cryoprotected in 35% sucrose (w/v) at 4˚C overnight, where they were then oriented in OTC using a dissecting needle and frozen at -80˚C. Larvae were sectioned on a cryostat (10 µm; -20˚C). Sections were transferred to Superfrost/Plus Slides and stored at -80˚C and stained the following day.

5.2.6 TUNEL Assay and Immunohistochemistry

Terminal deoxynucleotidyl transferase (TdT) dUTP nick-end labeling (TUNEL) assays were performed using the ApopTag Red *in situ* Apoptosis Detection Kit (Millipore), according to manufacturer's instructions (ApopTag Red; product number S7165; Millipore).

Following the TUNEL assay, sections were incubated with the primary antibody, BLBP- a neuronal marker specific to Müller glial cells (1:500; ab32423; Abcam) at room temperature for 1 hour in a moisture chamber. Following 3 subsequent rinses in 1X PBS, slides were

incubated with a secondary antibody labeled with Alexa Fluor 488 (1:250; ab150077; Abcam) and incubated for 1 hour at room temperature in a moisture chamber, rinsed 3 times in PBS, and stained with Hoechst (1:100,000,000 in blocking solution) for nuclear staining. Two slides, with 2 consecutive sections of each larvae were used for analysis (n=5 per treatment).

5.2.7 RNA Isolation and qPCR

Twenty larvae were pooled per replicate (n=3 replicate pools; n=3 biological replicates) for total RNA extraction using the Maxwell 16 Tissue and Cell Total RNA LEC System (Promega). Following extraction, RNA was analyzed on a NanoDrop (Thermofisher). RNA was diluted to 1000 ng and reverse transcribed to cDNA using iScript Reverse Transcription Supermix for RT-qPCR (Bio-Rad), using manufacturer's instructions. Upon completion, cDNA was stored at -20°C until qPCR was conducted. qPCR was performed using the SsoAdvanced Universal SYBR Green Supermix (Bio-Rad) on a Rotor-Gene 6000 (Corbett Life Science (Qiagen)). Each reaction had 100 ng cDNA with specific primer pairs (10 µM) for the genes of interest. The following thermal cycling conditions were used for qPCR: A denaturation step for 2 minutes at 95°C, with 40 cycles of a 10 second denaturation at 95°C and an annealing and extension for 60 seconds at an optimal temperature for each primer pair. A melt curve analysis was carried out from 54 to 95°C in increments of 0.5°C. A single peak was displayed for all primer pairs. Primer efficiencies were calculated using a 6-point standard curve and the Pfaffl method [16] used to calculate relative gene expression, and all genes normalized to the housekeeping gene *gapdh*.

5.2.8 Statistical Analysis

Statistical analyses were performed using SPSS (version 20). A one-way ANOVA, followed by a Bonferroni post-hoc test, was used to determine differences in total standard length, eye size, optokinetic responses, and mean, relative gene expression in 96 hpf larvae following oil-exposure. A non-parametric, Kruskal-Wallis, analysis was used to determine differences in immunofluorescence. A p-value < 0.05 was used to denote significance.

5.3 Results

5.3.1 Oil Composition

The HEWAFs predominantly consisted of 3-ring (68%) and 4-ring (27%) PAHs, with the majority represented as C2- and C3- phenanthrenes/anthracenes. The mean $tPAH_{50}$ concentration in 7% HEWAF was 54.78 ± 2.90 µg/L.

5.3.2 Morphological Assessment

Reductions in total standard length and eye diameters in oil-exposed larvae followed a dose-dependent relationship (Figure 5.1). Oil-exposed larvae were significantly smaller than controls ($p < 0.001$), with a reduced total standard length and eye diameter ($p < 0.001$). Exposed larvae had a 7.3% reduced total standard length (1.5 - 11.4 %) and a 7% smaller eye diameter (0.8 - 12.1 %) relative to controls (Figure 5.1).

5.3.3 Optokinetic Response (OKR)

All larvae used for OKR did not exhibit any spontaneous swimming activity and all exhibited an escape response before testing, with all larvae swimming away from a pipette tip.

Larvae that did not move from the bottom of exposure dishes were not used in OKR assay. Furthermore, there was no difference in the ability to respond to rotating stripes in the OKR assay, regardless of oil exposure (Figure 5.2). Eighty-six percent of the larvae tested exhibited an OKR, with eye saccades in the same direction as the rotating drum. There was, however, a significant difference in the number of saccades conducted per minute in oil-exposed larvae versus control (Figure 5.2). Larvae exposed to 1, 3, 5, and 7% HEWAF had a 47, 52, 36, and 26 % reduction in eye saccades per minute (Figure 5.2). Control larvae had an average of 23 eye saccades per minute, with 1, 3, 5, and 7% exposed larvae having an average of 13, 11, 15, and 17 saccades per minute, respectively.

5.3.4 Gene Expression

Genes important in eye development and visual function were significantly downregulated in larvae following oil exposure (Figure 5.3). *Arr3b, gnat2, opn1mw, rgr, rho, rpe65a, sws1* were all significantly downregulated in larvae exposed to 3, 5, and 7% HEWAF, when compared to controls (Figure 5.3), though not when exposed to 1% HEWAF. *Pde6c* and *pde6h* were significantly downregulated in larvae exposed to 5 and 7% HEWAF (Figure 5.3).

5.3.5 Immunohistochemistry

Significant decreases in Müller glia fluorescence was seen in larvae exposed to 1, 3, and 5% HEWAF, relative to controls. However, no significant change was seen in larvae exposed to 5% HEWAF (Figure 5.4 A,B). The highest fluorescence of Müller glia were in the inner plexiform layer, where the cell body spans. TUNEL-stained cells were primarily located in the outer membrane of the retinal pigmented epithelial layer and associated choroid (Figure 5.4A,C).

Larvae exposed to 1 and 3 % HEWAF had significantly increased TUNEL-stained cells relative to controls. However, larvae exposed to 5 and 7 % HEWAF did not significantly differ than controls in the amount of apoptotic fluorescence.

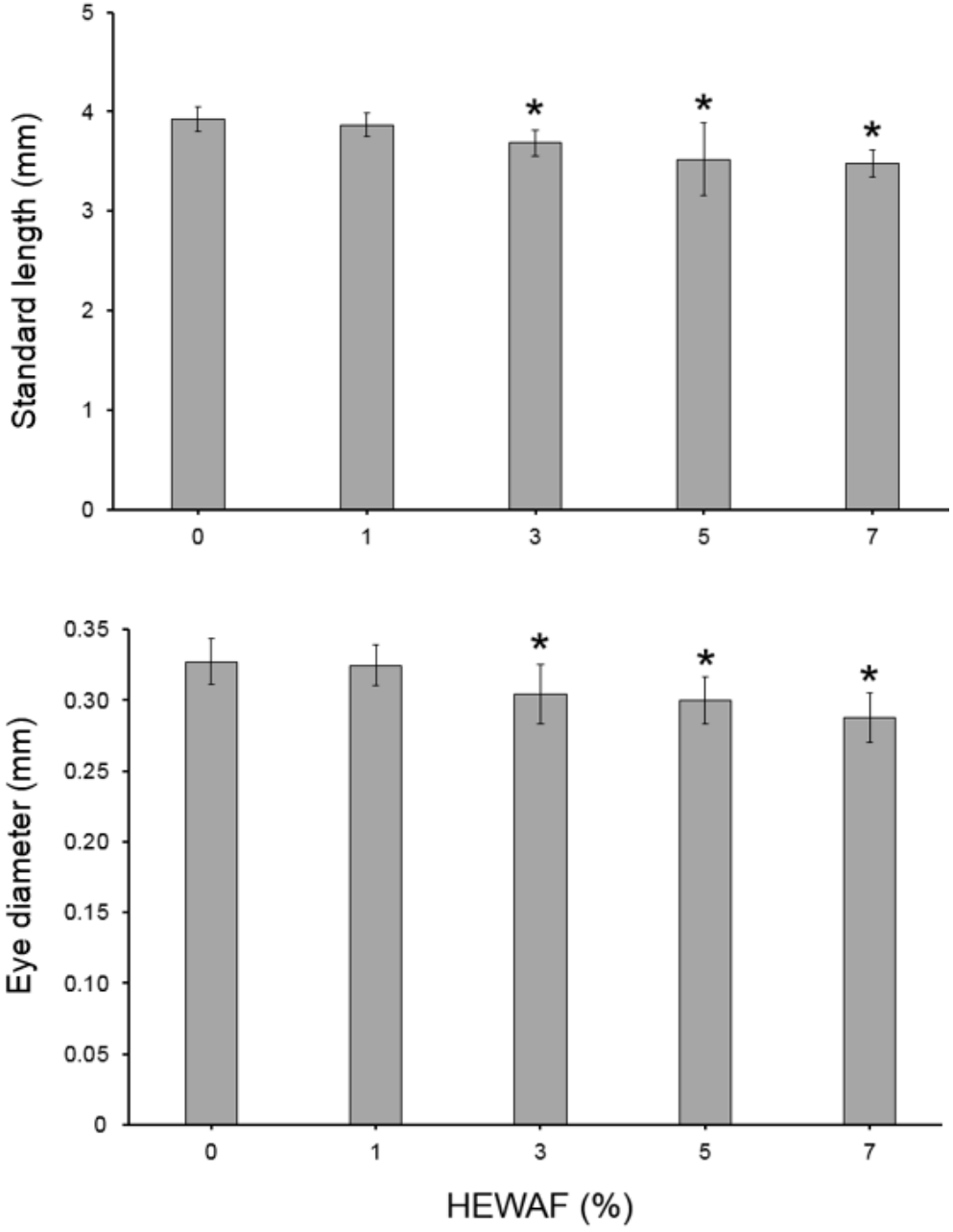

Figure 5.1: Mean (A) standard length and (B) eye diameter (mm) (±SD) in 96 hour post fertilized zebrafish exposed to 0, 1, 3, 5, and 7 % HEWAF. Asterisks (*) denote significance at ($p < 0.05$).

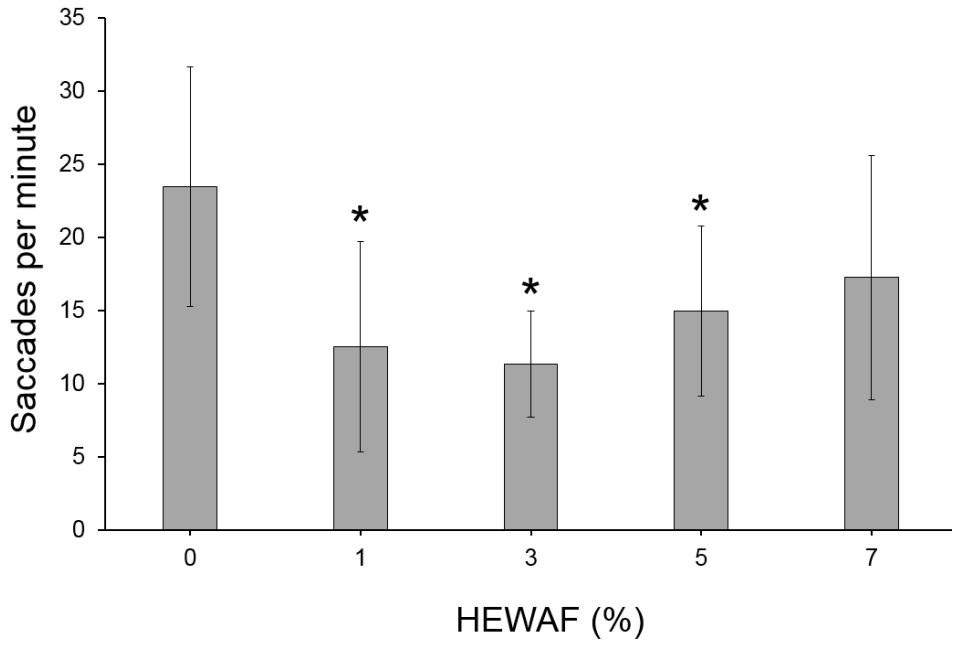

Figure 5.2: Mean saccades per minute (±SD) in 96 hour post fertilized zebrafish exposed to 0, 1, 3, 5, and 7 % HEWAF. Asterisks (*) denote significance at ($p < 0.05$).

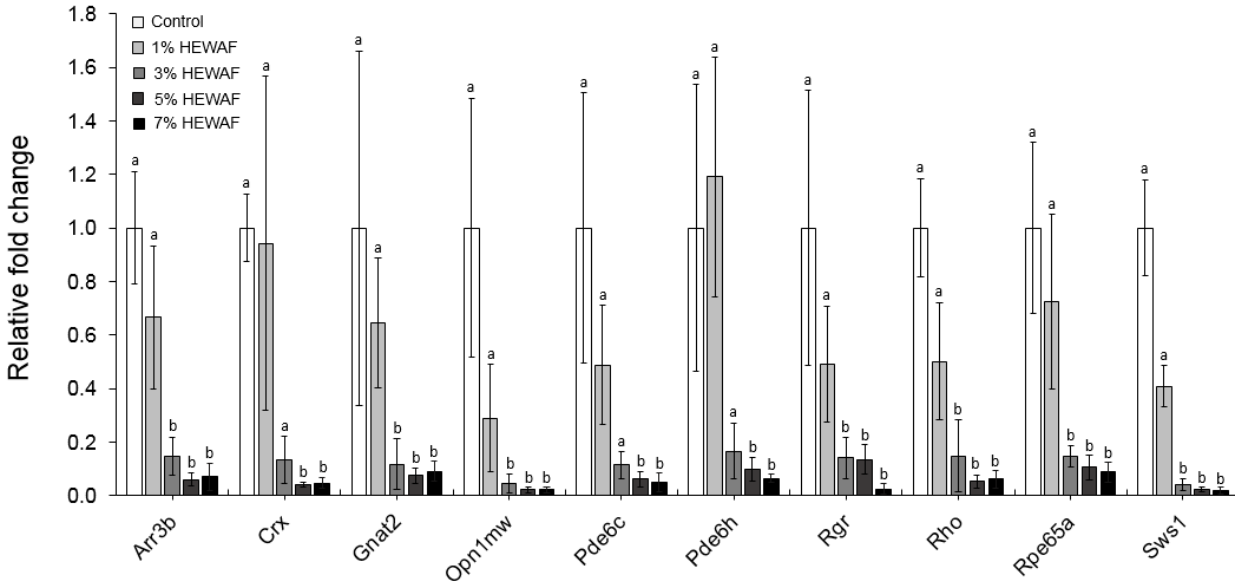

Figure 5.3: Relative fold change of *arr3b, crx, gnat2, opn1mw, pde6c, pde6h. rgr, rho, rpe65a,* and *sws1* in 96 hour post fertilized zebrafish exposed to 0, 1, 3, 5, and 7 % HEWAF. Lowercase letters are used to denote significance between exposure treatments and control ($p < 0.05$).

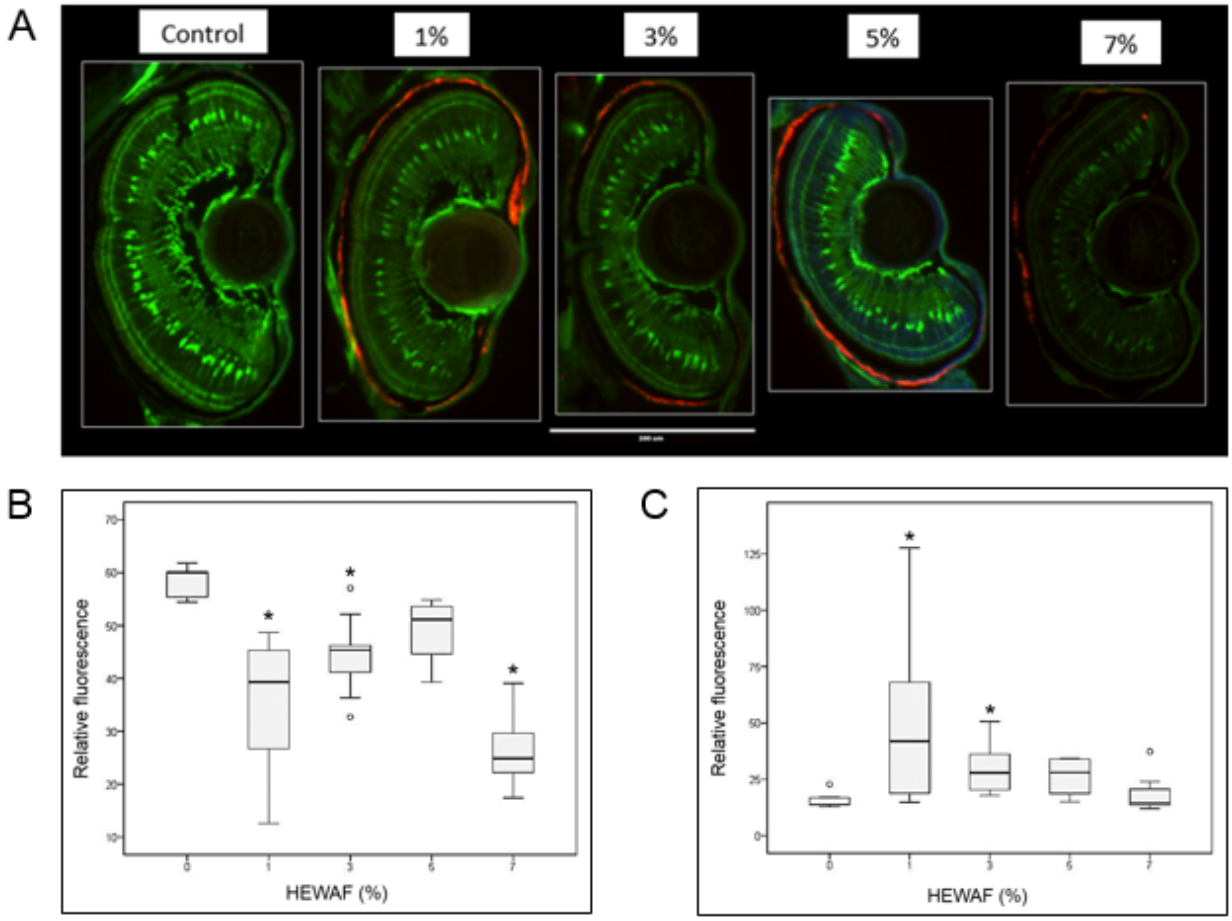

Figure 5.4: (A) Müller glial cell (green) and TUNEL (red) labeling, (B) relative fluorescence of Müller glial cells, and (C) relative TUNEL fluorescence in 96 hour post fertilized zebrafish exposed to 0, 1, 3, 5, and 7% HEWAF (scale bar 200 µm). Asterisks (*) denote significance at ($p < 0.05$).

5.4 Discussion

Vision plays an important role in predator avoidance and foraging behavior in larval teleosts [17–19]. Recent studies have shown that exposure to PAHs present in DWH crude oil can cause developmental defects and dysregulation of genes related to eye development and visual processing in oil-exposed larval fish [2,4]. However, the mechanism of how these transcriptomic-level changes impact visually-induced toxicity remains unclear. This is the first known study to provide direct evidence that larval fish have site-specific cell death in the retina, reduced Müller

glia and eye-associated gene expression, while impacting visually-mediated behavioral effects following exposure to crude oil.

Genes important in phototransduction and eye development (*arr3b*, *crx*, *gnat2*, *opn1mw*, *pde6c*, *pde6h*, *rgr*, *rho*, *rpe65a*, and *sws1*) were significantly downregulated in oil-exposed larvae, relative to controls. Similarly, Xu et al. (2016, 2017) and Diamante et al. (2017) found that vision-related, biological processes were among the most impacted pathways associated with exposure of crude oil in mahi-mahi and red drum larvae. Common genes found to be dysregulated following oil exposure in mahi-mahi were *crx*, *pde6c*, *rho*, and *rgr* [2], and *gnat2* and *rpe5a* in larval red drum [4]. A reduction in *rpe65* can further inhibit proper rod function in zebrafish [20]. A downregulation of genes important in eye development has also been observed in larval zebrafish following individual PAH exposures, including *opn1mw*, *gnat2*, and *pde6h* [13,21].

The binding of PAHs to aryl hydrocarbon receptors (AhR) has been well characterized in teleosts [22]. AhR is repressed by the aryl hydrocarbon receptor repressor (AHRR), which consists of two forms, AHRRa and AHRRb. AHRRa regulates AhR signaling during development, while AHRRa regulates PAH-induced gene expression [23]. Interestingly, Aluru et al. (2014) found that when AHRRa and AHRRb are knocked down in zebrafish exposed to TCDD, *pde6c*, *pde6h*, and *arr3b* (which is in part influenced by *crx* expression) were significantly downregulated in AHRRa knockdowns. However, they were not dysregulated in AHRRb knockdown fish. This suggests that AHRRa plays an important role in regulating several genes involved in photoreceptor signaling, and these genes are not directly regulated by the aryl hydrocarbon receptor, as when exposed to TCDD, these genes were not altered. However, further study is needed to determine the mechanism behind visual impairments in oil-exposed fish, with a focus on genes, such as *crx*, that influence multiple downstream effects.

crx plays an important role in the regulation of transcription for several genes important in phototransduction, such as *gnat2*, *pde6c*, *pde6h*, and *arr3*. *crx* is predominantly expressed in the outer part of the inner nuclear layer and photoreceptor layer [11,24]. Furthermore, site-specific apoptosis was seen in the outer limiting membrane of the retinal pigmented epithelial layer, which play a role in retinal cell differentiation, suggesting that *crx* is a major target of oil-induced toxicity in the developing larvae. When eyes were stained for Müller glial cells in zebrafish *crx* morphant embryos, Shen and Raymond (2004) saw a reduced levels of *crx* protein in *crx* morpholinos, relative to controls, which may suggest a role of *crx* in Müller glial cell expression. We found a similar response in oil-exposed larvae, with reduced connections seen, relative to controls. This further relates the apoptotic effects seen in the outer retinal pigmented epithelial layer, with a reduction in *crx* expression, inducing Müller glial expression in oil-exposed larvae.

Müller glial cells span across the retina where they provide a scaffold for neurons while interacting with all retinal neuronal bodies and associated processes [12]. They also play a critical role in regulating neurotransmitters and gas and ion homeostasis within the eye [25]. Reduced fluorescent expression was seen in larval eye, with increased oil-exposure further inhibiting retinal connections. Several processes are required for proper Müller glial cell function in the retina. Following oil exposure, CREB signaling in neurons (Xu et al., 2017a) was the top canonical pathway impacted in red drum. CREB plays an important role in the stability of dendritic branches in the ganglion, which is regulated by intracellular calcium [26], with reduced dendrites following suppressed calcium. Calcium signaling is a major pathway impacted following oil exposure in larval fish, suggesting that a suppression in Müller glial cells could play a role in the dysregulation of calcium levels in the retina. Furthermore, *lin-28* mRNAs were

rapidly induced in Müller glial cells in zebrafish following retinal injury [27]. Oil-exposed mahi-mahi had an upregulation of *lin-28,* relative to controls [3], suggesting site-specific damage in Müller glial cells, which we observed in oil-exposed zebrafish.

Visually-mediated effects at the molecular and cellular level induce subsequent downstream effects at the behavioral level. We have previously demonstrated that exposure to oil reduced an optomotor response (OMR) in larval mahi-mahi, red drum, and sheepshead minnow (in prep), though no known study has used an OKR to assess visual function in oil-exposed fish. Oil-exposed larvae had fewer eye saccades, relative to controls, as determined through OKR assays. Similar results were seen in larval duorado exposed to individual PAHs [28], with a decreased OMR response. Both responses have been used as common screening assays for visual function in fish [29,30], as an optomotor response relies on the fish to swim in the same direction as the rotating stripes, as opposed to an optokinetic response, which allows the fish to be restricted in a medium to view eye movements. We saw a dose-dependent decrease in eye saccades in 1 and 3% oil-exposed larvae, however, larvae exposed to both 5 and 7% HEWAF had subsequent increases in eye saccades, relative to 3% exposed larvae. Furthermore, there was no significant change in eye saccades in 7% oil-exposed larvae. Interestingly, a similar trend was observed when apoptosis was examined in the retina, with increased apoptosis occurring in 1 and 3% exposed larvae, with no significant difference in 5 or 7% exposed, which further relates molecular and cellular effects to behavioral-level impacts.

There was a downregulation of genes important in eye development and visual transduction in larvae following oil exposure, with an increased amount of apoptosis associated with the outer layer of the retinal pigment epithelium and associated choroid. We further saw a decrease in Müller glial cell connections in oil-exposed larvae, with subsequent decreases in eye

saccades, as determined through OKR. These results help further our understanding of oil-induced effects to eye development in larval teleosts, while relating gene expression, morphological, and behavioral-level effects. These visually-mediated effects are occurring at environmentally relevant concentrations of PAHs following the spill, and have implications for foraging ability and predator avoidance in the wild. Further research is needed to determine what other factors may be contributing reduced visual function in teleosts following oil exposure.

5.5 References

(1) Beyer, J.; Trannum, H. C.; Bakke, T.; Hodson, P. V.; Collier, T. K. Environmental Effects of the Deepwater Horizon Oil Spill: A Review. *Mar. Pollut. Bull.* **2016**, *110* (1), 28–51.

(2) Xu, E. G.; Mager, E. M.; Grosell, M.; Pasparakis, C.; Schlenker, L. S.; Stieglitz, J. D.; Benetti, D.; Hazard, E. S.; Courtney, S. M.; Diamante, G.; et al. Time- and Oil-Dependent Transcriptomic and Physiological Responses to Deepwater Horizon Oil in Mahi-Mahi (*Coryphaena Hippurus*) Embryos and Larvae. *Environ. Sci. Technol.* **2016**, *50* (14), 7842–7851.

(3) Diamante, G.; Xu, E. G.; Chen, S.; Mager, E.; Grosell, M.; Schlenk, D. Differential Expression of MicroRNAs in Embryos and Larvae of Mahi-Mahi (*Coryphaena Hippurus*) Exposed to Deepwater Horizon Oil. *Environ. Sci. Technol. Lett.* **2017**, *4*, 523–529.

(4) Xu, E. G.; Khursigara, A. J.; Magnuson, J.; Hazard, E. S.; Hardiman, G.; Esbaugh, A. J.; Roberts, A. P.; Schlenk, D. Larval Red Drum (*Sciaenops Ocellatus*) Sublethal Exposure to Weathered Deepwater Horizon Crude Oil: Developmental and Transcriptomic Consequences. *Environ. Sci. Technol.* **2017**, *51*, 10162–10172.

(5) Xu, E. G.; Mager, E. M.; Grosell, M.; Hazard, E. S.; Hardiman, G.; Schlenk, D. Novel Transcriptome Assembly and Comparative Toxicity Pathway Analysis in Mahi-Mahi (*Coryphaena Hippurus*) Embryos and Larvae Exposed to Deepwater Horizon Oil. *Sci. Rep.* **2017**, *7*, 44546.

(6) Esbaugh, A. J.; Mager, E. M.; Stieglitz, J. D.; Hoenig, R.; Brown, T. L.; French, B. L.; Linbo, T. L.; Lay, C.; Forth, H.; Scholz, N. L.; et al. The Effects of Weathering and Chemical Dispersion on Deepwater Horizon Crude Oil Toxicity to Mahi-Mahi (*Coryphaena Hippurus*) Early Life Stages. *Sci. Total Environ.* **2016**, *543*, 644–651.

(7) Mager, E. M.; Esbaugh, A. J.; Stieglitz, J. D.; Hoenig, R.; Bodinier, C.; Incardona, J. P.;

Scholz, N. L.; Benetti, D. D.; Grosell, M. Acute Embryonic or Juvenile Exposure to Deepwater Horizon Crude Oil Impairs the Swimming Performance of Mahi-Mahi (*Coryphaena Hippurus*). *Environ. Sci. Technol.* **2014**, *48* (12), 7053–7061.

(8) Incardona, J. P.; Gardner, L. D.; Linbo, T. L.; Brown, T. L.; Esbaugh, A. J.; Mager, E. M.; Stieglitz, J. D.; French, B. L.; Labenia, J. S.; Laetz, C. A.; et al. Deepwater Horizon Crude Oil Impacts the Developing Hearts of Large Predatory Pelagic Fish. *PNAS* **2014**, *111* (15), 1510–1518.

(9) Kohl, S.; Baumann, B.; Rosenberg, T.; Kellner, U.; Lorenz, B.; Jacobson, S. G.; Wissinger, B. Mutations in the Cone Photoreceptor G-Protein a -Subunit Gene GNAT2 in Patients with Achromatopsia. *Am. J. Hum. Genet.* **2002**, *71*, 422–425.

(10) Cai, K.; Itoh, Y.; Khorana, H. G. Mapping of Contact Sites in Complex Formation between Transducin and Light-Activated Rhodopsin by Covalent Crosslinking : Use of a Photoactivatable Reagent. *PNAS* **2001**, *98* (9), 4877–4882.

(11) Shen, Y.; Raymond, P. A. Zebrafish Cone-Rod (Crx) Homeobox Gene Promotes Retinogenesis. *Dev. Biol.* **2004**, *269*, 237–251.

(12) Bringmann, A.; Pannicke, T.; Grosche, J.; Francke, M.; Wiedemann, P.; Skatchkov, S. N.; Osborne, N. N.; Reichenbach, A. Müller Cells in the Healthy and Diseased Retina. *Prog. Retin. Eye Res.* **2006**, *25*, 397–424.

(13) Huang, L.; Wang, C.; Zhang, Y.; Wu, M.; Zuo, Z. Phenanthrene Causes Ocular Developmental Toxicity in Zebrafish Embryos and the Possible Mechanisms Involved. *J. Hazard. Mater.* **2013**, *261*, 172–180.

(14) Westerfield, M. *The Zebrafish Book: A Guide for the Laboratory Use of Zebrafish (*Danio Rerio, 5th ed.; University of Oregon Press, 2007.

(15) Spence, R.; Gerlach, G.; Lawrence, C.; Smith, C. The Behaviour and Ecology of the Zebrafish, *Danio Rerio*. *Bio. Rev.* **2008**, *83*, 13–34.

(16) Pfaffl, M. W. *A New Mathematical Model for Relative Quantification in Real-Time RT–PCR*; 2001; Vol. 29.

(17) Job, S. D.; Bellwood, D. R. Visual Acuity and Feeding in Larval *Premnas Biaculeatus*. *J. Fish Biol.* **1996**, *48*, 952–963.

(18) Blaxter, J. H. S. Development of Sense Organs and Behaviour of Teleost Larvae with Special Reference to Feeding and Predator Avoidance. *Trans. Am. Fish. Soc.* **1986**, *115*, 98–114.

(19) Blaxter, J. H. S. *The Eyes of Larval Fish. In: Vision in Fishes*, 1st ed.; Ali, M. A., Ed.; Plenum, New York, 1974.

(20) Schonthaler, H. B.; Lampert, J. M.; Isken, A.; Rinner, O.; Mader, A.; Gesemann, M.;

Oberhauser, V.; Golczak, M.; Palczewski, K.; Neuhauss, S. C. F.; et al. Evidence for RPE65-Independent Vision in the Cone-Dominated Zebrafish Retina. *Eur. J. Neurosci.* **2007**, *26* (7), 1940–1949.

(21) Huang, L.; Zuo, Z.; Zhang, Y.; Wu, M.; Lin, J. J.; Wang, C. Use of Toxicogenomics to Predict the Potential Toxic Effect of Benzo(a)pyrene on Zebrafish Embryos: Ocular Developmental Toxicity. *Chemosphere* **2014**, *108*, 55–61.

(22) Billiard, S. M.; Hahn, M. E.; Franks, D. G.; Peterson, R. E.; Bols, N. C.; Hodson, P. V. Binding of Polycyclic Aromatic Hydrocarbons (PAHs) to Teleost Aryl Hydrocarbon Receptors (AHRs). *Comp. Biochem. Physiol. - B Biochem. Mol. Biol.* **2002**, *133* (1), 55–68.

(23) Aluru, N.; Jenny, M. J.; Hahn, M. E. Knockdown of a Zebrafish Aryl Hydrocarbon Receptor Repressor (AHRRa) Affects Expression of Genes Related to Photoreceptor Development and Hematopoiesis. *Toxicol. Sci.* **2014**, *139* (2), 381–395.

(24) Laranjeiro, R.; Whitmore, D. Transcription Factors Involved in Retinogenesis Are Co-Opted by the Circadian Clock Following Photoreceptor Differentiation. *Development* **2014**, *141*, 1–13.

(25) Peterson, R. E.; Fadool, J. M.; McClintock, J.; Linser, P. J. Müller Cell Differentiation in the Zebrafish Neural Retina: Evidence of Distinct Early and Late Stages in Cell Maturation. *J. Comp. Neurol.* **2001**, *429*, 530–540.

(26) Redmond, L.; Kashani, A. H.; Ghosh, A. Calcium Regulation of Dendritic Growth via CaM Kinase IV and CREB-Mediated Transcription. *Neuron* **2002**, *34*, 999–1010.

(27) Ramachandran, R.; Fausett, B. V; Goldman, D. Ascl1a Regulates Müller Glia Dedifferentiation and Retinal Regeneration through a Lin- 28-Dependent, *Let* -7 microRNA Signalling Pathway. *Nat. Cell Biol.* **2010**, *12* (11), 1101–1107.

(28) Carvalho, P. S. M.; Kalil, D. da C. B.; Novelli, G. A. A.; Bainy, A. C. D.; Fraga, A. P. M. Effects of Naphthalene and Phenanthrene on Visual and Prey Capture Endpoints during Early Stages of the Dourado *Salminus Brasiliensis*. *Mar. Environ. Res.* **2008**, *66* (1), 205–207.

(29) Muto, A.; Orger, M. B.; Wehman, A. M.; Smear, M. C.; Kay, J. N.; Page-McCaw, P. S.; Gahtan, E.; Xiao, T.; Nevin, L. M.; Gosse, N. J.; et al. Forward Genetic Analysis of Visual Behavior in Zebrafish. *PLoS Genet.* **2005**, *1* (5), 575–588.

(30) Orger, M. B.; Gahtan, E.; Muto, A.; Page-McCaw, P. S.; Smear, M. C.; Baier, H. Behavioral Screening Assays in Zebrafish. *Methods Cell Biol* **2004**, *77*, 53–68.

CHAPTER 6

DISCUSSION

6.1 Optomotor, Optokinetic, and Electroretinogram Assays

The optomotor response (OMR) measures the ability of a fish to orient its body by swimming in the same direction as an external stimuli. Individual and multiple larvae can be assessed for an OMR at once, which can make it a great tool to measure visual ability using high throughput techniques [1,2]. Individual stripes can be adhered to a rotating drum while changing light levels to assess both scotopic and photopic responses. To assess overall visual function without the need to change the stripes or light levels displayed on the rotating drum, a moving grating system can be used, along with varying light intensities, through a computer system to test multiple larvae at once [1]. This behavioral assay has been used to determine several visually-impaired mutant strains [2], as well as visually deficient larvae following exposure to contaminants [3,4]. Though utilizing different motor outputs, an optokinetic response (OKR) has been used to assess visual function in larval fishes. Though similar to the OMR, as the fish will focus on the alternating stripes adhered to a rotating drum apparatus, this assay focuses on the ability of a fish to move its eyes in response to a rotating drum apparatus, as opposed to a swimming response-as seen with an OMR. The OKR can elicit a behavioral response in larvae as young as 73 hpf [5], whereas an OMR is exhibited about 4 dpf [1]. OKR has also been used to screen larvae to find visual mutants [6], with the ability to look at multiple larvae at a time [1]. Some visual mutants are capable of assessing an OMR though not an OKR, and vis-versa, while others exhibit both [2], suggesting possible limitations for each assay. It has been proposed that an OMR is better utilized for presorting mutants, while an OKR would be better utilized for weeding-out false

positives. As such, utilizing multiple screening assays together would provide the most effective assessment of visual function [2].

Furthermore, as both the OMR and OKR do not require sacrificing larvae for visual assessment, an electroretinogram (ERG) could be used concomitantly following both behavioral assays. An ERG is a non-invasive method that measures the electrical activity of the eye through the stimulation of the retina by various light intensities. Electrical signals originate in the photoreceptor layer which will generate three successive waves [7]. These waves assess electrical impulses from photoreceptor activity, and the on and off responses of bipolar cells, where it primarily assess outer retinal function. ERGs are commonly used as a subsequent assay to measure visual function in larval fish, and can be used in zebrafish larvae as early at 5 dpf.

Utilizing multiple behavioral assays, with a subsequent ERG assessment would be ideal to determine visually-mediated effects following exposure to contaminants, while providing a means to find visual mutants. However, due to the sensitivity of several larval fish, especially once exposed to contaminants, using all three assays would not be feasible to assess visual function. As zebrafish larvae can exhibit an OKR prior to an OMR, it can be suggested that this is a preferable means to determine visual activity in larval fish. Though the amount of equipment and supplies needed to conduct an ERG is quite extensive, a subsequent ERG could further measure electrical responses following various light intensities to assess phototransduction and retinal function.

6.2 Behavioral Assessment

While using common behavioral assays we were able to determine visual function in mahi-mahi, red drum, sheepshead minnow, and zebrafish larvae following exposure to

environmentally relevant concentrations of oil found in the Gulf of Mexico following the *Deepwater Horizon* oil spill [8]. Prior studies conducted on mahi-mahi vision have been on juveniles and adults [9–12], with no baseline information available for early life stages. Understanding when larvae are capable of exhibiting an optomotor response, while combating early life stage sensitivity, provided us with a starting point for oil exposures. The optomotor response and optokinetic response were used to assess visual function in larvae, as both have been utilized in studies following contaminant exposure [3,4] and identifying visual mutants [2]. The rotating drum apparatus used in both behavioral tests were adjusted to each species and life stage tested so results could be comparable across fish species inhabiting different locations. A range of weathered oil concentrations were used to assess these visually-mediated behavioral changes due to species sensitivity, which has been further shown to change depending on life stage [13]. Following oil-exposure, there was a decreased ability of larval fish to exhibit either an optomotor or optokinetic response relative to unexposed larvae. These changes were directly related to visual effects, as concentrations used did not impair swimming behavior until far greater speeds than used in this assay [14]. Furthermore, reductions in the ability to exhibit optomotor and optokinetic responses have similar endpoints when feeding studies were conducted following individual PAH-exposure [4], further suggesting implications for survival in the environment.

6.3 Morphological and Histological Assessment

A common effect following oil exposure in microphthalmia (reduced eye size) [15,16]. Following oil exposure, reduced eye size was seen in red drum, sheepshead minnow, and zebrafish, though not in mahi-mahi. We suggest that effects to eye size is dependent on oil concentration, and may also be a species dependent response. Though mahi-mahi were exposed

to the lowest concentration of oil compared to other fish tested unchanged eye size was observed when exposed to higher concentrations of crude oil, as well (Edmunds et al. 2015). When assessed for histological effects in the retina, layers important in visual function were reduced in size in the sheepshead minnow, with concurrent impacts in nuclear layers in red drum. However, these reductions in retinal layers were not seen in later stages of development in red drum, nor at any age examined in mahi-mahi. It has been suggested that transcriptomic level changes may be occurring prior to the initiation of histological damage in the retina as seen in benzo(a)pyrene-exposed zebrafish [17], as relying on morphological and histological assessment alone is not enough to determine direct impacts to visual ability.

6.4 miRNA-mRNA Interactions and Gene Expression

To further understand these underlying, molecular-level effects impacting visual function following oil exposure, miRNA-mRNA interactions were assessed in mahi-mahi. miR-181b and miR-23b among the most affected miRNAs, where they were upregulated in larvae following oil exposure. They both play important roles in visual function, eye development, and capillary formation in teleosts. miR-181b plays important functions in the ganglion and inner nuclear layer where it is involved in mediating downstream visual processing in the tectum [18], and was subsequently upregulated in oil-exposed mahi-mahi. miR-23b plays an important role in mediating capillary and choroid formation in the retina [19], where it was also upregulated in exposed larvae. Due to the role miRNAs play in regulating mRNA stability and translation, the associated interactions between miRNA and mRNA help us further understand oil-induced effects to retinal processes, impacting both eye development and function.

As oil-exposed larvae did not have subsequent reductions in morphological or histological assessments of retinal impacts, though biological pathways involved with visual function were impacted, genes important in eye development and phototransductions were assessed in larval zebrafish. Following exposure to oil, a downregulation was seen in all genes examined. These genes have been further shown to be down regulated in larval zebrafish exposed to benzo(a)pyrene [17], mahi-mahi [20], and red drum [16]. One of the genes, *crx*, is involved in the regulation of several genes involved in phototransduction [21]. Furthermore, *crx* is downregulated in oil-exposed mahi-mahi [20], and further explains subsequent dysregulations of genes.

6.5 Immunohistochemistry and Apoptosis

Site-specific damage was seen in Müller glial cells in exposed zebrafish. miRNA *lin-28*, was upregulated in oil-exposed mahi-mahi [22], which has further been shown to specifically impact Müller glial cell function in the retina following injury [23]. Interesting, a majority of apoptotic cells were seen in the outer layer of the retinal pigmented epithelium and associated choroid, with none associated with Müller glia themselves. Multiple processes could impact Müller glial activity following retinal injury, such as reduced *crx* expression [24], dysregulation of CREB [25], and further influence in notch, wnt, and fgf- which were dysregulated following oil exposure in mahi-mahi [22].

6.6 Mechanisms

The aryl hydrocarbon receptor (AhR) pathway plays an important role in mediating the breakdown and removal of TCDD, halogenated aromatic hydrocarbons (HAHs), and PAHs [26].

However, HAH and PAH ligands do not possess the same affinity towards AhR as TCDD. These ligands will bind to an AhR in the cytoplasm with two associated heat shock proteins (hsp90), an x-associated protein 2 (xap2), and a p23 chaperone protein. This complex will undergo a conformational change where it will translocate into the nucleus, binding to an aryl hydrocarbon nuclear translocator (ARNT). Following dimerization, the complex will bind to a DNA recognition site (DRE), which will stimulate the transcription of CYP1A1 and other downstream AhR-responsive genes [26]. Though phenanthrene is a weak AhR agonist, Huang et al. [27] indicated that following exposure zebrafish had an upregulation of AhR in the retina at both the transcriptional and translational level. Following an upregulation of AhR, it was proposed that AhR serves as a transcription factor for *zeb1*, which was subsequently inhibited, further reducing *mitf* expression, and reducing cell proliferation within the retina [27]. Furthermore, trout exposed to TCDD had increased CYP1A1 expression in the choroid layer, surrounding the retina, though not in any associated retinal layers [3]. Interestingly, Colavecchia et al. [28], reported increased levels of CYP1A in the lens epithelium and innermost retinal layers in fathead minnow larvae exposed to oil sands, though no induced CYP1A expression was noted in larval white suckers. These findings suggest that there could be species sensitivity differences, along with differences in the subcellular compartmentalization of CYP1A in larval fish.

It has been further proposed that, though playing a predominant role in reducing TCDD toxicity, a non-AhR pathway is involved in PAH-associated toxicity. The use of transgenic knockouts or by injecting embryos with morpholinos has allowed us to further understand the mechanism of toxicity following contaminant exposure. To better understand the mechanism of PAH-exposed fish, a mutant zebrafish with a dysfunctional troponin was exposed to several PAHs consisting of different ring structures [29]. Reduced eye development was noted following

exposure to three-ring PAHs, suggesting that cardiac impairment was sufficient for secondary, downstream, eye-associated effects. It was further suggested that most or all induced morphological defects following PAH-exposure were associated with cardiac dysfunction [29].

Alternative, non-AhR pathways have been proposed to directly impair proper eye formation in larval fish, with eye-specific effects. Aluru et al. [30] used zebrafish that were knockdowned in aryl hydrocarbon receptor repressor (AHRR)- either AHRRa or AHRRb. AHRR plays an important role in repressing AhR and hypoxia-inducible factor (HIF). AHRRa regulates AhR signal during development, whereas AHRRb regulates PAH-induced gene expression. When morpholino knockdowns were exposed to TCDD, the expression of genes important in proper phototransduction were downregulated in AHRRa knockdowns, whereas AHRRb knockdowns were not different than controls. This suggests that AHRRa plays an important role in the developing eye, where it could regulate AhR, HIF, among other transcription factors, with subsequent roles in exhibiting a protective response to xenobiotics [30]. This could further help explain eye-associated toxicity following PAH or TCDD exposure noted in larval zebrafish [27] and trout [3]. Further use of transgenic lines should be used to determine the target of PAH-associated toxicity in the developing fish eye. Subsequent behavioral assays have been used to determine the role of eye-associated genes in visual function, with further research needed to understand eye-specific toxicity following PAH exposure.

6.7 Future Directions

The optomotor and optokinetic assays can tell us a lot of information about visual function, though conducting an electroretinogram could help connect these behavioral-level effects with Müller glial cell activity, due to their neuronal interactions and role in transmitting

light to photoreceptors. This would help further confirm retinal-induced injury following oil exposure. The majority of apoptosis resulting in the associated choroid layer leaves reason to believe there is a reduced capillary network in oil-exposed larvae. Looking at *Gfp*-transgenic zebrafish could help provide further answers to what is occurring in the retinal vasculature in exposed larvae, influencing oxygen delivery and ion exchange. Furthermore, it has been proposed that the mosaic arrangement of rods and cones in the retina are altered during injury, and following retinal repair can be regenerated, though not in the same mosaic arrangement. It would be interesting to further understand if this occurs in oil-exposed fish, and the implications this has on visual function.

6.8 References

(1) Orger, M. B.; Gahtan, E.; Muto, A.; Page-McCaw, P. S.; Smear, M. C.; Baier, H. Behavioral Screening Assays in Zebrafish. *Methods Cell Biol* **2004**, *77*, 53–68.

(2) Muto, A.; Orger, M. B.; Wehman, A. M.; Smear, M. C.; Kay, J. N.; Page-McCaw, P. S.; Gahtan, E.; Xiao, T.; Nevin, L. M.; Gosse, N. J.; et al. Forward Genetic Analysis of Visual Behavior in Zebrafish. *PLoS Genet.* **2005**, *1* (5), 575–588.

(3) Carvalho, P. S. M.; Tillitt, D. E. 2,3,7,8-TCDD Effects on Visual Structure and Function in Swim-up Rainbow Trout. *Environ. Sci. Technol.* **2004**, *38* (23), 6300–6306.

(4) Carvalho, P. S. M.; Kalil, D. da C. B.; Novelli, G. A. A.; Bainy, A. C. D.; Fraga, A. P. M. Effects of Naphthalene and Phenanthrene on Visual and Prey Capture Endpoints during Early Stages of the Dourado *Salminus Brasiliensis*. *Mar. Environ. Res.* **2008**, *66* (1), 205–207.

(5) Easter, S. S.; Nicola, G. N. The Development of Vision in the Zebrafish (*Danio Rerio*). *Dev. Biol.* **1996**, *180* (2), 646–663.

(6) Brockerhoff, S. E.; Hurley, J. B.; Janssen-Bienhold, U.; Neuhauss, S. C.; Driever, W.; Dowling, J. E. A Behavioral Screen for Isolating Zebrafish Mutants with Visual System Defects. *Proc. Natl. Acad. Sci.* **1995**, *92* (23), 10545–10549.

(7) Makhankov, Y. V.; Rinner, O.; Neuhauss, S. C. F. An Inexpensive Device for Non-Invasive Electroretinography in Small Aquatic Vertebrates. *J. Neurosci. Methods* **2004**, *135* (1–2), 205–210.

(8) Diercks, A. R.; Highsmith, R. C.; Asper, V. L.; Joung, D.; Zhou, Z.; Guo, L.; Shiller, A. M.; Joye, S. B.; Teske, A. P.; Guinasso, N.; et al. Characterization of Subsurface Polycyclic Aromatic Hydrocarbons at the Deepwater Horizon Site. *Geophys. Res. Lett.* **2010**, *37* (20), 1–6.

(9) Kröger, R. H. H.; Fritsches, K. A.; Warrant, E. J. Lens Optical Properties in the Eyes of Large Marine Predatory Teleosts. *J. Comp. Physiol. A* **2009**, *195* (2), 175–182.

(10) McFarland, W. N.; Munz, F. W. Part III: The Evolution of Photopic Visual Pigments in Fishes. *Vis. Res.* **1975**, *15*, 1071–1080.

(11) Munz, F. W.; McFarland, W. N. Part I: Presumptive Cone Pigments Extracted from Tropical Marine Fishes. *Vis. Res.* **1975**, *15*, 1045–1062.

(12) Tamura, T.; Wisby, W. J. The Visual Sense of Pelagic Fishes Especially the Visual Axis and Accommodation. *Bull. Mar. Sci. Gulf Caribb.* **1963**, *13*, 433–448.

(13) Mager, E. M.; Pasparakis, C.; Schlenker, L. S.; Yao, Z.; Bodinier, C.; Stieglitz, J. D.; Hoenig, R.; Morris, J. M.; Benetti, D. D.; Grosell, M. Assessment of Early Life Stage Mahi-Mahi Windows of Sensitivity during Acute Exposures to *Deepwater Horizon* Crude Oil. *Environ. Toxicol. Chem.* **2017**, *36* (7), 1887–1895.

(14) Mager, E. M.; Esbaugh, A. J.; Stieglitz, J. D.; Hoenig, R.; Bodinier, C.; Incardona, J. P.; Scholz, N. L.; Benetti, D. D.; Grosell, M. Acute Embryonic or Juvenile Exposure to Deepwater Horizon Crude Oil Impairs the Swimming Performance of Mahi-Mahi (*Coryphaena Hippurus*). *Environ. Sci. Technol.* **2014**, *48* (12), 7053–7061.

(15) Hose, J. E.; McGurk, M. D.; Marty, G. D.; Hinton, D. E.; Brown, E. D.; Baker, T. T. Sublethal Effects of the Exxon Valdez Oil Spill on Herring Embyros and Larvae: Morphological, Cytogenetic, and Histopathological Assessments, 1989-1991. *Can. J. Fish. Aquat. Sci.* **1996**, *53* (10), 2355–2365.

(16) Xu, E. G.; Khursigara, A. J.; Magnuson, J.; Hazard, E. S.; Hardiman, G.; Esbaugh, A. J.; Roberts, A. P.; Schlenk, D. Larval Red Drum (*Sciaenops Ocellatus*) Sublethal Exposure to Weathered Deepwater Horizon Crude Oil: Developmental and Transcriptomic Consequences. *Environ. Sci. Technol.* **2017**, *51*, 10162–10172.

(17) Huang, L.; Zuo, Z.; Zhang, Y.; Wu, M.; Lin, J. J.; Wang, C. Use of Toxicogenomics to Predict the Potential Toxic Effect of Benzo(a)pyrene on Zebrafish Embryos: Ocular Developmental Toxicity. *Chemosphere* **2014**, *108*, 55–61.

(18) Carrella, S.; D'Agostino, Y.; Barbato, S.; Huber-Reggi, S. P.; Salierno, F. G.; Manfredi, A.; Neuhauss, S. C. F.; Banfi, S.; Conte, I. miR-181a/b Control the Assembly of Visual Circuitry by Regulating Retinal Axon Specification and Growth. *Dev. Neurobiol.* **2015**, *75* (11), 1252–1267.

(19) Agrawal, S.; Chaqour, B. MicroRNA Signature and Function in Retinal Neovascularization. *World J Biol Chem* **2014**, *5* (1), 1–11.

(20) Xu, E. G.; Mager, E. M.; Grosell, M.; Pasparakis, C.; Schlenker, L. S.; Stieglitz, J. D.; Benetti, D.; Hazard, E. S.; Courtney, S. M.; Diamante, G.; et al. Time- and Oil-Dependent Transcriptomic and Physiological Responses to Deepwater Horizon Oil in Mahi-Mahi (*Coryphaena Hippurus*) Embryos and Larvae. *Environ. Sci. Technol.* **2016**, *50* (14), 7842–7851.

(21) Freund, C. L.; Gregory-evans, C. Y.; Furukawa, T.; Papaioannou, M.; Looser, J.; Ploder, L.; Bellingham, J.; Ng, D.; Herbrick, J. S.; Duncan, A.; et al. Cone-Rod Dystrophy Due to Mutations in a Novel Photoreceptor-Specific Homeobox Gene (CRX) Essential for Maintenance of the Photoreceptor. *Cell* **1997**, *91*, 543–553.

(22) Diamante, G.; Xu, E. G.; Chen, S.; Mager, E.; Grosell, M.; Schlenk, D. Differential Expression of MicroRNAs in Embryos and Larvae of Mahi-Mahi (*Coryphaena Hippurus*) Exposed to Deepwater Horizon Oil. *Environ. Sci. Technol. Lett.* **2017**, *4*, 523–529.

(23) Ramachandran, R.; Fausett, B. V; Goldman, D. Ascl1a Regulates Müller Glia Dedifferentiation and Retinal Regeneration through a Lin-28-Dependent, *Let*-7 microRNA Signalling Pathway. *Nat. Cell Biol.* **2010**, *12* (11), 1101–1107.

(24) Shen, Y.; Raymond, P. A. Zebrafish Cone-Rod (Crx) Homeobox Gene Promotes Retinogenesis. *Dev. Biol.* **2004**, *269*, 237–251.

(25) Redmond, L.; Kashani, A. H.; Ghosh, A. Calcium Regulation of Dendritic Growth via CaM Kinase IV and CREB-Mediated Transcription. *Neuron* **2002**, *34*, 999–1010.

(26) Denison, M. S.; Nagy, S. R. Actication of the Aryl Hydrocarbon Receptor by Structurally Diverse Exogenous and Endogenous Chemicals. *Annu. Rev. Pharmacol. Toxicol.* **2003**, *43* (1), 309–334.

(27) Huang, L.; Wang, C.; Zhang, Y.; Wu, M.; Zuo, Z. Phenanthrene Causes Ocular Developmental Toxicity in Zebrafish Embryos and the Possible Mechanisms Involved. *J. Hazard. Mater.* **2013**, *261*, 172–180.

(28) Colavecchia, M. V.; Hodson, P. V.; Parrott, J. L. The Relationships among CYP1A Induction, Toxicity, and Eye Pathology in Early Life Stages of Fish Exposed to Oil Sands. *J. Toxicol. Environ. Heal. Part A* **2007**, *70*, 1542–1555.

(29) Incardona, J. P.; Collier, T. K.; Scholz, N. L. Defects in Cardiac Function Precede Morphological Abnormalities in Fish Embryos Exposed to Polycyclic Aromatic Hydrocarbons. *Toxicol. Appl. Pharmacol.* **2004**, *196* (2), 191–205.

(30) Aluru, N.; Jenny, M. J.; Hahn, M. E. Knockdown of a Zebrafish Aryl Hydrocarbon Receptor Repressor (AHRRa) Affects Expression of Genes Related to Photoreceptor Development and Hematopoiesis. *Toxicol. Sci.* **2014**, *139* (2), 381–395.